ENGINEERING RESEARCH INSTITUTE
THE UNIVERSITY OF MICHIGAN
ANN ARBOR

APPLICATION OF NUCLEAR ENERGY TO TRANSPORTATION

Progress Report No. 6

PRELIMINARY NUCLEAR HEAT POWERPLANT ENGINE STUDIES

F. G. HAMMITT
E. M. BROWER
R. K. FU
J. L. SUMMERS

Approved by:

H. A. OHLGREN

Project 2427

CHRYSLER CORPORATION
DETROIT, MICHIGAN

April 1956

TABLE OF CONTENTS

Table of Contents, Continued

LIST OF ILLUSTRATIONS - PART I

LIST OF ILLUSTRATIONS - PART II

List of Illustrations - Part II, Continued

List of Illustrations - Part II, Continued

LIST OF TABLES - PART I

LIST OF TABLES - PART II

1.0 ABSTRACT

This report includes a preliminary overall appraisal of the various conceivable heat engine cycles which might be used with a nuclear powerplant, as well as a detailed investigation of the gas turbine cycle in this application - particularly from the viewpoint of the turbomachinery. The report is divided into Part I and Part II, with Part I comprising the overall investigation and Part II the gas turbine study.

Part I.

It is the function of this portion of the report to review in a preliminary fashion all heat engine cycles feasible for use in nuclear powerplants. It is concluded that the gas turbine type, the steam type, and the binary or trinary vapor cycle type include all the modes of design which are presently practical. These cycles are reviewed primarily with respect to attainable thermal efficiency as a function of source and receiver temperature.

It is concluded that within the range of source temperature up to 1500 F, the highest efficiencies may be obtained with the binary or trinary cycle (about 59% at 1500 F), with a maximum of about 45% for the gas turbine and about 49% for the steam cycle (Figure 11). It is further concluded that the development of a 1500 F gas turbine plant with an efficiency approaching this figure, except for very large outputs, is less difficult than the development of either the steam or binary plant for the same temperature.

The machinery requirements of a binary plant are examined briefly, and it is concluded that inherently no insuperable problem is involved. The possibility of the utilization of sodium, mercury, or possible other fluids as direct reactor coolant in a boiling-type reactor concurrent with its use as a heat engine fluid for the high temperature portion of a binary vapor cycle is discussed.

A listing of anticipated future efforts to compliment the work herein reported is included.

Part II.

This portion of the report is concerned with a detailed investigation of the gas turbine cycle as it may be applied to nuclear powerplants. It includes a theoretical "perfect gas" investigation, and also a detailed study of the effects of power output, pressure, and temperature on the overall plant efficiency in terms of the variation of turbomachinery component efficiencies. The "perfect gas" studies are applied to both monatomic and diatomic gases, while both air and helium were considered in the machinery studies.

A "basic cycle", consisting of a highly effective regenerator, a single intercooler, a heat source and sink, and a compressor and turbine is considered. This type of cycle was chosen rather than a "simple cycle" (no intercooler or regenerator) because of higher efficiencies, though sacrificing size and weight considerations to some extent. The conceivable variations in component efficiencies and cycle arrangement from the "basic cycle" were considered, and thus a method for estimating the attainable efficiency for any other cycle arrangement provided.

For the "perfect gas" study, it was noted that, for given temperature limitations and cycle arrangement, the plant thermal efficiency is affected only by the ratio of specific heats and the pressure ratio. Under these assumptions, monatomic gases differ in attainable efficiency from diatomic, but the gas molecular weight has no effect. Diatomic gases appear somewhat superior in this respect. It is shown that the result may be somewhat misleading since, in some instances, monatomic gases may show certain superior qualities which may allow the attainment of a given level of component efficiency at reduced cost.

For the machinery studies with air and helium, the variations in turbomachinery efficiency, size, and type with output, fluid, temperature, and pressure were investigated for the "basic cycle". Constant heat exchanger effectivenesses were assumed. All significant results are tabulated, plotted and discussed. In combination with the "perfect gas" study, these efficiency results may be used to estimate the attainable efficiency with other cycle arrangements.

The anticipated course of future work is outlined.

2.0 INTRODUCTION

A nuclear reactor, as presently conceived, is essentially a heat-producing device. If usable power is to be generated, it is necessary, under present day technology to convert this heat through a suitable means to mechanical and/or electrical energy. Thus a "heat engine" of some sort is required. Although very considerable experience and knowledge exists relating to heat engines as used in conventional fossil-fueled powerplants, the step to nuclear energy introduces many new factors and variables into the overall design. It requires a reappraisal of the existing practice in order to adapt successfully to the new boundary conditions. If nuclear powerplants are to be successfully applied to transportation devices, where size and weight become of paramount importance, it is necessary that the energy level be raised considerably above that obtained in present day nuclear plants, and even above that common to fossil-fueled units.

In general it is necessary to consider various new working fluids and cycles, and also to reconsider the conventional ones in the light of higher temperatures, exposure to radiation, possible inaccessibility of machinery, stringent sealing requirements, unusual relations between fuel costs and capital costs, etc. As is well known, the suitability of the various conceivable heat engine devices depends upon the available source and receiver temperatures, the size of the plant (i.e. power output), and various other factors involving type of application, particular type and arrangement of the reactor, etc.

A general appraisal of the possible working fluids for heat engine cycles (which comprise the only presently known practical large scale devices for the conversion of heat energy into mechanical energy) shows that these are either of the single phase type in the working range (as a gas) or exhibit phase change within the cycle range (as water). There is also, of course, the possibility of advantageously combining fluids of the same or different types in this respect into the same cycle.

The present report reviews the various possible cycles from the standpoint of attainable efficiency. The cycles being considered are the gas turbine, the steam, and the binary (or trinary) vapor cycles which utilize combinations of a low vapor pressure fluid for the high temperature portion of the cycle and water or gas for the lower temperature portion.

In addition, detailed studies of the gas turbine cycle are included. These consider "perfect gas" cycles, and also real fluid cycles, in which the influences on efficiency of the plant output, pressure level, temperature, and working fluid as they affect the turbomachinery are considered.

The work reported covers the preliminary phases and progress of these investigations. Major items remaining to be considered are:

a) Additional working fluid combinations and further refinement of those studies presently underway,

b) Evaluation of probable developmental difficulties for the various cycles,

c) Radioactivity effects on working fluid and machinery,

d) Effects on gas turbine cycle of heat exchanger component variations,

e) Overall economic optimization of nuclear powerplants for typical applications,

f) Control problems of an integrated nuclear-gas-turbine powerplant.

3.0 OBJECTIVES

The work herein reported is being undertaken in partial fulfillment of the contract between the University of Michigan and the Chrysler Corporation. The general objective of this work is the examination of possible heat engine cycles as components of nuclear powerplants, particularly with respect to those features by which the imposed boundary conditions for this type of plant may alter the previously established design philosopies. A specific objective is the investigation in detail of the gas turbine cycle for application to a nuclear powerplant.

4.0 ACKNOWLEDGEMENTS

The authors wish to express their appreciation to Professor H. A. Ohlgren for his aid and suggestions in the preparation of this report, and to Philip Allen, William Beckman and Jacques Boegli for their assistance with the calculations.

The authors also wish to thank Robert Thomas and Ronald Hanson who drafted the figures and Mrs. Autumn Jenkins for her secretarial help.

PART I. GENERALIZED HEAT ENGINE STUDIES FOR NUCLEAR POWERPLANTS

1.0 GENERAL THERMODYNAMIC PARAMETERS

1.1 Application to Nuclear Powerplant

For the successful utilization of a nuclear powerplant, heat generated by nuclear fission in the core of the reactor must be converted in as large a proportion as possible into useful mechanical work. This realizable proportion is largely controlled by the temperature ratio available to the heat engine: i.e., the ratio of the maximum absolute temperature available to the heat engine fluid to the minimum absolute temperature at which heat may be rejected to the environment.* The minimum temperature is a function of the application and of ambient conditions. For example, it may be as low as 60 F for a plant located in proximity to a suitable supply of cooling water. On the other hand, it may be as high as 300-400 F in cases where an adequate cooling medium may not be available.

The upper temperature limit is fixed by the nuclear reactor. Depending on the choice of reactor type, it may assume a wide range of values. Because increased maximum temperature, and hence increased heat engine temperature ratio**, leads to the conversion of a greater proportion of the heat energy produced in the reactor to useful work, there exists a large scale effort to increase the maximum available temperature for the existing reactor types, and to investigate those apparently capable of higher temperatures. For this reason it is necessary to examine the various heat engine alternatives and to outline, from the viewpoint of thermodynamic efficiency, those most suitable for various ranges of temperature. With this information in hand, it becomes possible to intelligently consider the other factors involved in the selection of a suitable arrangement for a given application.

1.2 General Discussion of Thermodynamic Factors

As is well known from the Second Law of Thermodynamics, the greatest thermal efficiency which is possible for a heat engine cycle operating between prescribed temperature limits is that of the Carnot cycle (Figure 1a), where heat is received and rejected at constant temperatures, equal respectively to the prescribed upper and lower cycle temperature limits, and where expansion and compression are accomplished isentropically. This maximum efficiency may be expressed as

---

* The general relations are well illustrated in Reference 11.

** It should be emphasized that this efficiency increase is generally a function of temperature ratio and not simply of additional temperature. Thus the possible efficiency increase for a fixed temperature increase becomes less for higher temperatures.

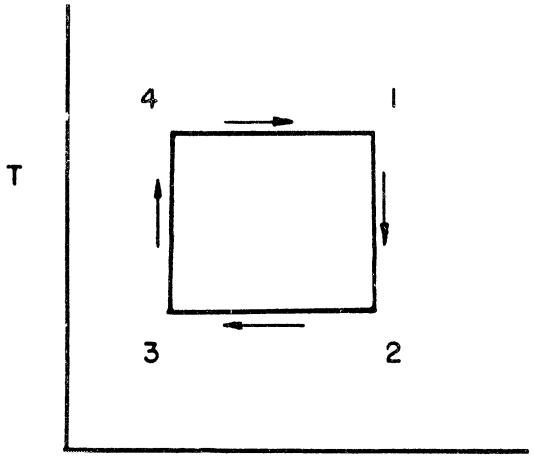

(a.) CARNOT CYCLE

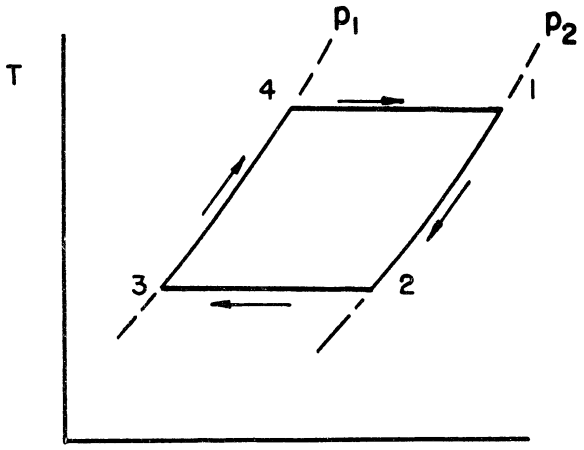

(b.) ERICCSON CYCLE

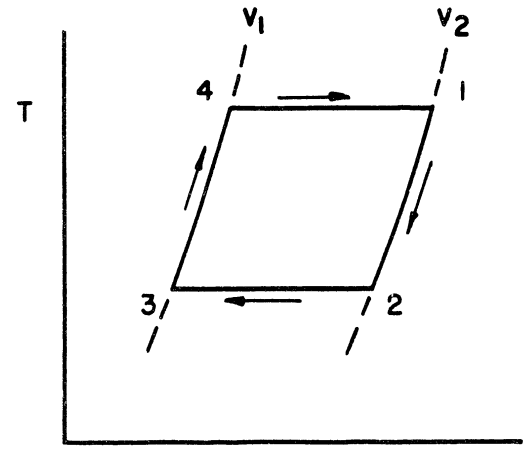

(c.) STIRLING CYCLE

FIG. 1 TEMPERATURE – ENTROPY DIAGRAMS OF VARIOUS CYCLES

$$\eta_{th} = \frac{T_{in} - T_{out}}{T_{in}}$$

Where T refers to the absolute temperature scale.

The Ericsson and Stirling cycles (Figures 1b and 1c) are also theoretically capable of attaining the maximum possible thermal efficiency between prescribed temperature limits. In the first case the isentropics of the Carnot cycle are replaced by constant pressure, and in the second case by constant volume processes. In both cases heat is received and rejected along constant temperature lines as in the Carnot cycle. Here it is necessary to postulate a regenerator so that heat rejected along 1-2 may be reabsorbed along 3-4. Thus it is implied that the working fluid be such that the specific heat is not a function of temperature or pressure. (An example of such a fluid is, of course, a perfect gas.)

Although it is not possible to duplicate these ideal processes with actual machinery, they may be approached. In general, the degree by which the ideal overall efficiency is approximated is controlled by the

1) approach to constant temperature heat admission and rejection from the cycle at the maximum and minimum temperatures available respectively; and by the

2) degree by which irreversibilities can be eliminated from the cycle.

With these basic considerations in mind, one can examine the feasible real cycles and postulate certain general statements as to their attainable efficiencies.

1.2.1 Gas Turbine Cycle

To attain theoretically the ideal Carnot efficiency with the gas turbine type cycle, there are two alternatives. If the "simple" cycle is considered (Figure 2a), consisting of heat source, expander, heat sink*, and compressor, the ideal efficiency can be attained only by infinite pressure ratio. In this case, the heat addition and rejection may be at relatively constant temperature compared to the overall temperature spread (Figure 2b). This alternative is often used for aircraft type powerplants where space and weight are of great importance, and large heat exchangers prohibitive.

On the other hand, ideal efficiency may be attained with the regenerative type cycle with an infinite number of reheat and expansion stages. This cycle is illustrated in Figure 3b, where the arrangement

* In an "open" cycle, this component effectively becomes the infinte mixing medium of the atmosphere. Thus thermodynamically there is no difference between open and closed gas turbine cycles.

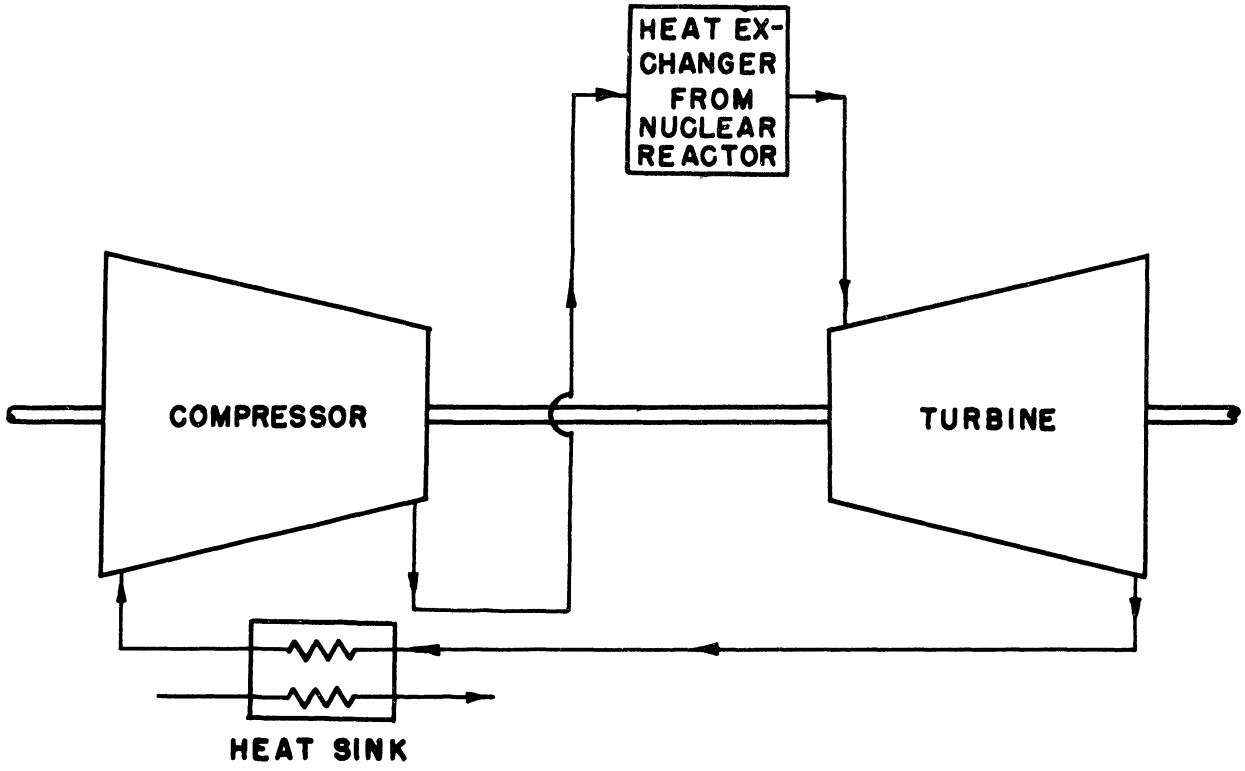

(a.) FLOW DIAGRAM

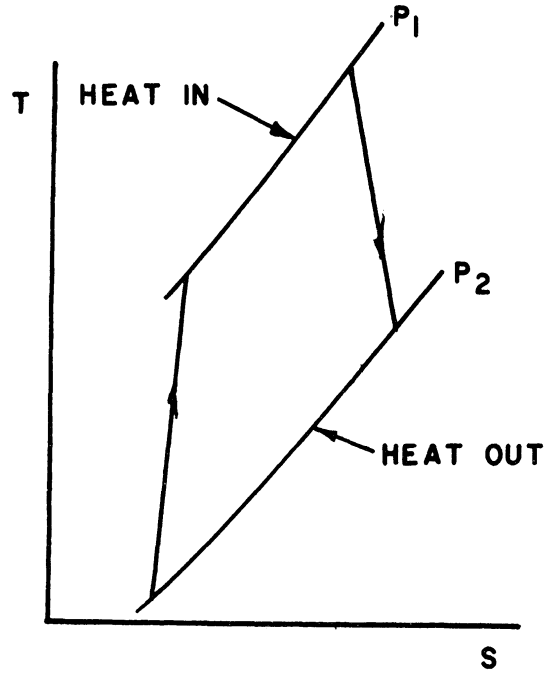

(b.) TEMPERATURE – ENTROPY DIAGRAM WITH A HIGH PRESSURE RATIO

FIG. 2 SIMPLE GAS TURBINE CYCLE

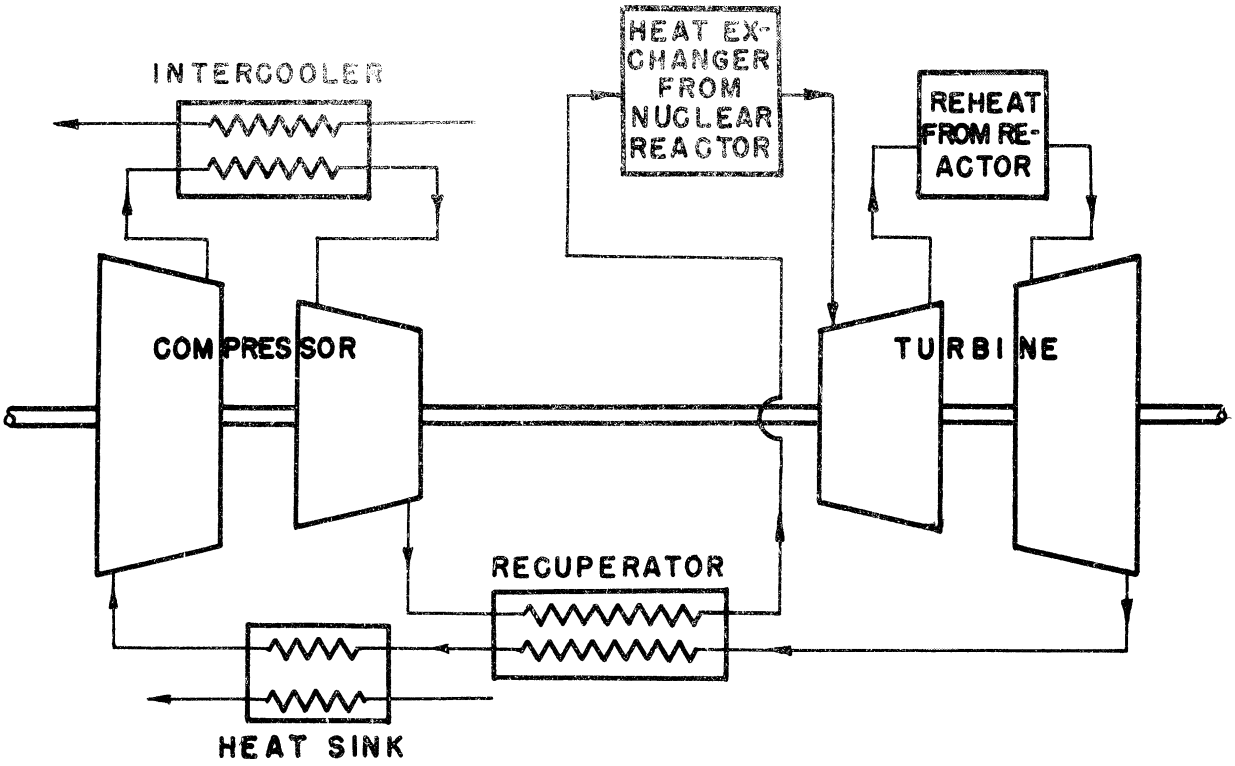

(a.) FLOW DIAGRAM WITH REHEATER AND INTERCOOLER.

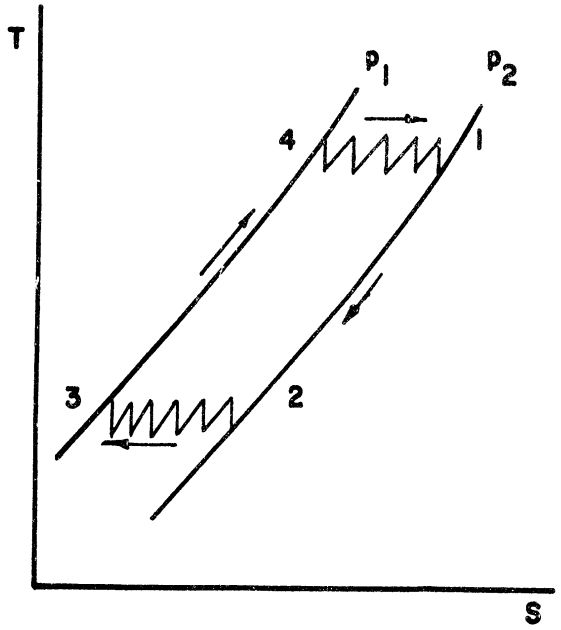

(b.) TEMPERATURE-ENTROPY DIAGRAM WITH LARGE NUMBER OF REHEAT AND INTERCOOLER STAGES.

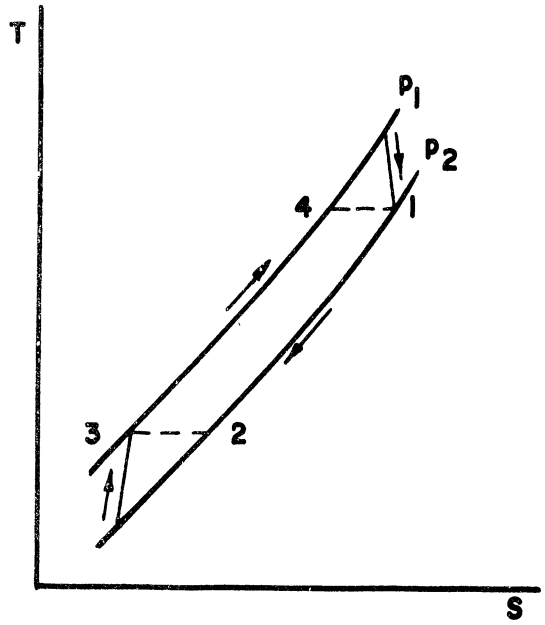

(c.) TEMPERATURE-ENTROPY DIAGRAM WITH VERY LOW PRESSURE RATIO

FIG. 3 REGENERATIVE GAS TURBINE CYCLE

closely approaches the previously described Ericsson cycle. The same result would be approached by a regenerative cycle with no reheat or intercooling but with a pressure ratio approaching zero (Figure 3c) since here heat addition and rejection are accomplished at substantially constant pressures (compared to the overall range). Practically, this is not a particularly useful approach because the work output per unit mass of fluid would be very small and the required mass flow rates and machinery sizes excessive.

A combination of these approaches, i.e. a cycle, with perhaps one reheat and one intercooler stage, and with a highly effective regenerator appears desirable either for

1) an elevated-pressure closed cycle large output plant (pressure ratio small so that all components can be at reasonably high pressure to reduce machinery and heat exchanger sizes), or

2) small output plants where the reduced flow rates do not allow sufficiently high turbomachinery efficiencies to profit fully from a high pressure ratio cycle, and the large flow rate per output is not embarassing.

1.2.2 Steam Cycle

The ordinary saturated steam cycle (Figure 4a) approaches the Carnot cycle in so far as the main portion of the heat is added along the constant temperature boiling line (and the expansion and compression are isentropic). If extraction feed water heating is employed, the approach is closer, since, in the limiting case, all net heat to the cycle is supplied along the constant temperature boiling line, and all net heat rejected in the constant temperature condensing process.

Thus, in many cases, surprisingly high efficiencies are obtained with a very limited maximum temperature with this type of cycle (Army Package Reactor reports an overall thermal efficiency of 19.3% with 407 F peak temperature. Reference 1). It has found general acceptance with the initial types of nuclear power reactors where only moderate temperatures were possible because of the types of reactors employed.

Actually, of course, the turbine efficiency is severely penalized by the necessity for handling a mixture of steam and water droplets (involving, as well as destructive erosion, the inefficient momentum transfer between the slow moving droplets and the steam). It has been found desirable in past experience with fossil-fueled plants to utilize superheater-cycles (Figure 4b) so that the expansion may be entirely

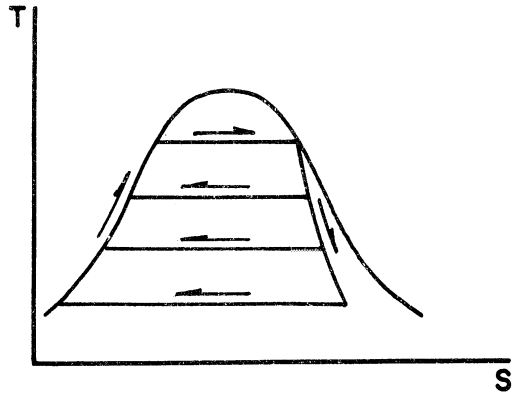

(a) SATURATED STEAM CYCLE

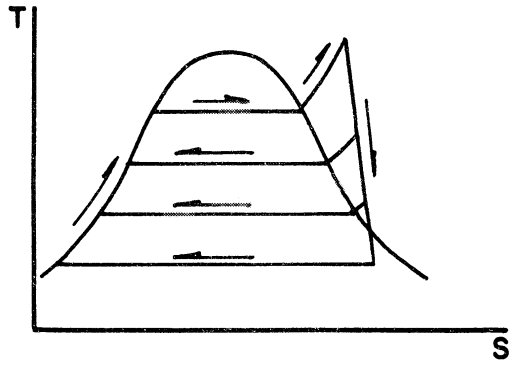

(b) SUPERHEATED STEAM CYCLE

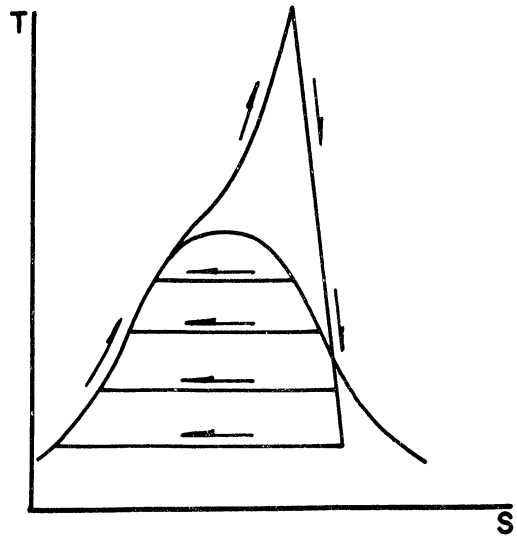

(c) SUPERCRITICAL STEAM CYCLE

FIG. 4. TEMPERATURE-ENTROPY DIAGRAMS FOR VARIOUS STEAM CYCLES WITH EXTRACTION

with dry steam. This affords an arrangement whereby the temperature level of the cycle can be raised without increasing the pressure level. Thermodynamically it does not take the maximum advantage of a given available temperature. However, for a given pressure level, it is superior in efficiency to the saturated cycle because of the increased temperature ratio, and also the increased turbine efficiency which can be attained. The pressure level, with a steam cycle, has perhaps more influence on the machinery cost and feasibility than the temperature. Therefore, a superheater is an economic advantage.

If the water is to be vaporized in the saturated region, the maximum boiling temperature and pressure must necessarily be less than the critical temperature and pressure (705 F and 3206 psia). Since the boiling temperature is so limited, the desirable superheat (or combination of reheat and superheat) temperature is also limited. In other words, if the superheat temperature, for a cycle of a given pressure level is raised beyond a certain point, the result is rejection of heat from superheated steam at a temperature in excess of the condensing temperature. From the viewpoint of efficiency, this is not desirable.

It is as a result of these conditions, that supercritical cycles (Figure 4c) have been considered and utilized (reference 2) since advancing metallurgy has allowed the use of higher and higher maximum temperatures and pressures. With the supercritical arrangement it is possible to utilize effectively, from the thermodynamic viewpoint, whatever maximum temperature may be metallurgically feasible. However, higher temperatures necessitate higher pressures, reaching the range of 5,000-10,000 psig (reference 2). This may become economically and mechanically inconvenient. Also, from the viewpoint of the ideal cycle, the heat is not added substantially at the maximum temperature, since no constant temperature addition is possible. Of course, the situation is improved considerably by extraction feed water heating.

1.2.3 Binary Vapor Cycles

The necessity for very high steam pressures as more elevated temperatures become feasible, makes apparent the advantage of a fluid in which high temperature is not accompanied by high vapor pressure. Such a fluid can be expanded through a turbine and condensed at a temperature at which its vapor pressure (and density) reaches a minimum for feasible turbomachine operation, but which is convenient for the addition of heat to a moderate pressure and temperature steam cycle.

These considerations led to the installation of several mercury-steam binary cycle central station plants in this country in the years prior to World War II. The maximum temperature employed was only 958 F, but the thermal efficiency (boiler losses excluded) was 44%, accomplished

with a maximum pressure of only 365 psig (reference 3). This temperature is too low for an advantageous recourse to a supercritical cycle.

Aside from the advantage of reduced pressure over the corresponding steam cycle, there is the further advantage of increased efficiency over the same limits of available temperature. This can be explained theoretically on the basis that heat addition to the binary cycle (with several extraction points) is substantially at a constant temperature equal to the maximum cycle temperature, since the mercury is used in a saturated cycle. On the other hand, in the superheated steam cycle with which the binary cycle must be compared (since a saturated steam cycle at 1000 F is not possible) the heat is added at a mean temperature substantially less than the maximum available (i.e. at a temperature corresponding to the boiling temperature at the existing pressure, say 550 F in this case).

2.0 SPECIFIC CYCLE ARRANGEMENTS

2.1 Gas Turbine Cycle

As previously indicated there are two possible approaches to the attainment of high efficiency in a gas turbine cycle. These are:

1) The utilization of very high pressure ratio and the consequent elimination of bulky heat transfer equipment such as a regenerator, and

2) The utilization of heat exchange equipment of maximum effectiveness including a regenerator, compressor intercoolers, and reheat stages.* This automatically leads to the selection of a moderate pressure ratio since the maximum efficiency occurs at such a value (see Figure 6a of Part II for example).

It can be shown that, with attainable component efficiencies, a higher cycle efficiency is feasible with the second arrangement, i.e. low pressure ratio and maximum utilization of heat exchangers. The interrelations of these efficiencies, the degree of their attainability, and the various alternative arrangements with various working fluids, are examined in detail in Part II of this report. For the present purpose, a cycle including a regenerator, a single intercooler, and a single reheat stage has been selected to give approximately the maximum gas turbine cycle efficiency, which may practically be obtained, as a function of temperature. This is not to say that such an efficiency represents an optimum economic design in all cases - only that if generous weight, space and financial allowance may be made for each component, this overall efficiency is obtainable for the imposed temperature limitations. For the purposes of the report, these temperature limitations are largely a function of reactor design and ambient environmental conditions.

The derivation for the thermal efficiency relation which was used for this cycle is shown in Part II (Section 8.1) and the assumed values of component efficiencies (Table III, Part II). Although these values are actually functions of the power level, pressure level, working fluid, temperature, etc. (these interrelations are examined in Part II), the values selected for this computation are believed to be fairly realistic assumptions. To

---

* Heat source and sink, necessary to all heat engine cycles, are not included in this discussion since from the viewpoint of the cycle they do not allow any freedom of choice. As a piece of physical equipment, the heat sink exists in the closed cycle gas turbine, but, of course, not in the open.

estimate the optimum efficiency for the given temperature level, curves were plotted of efficiency against pressure ratio (Figure 5). The values shown for the gas turbine cycle of Figure 11 represents the optimums.

A cycle utilizing a reciprocating compressor and/or expander for the purposes of this report is also considered to be a gas turbine cycle. Such a design might find application for low output power, in cases where the higher component efficiencies for low flow rates of the reciprocating machinery would be advantageous, and where the space-weight penalty not important. A very real thermodynamic advantage of an internal combustion engine is that high fluid temperatures are possible because of the intermittent nature of the process. This situation cannot be realized in a cycle which depends on steady-state heating as in a nuclear reactor. However, the possibilities of an intermittent critical reactor in a reciprocating device have been considered by the Baldwin Locomotive Company and others.

2.2 Steam Cycle

The steam cycle efficiencies plotted in Figure 11 for the various temperatures are based on existing commercial plants as reported in the literature. For the low temperature ranges, they involve simple saturated cycles (references 1 and 3). As the maximum temperature is increased, superheat, reheat, and extraction cycles are utilized where desirable (reference 3). For the very high temperature ranges, supercritical plants were considered, including both design studies and projected plants (references 2, 3, and 4). The detailed assumptions and sources for this data are shown in the Appendix (Section 7.1).

As is well known, the applicability and the attainable efficiency of high temperature and pressure steam cycles depends very strongly on the power range. For example, it is shown in reference 4 that for a given inlet temperature the pressure for optimum heat rate increases with plant output. Also the desirability of very high temperatures and pressures exists only in fairly large plants, because of the small volume flow rates to the turbine. On the other hand, if only moderate temperature is available, the saturated steam cycle may well be the most suitable choice down to quite low power ranges (reference 1 - considers a plant of 2500 hp output). However, in general, for fairly standard temperature and pressure conditions, it appears that the steam cycle is most suitable for power outputs in excess of 10,000 hp.

2.3 Binary Vapor Cycles

2.3.1 General Factors

As previously mentioned the required pressure for an efficient high temperature steam cycle becomes extremely excessive. This is of particular importance in the relatively low power ranges where the steam

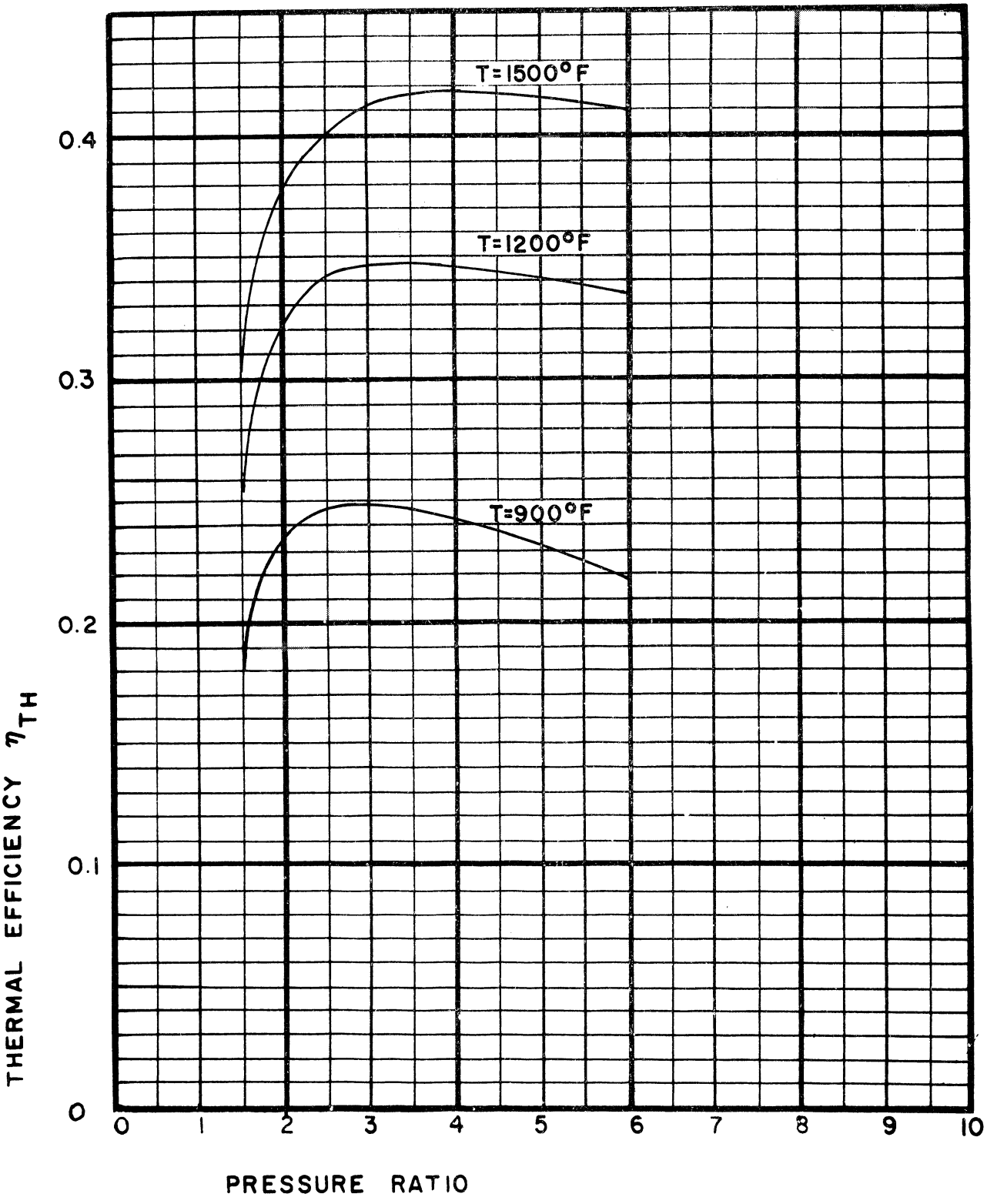

FIG. 5. THERMAL EFFICIENCY OF A REGENERATIVE AIR CYCLE WITH REHEATER & INTERCOOLER "BASIC"* CYCLE WITH REHEAT

*SEE TABLE 3, PART II

volume flow rate is not sufficient to allow an efficient turbine design. Hence, the desirability of utilizing a fluid for which the vapor pressure at a given elevated temperature is still moderate, is apparent. For these reasons, several mercury-vapor and steam binary cycle central station plants were constructed in this country and performed at extremely high thermal efficiency (reference 3) at temperatures, high at that time (about 950 F) but today relatively moderate.

The efficiency of the mercury-steam cycle in the 950 F temperature range is considerably in excess of that of either the steam cycle or the gas turbine cycle for the same temperature. Hence, it appears desirable to consider seriously cycles of this type for higher temperatures, which may eventually become available through advancing reactor technology. As was mentioned before, (Section 1.2.3) there is good theoretical justification for the expectation of extremely favorable efficiencies in the very high temperature range.

2.3.2 Working Fluids: Machinery and Nuclear Factors

In spite of its high efficiency, the mercury-steam cycle has not enjoyed very extensive application apparently because of the mechanical difficulties of sealing, pumping, etc. However, there have been very great efforts expended in the last few years toward the development of liquid metal pumps and seals in connection with the nuclear effort. It is believed that a great many of the mechanical difficulties which existed at the time of the original designs have been overcome.

Although the past operating experience with the binary vapor cycle has been restricted to the mercury and water combination, there are other possibilities for the high temperature fluid which may be more suitable in some applications. For example, sodium or sodium-potassium alloy may be considered. Sodium has a much lower vapor pressure at a given temperature than mercury, and would become applicable for maximum temperatures of at least the order of 1500 F. In this temperature range the vapor pressure of mercury becomes quite excessive.

The principle difficulty with sodium lies in its extremely low vapor pressure at temperatures suitable for transfer of the heat to the water cycle. However, it turns out that the low pressure turbine blading to handle sodium vapor at 1000 F is of the same order as steam turbine blading operating to $\frac{1}{2}$" Hg condenser pressure (Appendix, Section 7.2). Since the sonic velocity of the sodium vapor would lie between that of steam and air, no difficulty should accrue to the turbine design on this account. The general practicability of liquid metal vapor turbines has been demonstrated over the years by the performance of the steam-mercury plants.

The question of low vapor pressure at high temperature raises the possibility of a trinary cycle wherein the sodium portion would serve as a topping cycle to a mercury binary arrangement. Such a cycle is shown on the T-S diagram of Figure 6. Another possibility which would lead to a somewhat reduced efficiency would be the use of a sodium-steam binary cycle (Figure 7) in which the sodium plant exchanged heat with a superheated steam cycle operating to about 1200 F. This involves a considerable irreversibility in the heat transfer since a large portion of the heat to the steam cycle would be delivered across a large temperature differential. Another possible combination is a sodium topping cycle discharging its heat to a gas turbine. This is shown in the T-S diagram of Figure 8.

As a compromise between the low vapor pressure of sodium and the high vapor pressure of mercury, there are the possibilities of sodium-potassium alloy* or pure potassium. There are possibilities of other metals also for which exploratory calculations have been conducted by other agencies. However, since detailed thermodynamic data were available only for sodium and mercury, the preliminary calculations reported herein consider only these two fluids. The vapor pressures for various fluids at several temperatures are listed in Table I along with the applicable references.

Sodium as a direct reactor coolant in some such device as a sodium-boiler reactor is conceivable. Because of the high intensity gamma radiation from sodium, the sodium portion of the machinery would require extensive shielding. Since the pressure rises in the sodium are small, it appears that either electromagnetic pumping equipment or jet ejectors would be completely suitable, allowing a hermetically sealed system except for the turbine. The ejectors have the advantage of serving also as direct mixing heat exchangers and thus eliminating the necessity of closed type heaters.

A cycle of this type could transfer its heat to either a conventional water system or to a gas turbine system. In either case, the efficiency is quite high. Since the density of the sodium working fluid is low, the system might be quite adaptable to relatively small size units. Calculations have been performed for the sodium-mercury-steam cycle, for the sodium-steam cycle, and for the sodium-gas-turbine cycle. These are shown on T-S diagrams in Figures 6, 7 and 8 respectively. The results of all the binary and trinary cycles are tabulated in Table II where, for purposes of comparison, the best steam and gas turbine cycles are also shown.

---

* In this case the concentrations in the gas phase would depend on the partial pressures existing at the temperature, and would not be a choice of the designer.

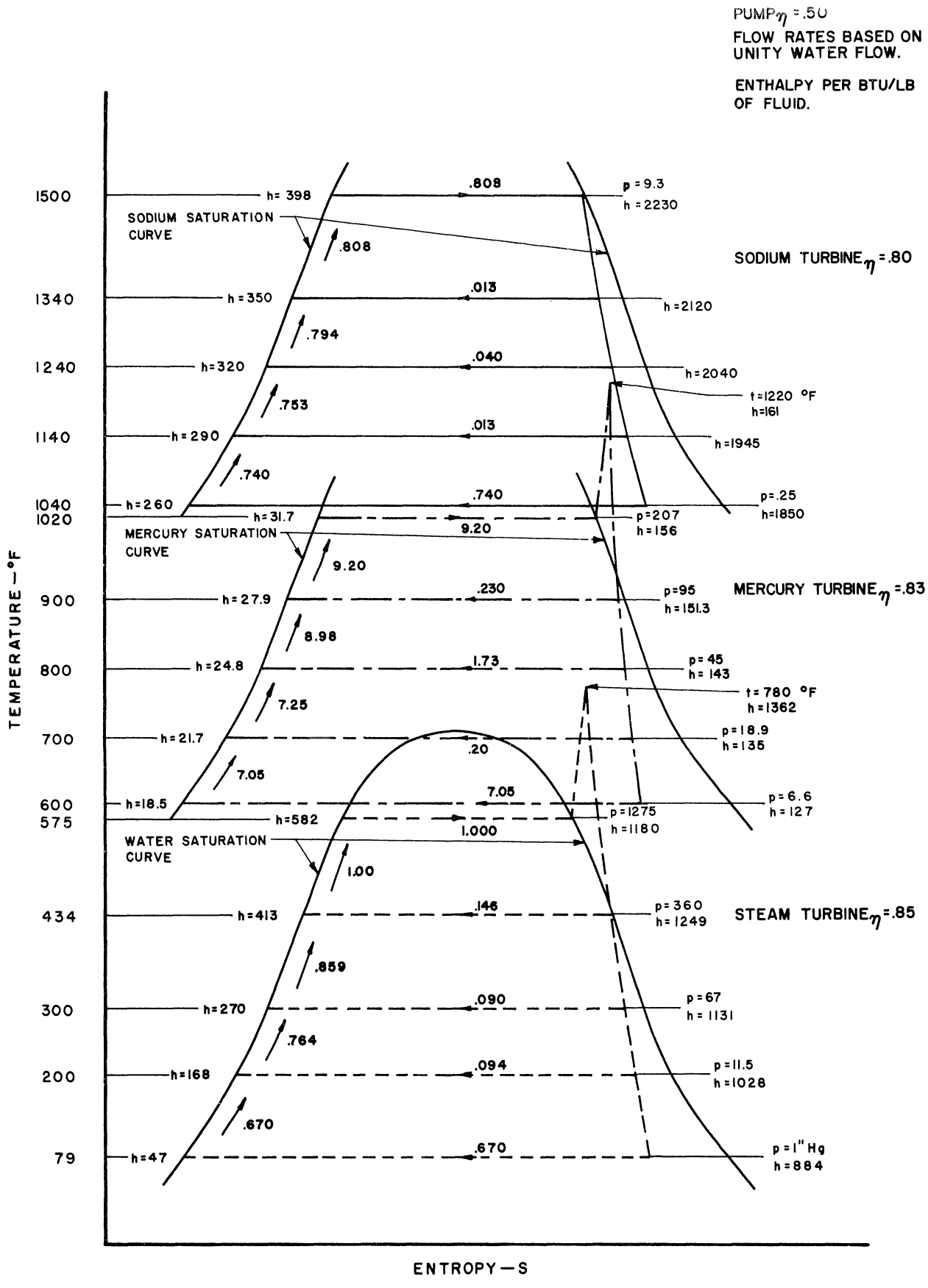

OVERALL EFFICIENCY = .600

FIG. 6a SODIUM-MERCURY-STEAM EXTRACTION TRINARY CYCLE I
TEMPERATURE-ENTROPY DIAGRAM

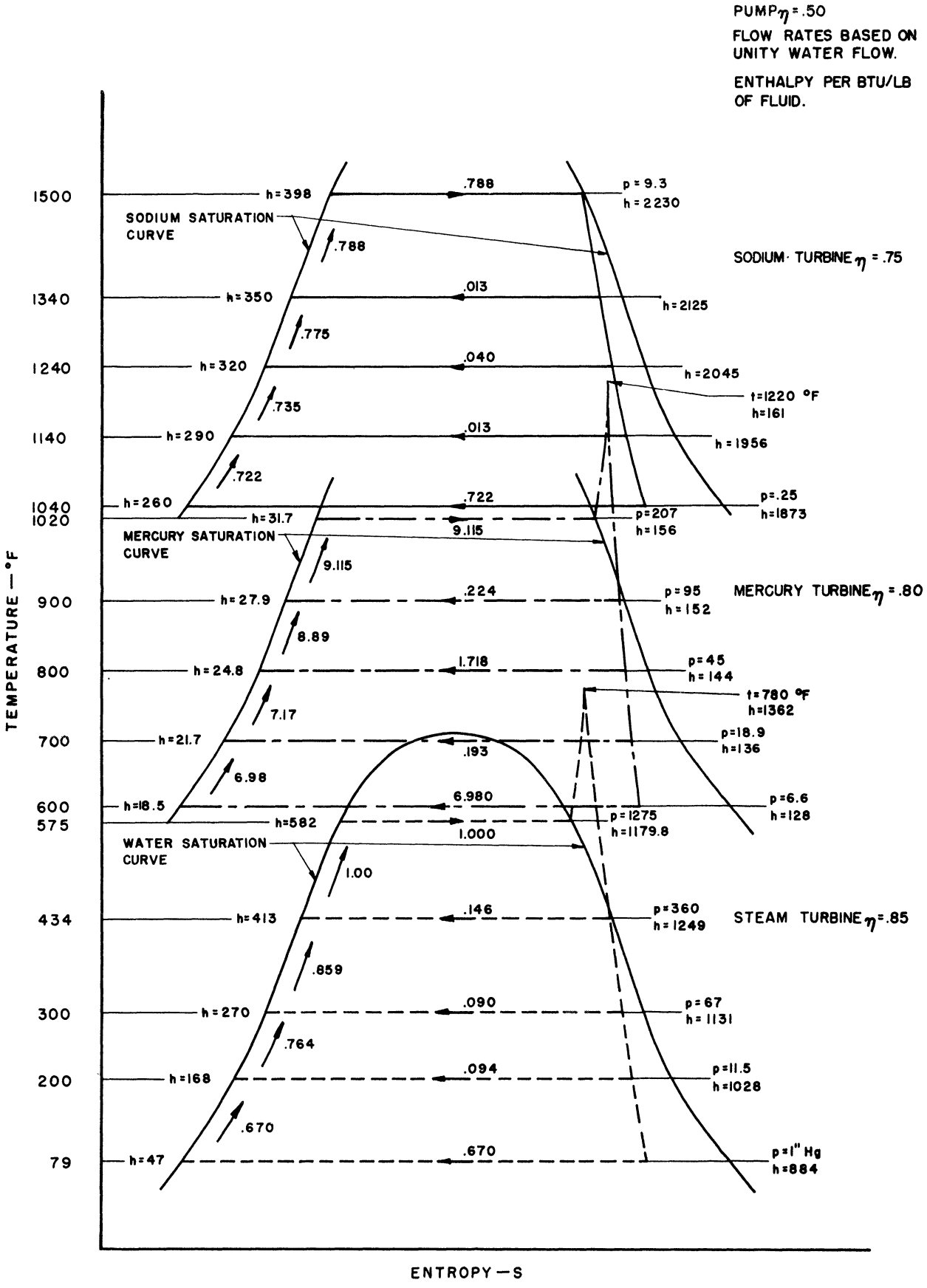

OVERALL EFFICIENCY = .588

FIG. 6b SODIUM–MERCURY–STEAM EXTRACTION TRINARY CYCLE II
TEMPERATURE–ENTROPY DIAGRAM

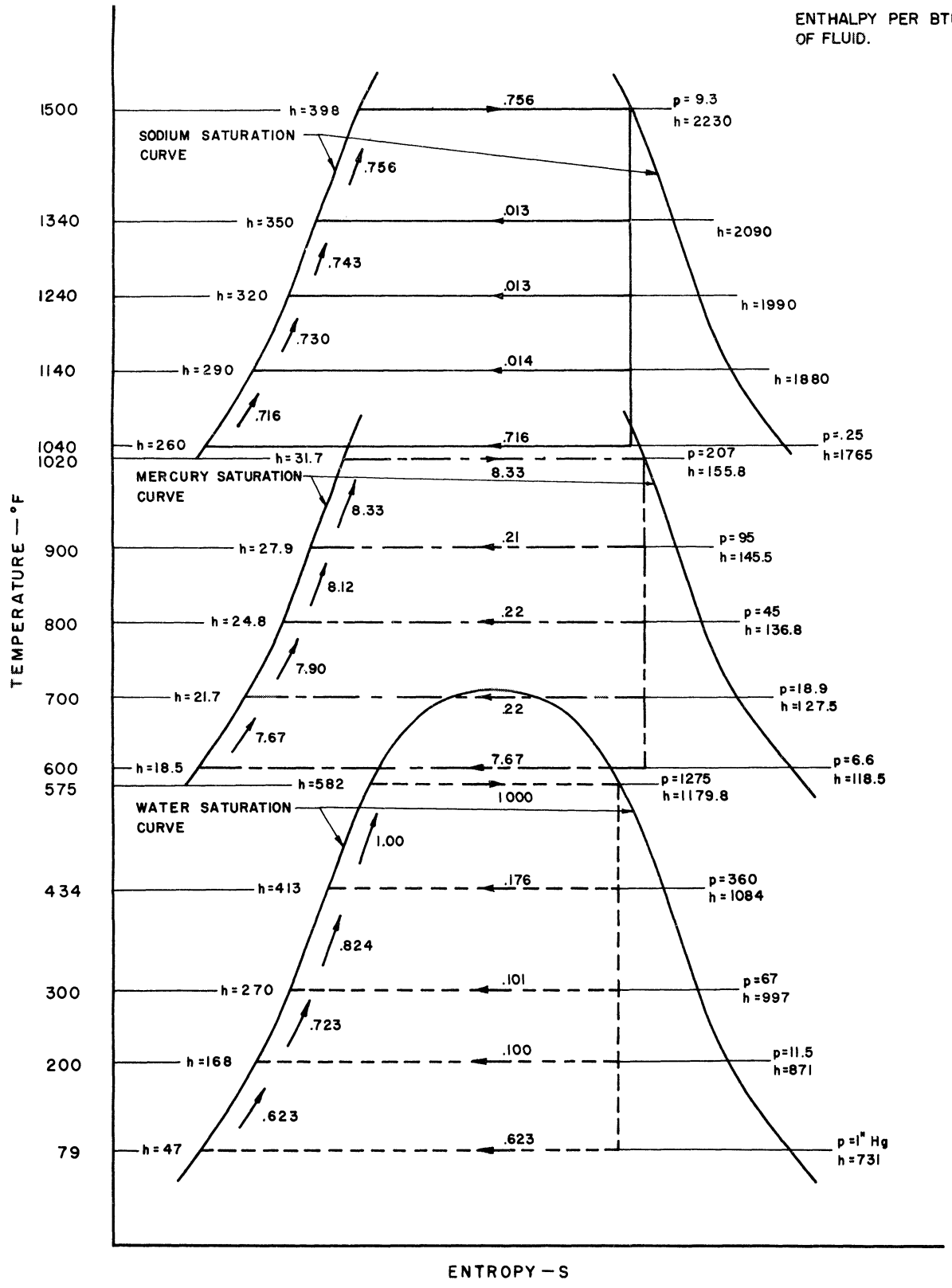

OVERALL EFFICIENCY = .671

FIG. 6c SODIUM-MERCURY-STEAM IDEAL EXTRACTION TRINARY CYCLE TEMPERATURE—ENTROPY DIAGRAM

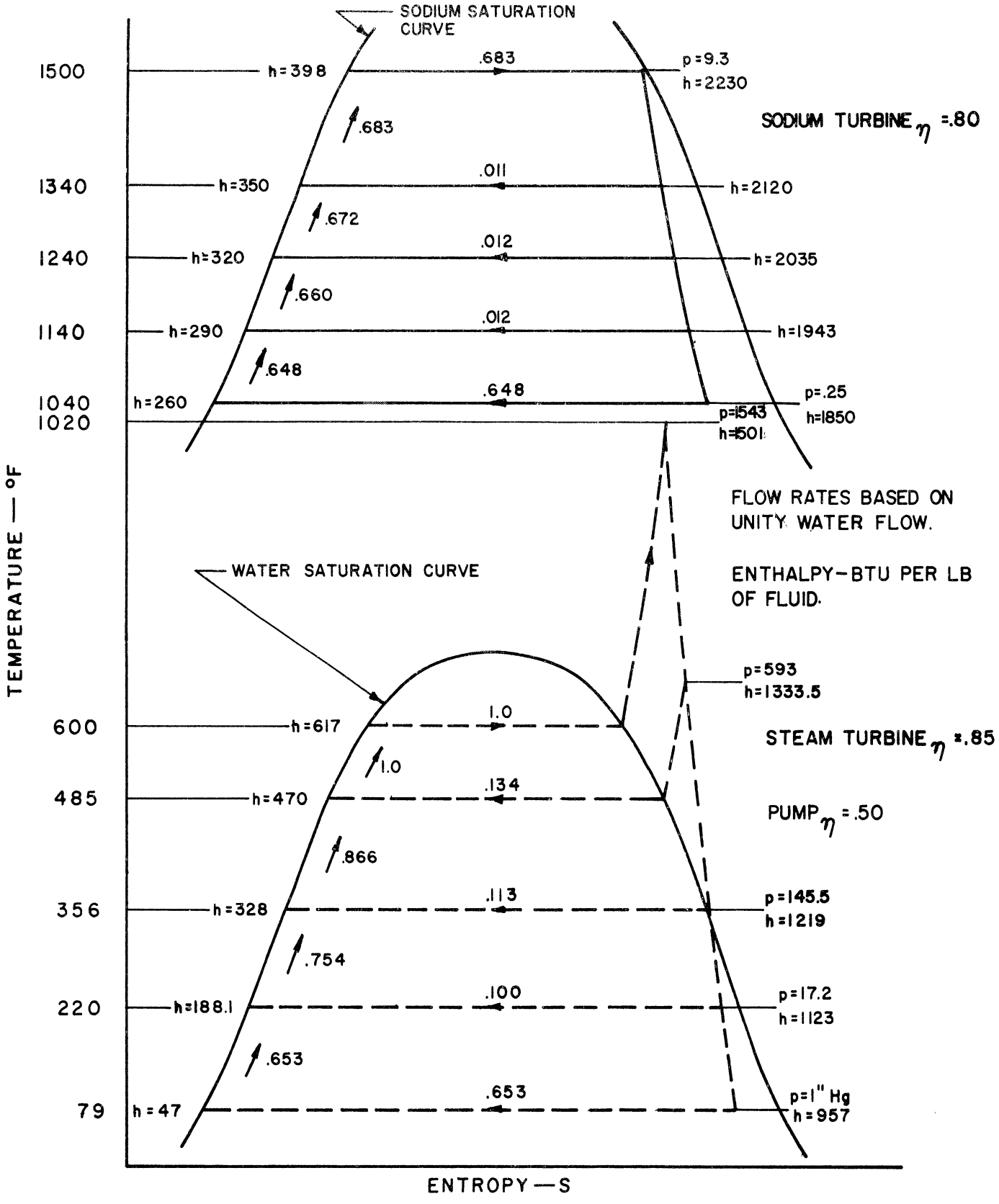

OVERALL EFFICIENCY = .516

FIG. 7 SODIUM — STEAM BINARY EXTRACTION CYCLE
TEMPERATURE-ENTROPY DIAGRAM

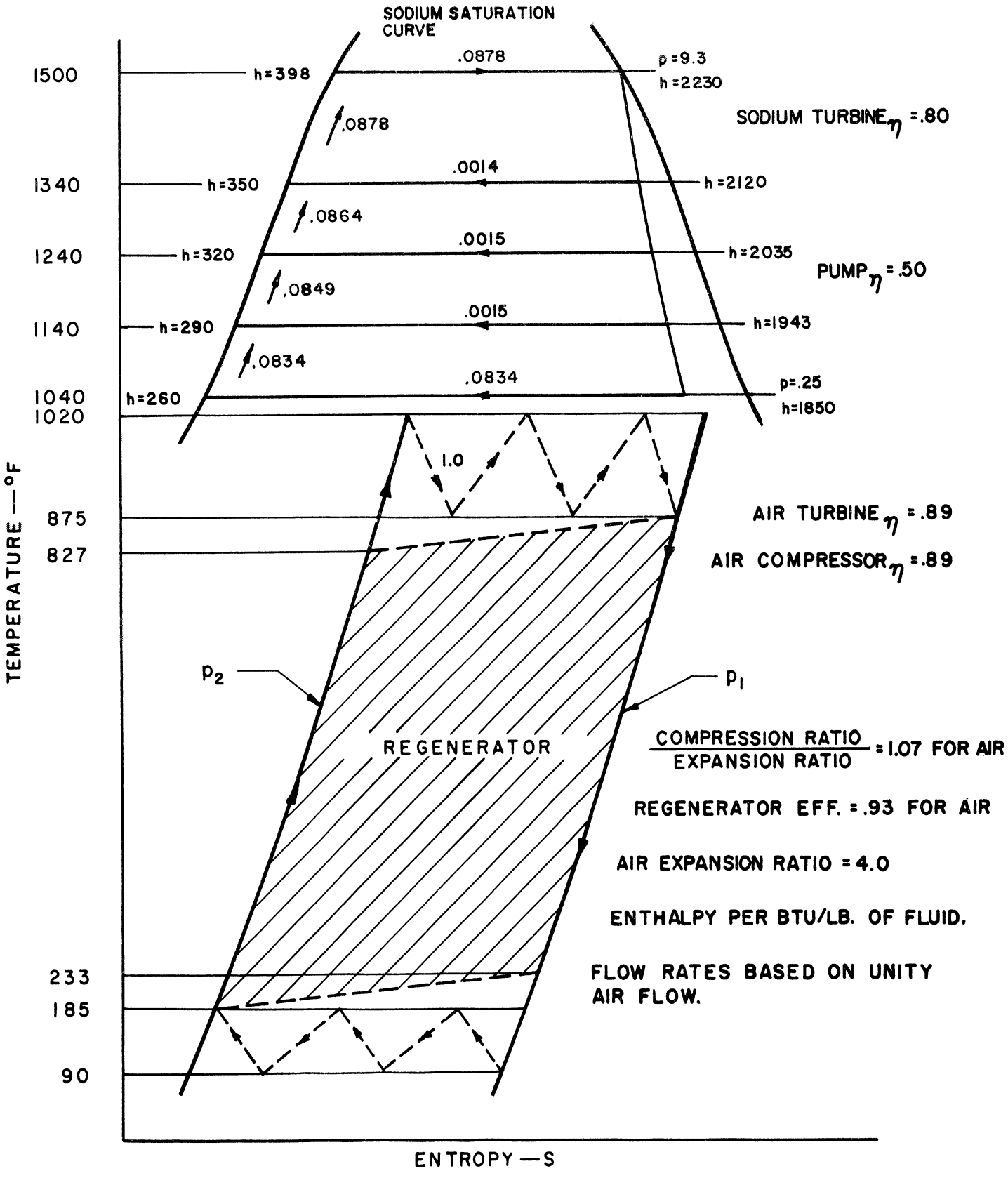

OVERALL EFFICIENCY = .486

FIG. 8 SODIUM–AIR BINARY EXTRACTION–REHEAT CYCLE TEMPERATURE–ENTROPY DIAGRAM

TABLE I. VAPOR PRESSURES FOR VARIOUS FLUIDS AT SEVERAL TEMPERATURES

Fluid	Temperature °F	Vapor Pressure psia	Reference
Mercury	600	6.64	5
	900	95.4	
	1200	509.5	
	1500	2000	
Sodium	600	.01	6
	900	.1	
	1200	1.0	
	1500	9.0	
	1620	14.7	
Potassium	1400	14.7	7
Rubidium	1270	14.7	

Mercury, due to its high neutron capture cross-section, is not in general a desirable reactor moderator or coolant. However, it can be used as coolant for a fast reactor (Los Alamos Clementine) where high capture cross-sections are not so disadvantageous. Potassium, and perhaps other suitable fluids which may be determined, could be used with varying degrees of success directly in a reactor. The mercury cycles which were calculated are shown in the T-S diagrams of Figures 9 and 10.

2.3.3 Thermodynamic Calculations

In order to achieve optimum efficiency with cycles of these types, it is necessary that irreversibilities in the heat transfer be eliminated as far as possible. This has been approached by including three extraction "feed water" heaters for both the liquid metal and the steam portions. To take maximum advantage of the obtainable efficiency with steam turbines operating with dry steam, the lowest liquid metal extraction is used to superheat the steam. An efficiency of 0.85, including reheat factor, was used. This was based on current figures for large plant steam turbine efficiency. A liquid metal vapor turbine efficiency of 0.80, including reheat factor, was used. This reduced value is assumed because of the unknown performance, and operation in the saturated region. In the case of the sodium-mercury-steam cycle a mercury turbine efficiency of 0.83 was used because of the superheat afforded by a sodium extraction.

Several cycle arrangements with the mercury steam cycle were

TABLE II. TABULATED EFFICIENCIES OF BINARY AND TRINARY VAPOR CYCLES AT 1500 F INLET, 70 F COOLING WATER (1" Hg cond.)

Cycle Description	T-S Diagram	Efficiency
1) Mercury-Steam, Extraction Mercury Turbine Eff. - .80 Steam Turbine Eff. - .85 Steam Superheated	Fig. 9	.588
2) Mercury-Steam, Non-Extraction Mercury Turbine Eff. - .80 Steam Turbine Eff. - .85 Steam Superheated	Fig. 10	.550
3) Sodium-Mercury-Steam, Extraction Sodium Turbine Eff. - .75 Mercury Turbine Eff. - .80 Steam Turbine Eff. - .85 Mercury and Steam Superheated	Fig. 6	.588
4) Sodium-Mercury-Steam, Extraction Sodium Turbine Eff. - .80 Mercury Turbine Eff. - .83 Steam Turbine Eff. - .85 Mercury and Steam Superheated	Fig. 6	.600
5) Sodium-Mercury-Steam, Extraction Sodium Turbine Eff. - 1.00 Mercury Turbine Eff. - 1.00 Steam Turbine Eff. - 1.00 No Superheat	Fig. 6	.671
6) Sodium-Steam, Extraction Sodium Turbine Eff. - .80 Steam Turbine Eff. - .85 Steam Superheated	Fig. 7	.518
7) Sodium-Air, Extraction Sodium Turbine Eff. - .80 Air Turbine Eff. - .89 Air Compressor Eff. - .89 Regenerator Effectiveness - .93 Precooler Terminal Δt - 20 F Compression to Expansion Ratio - 1.07	Fig. 8	.486
8) Supercritical Steam Cycle 7000 psig - 1500 F Reference 4		.485
9) Gas Turbine Cycle - 1500 F Regenerator, Reheat, Intercooler		.448

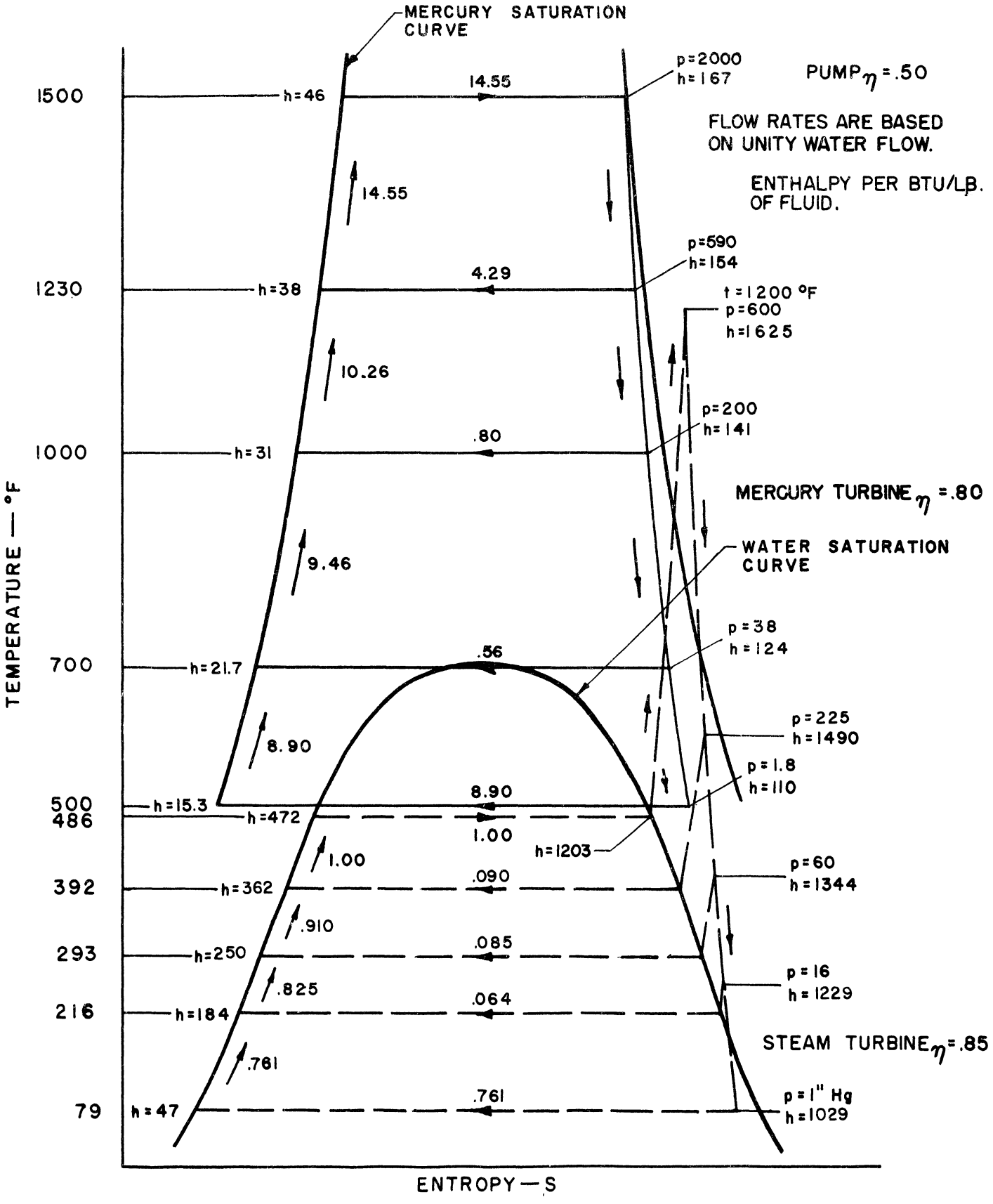

OVERALL EFFICIENCY = .590

FIG. 9 MERCURY–STEAM BINARY EXTRACTION CYCLE
TEMPERATURE–ENTROPY DIAGRAM

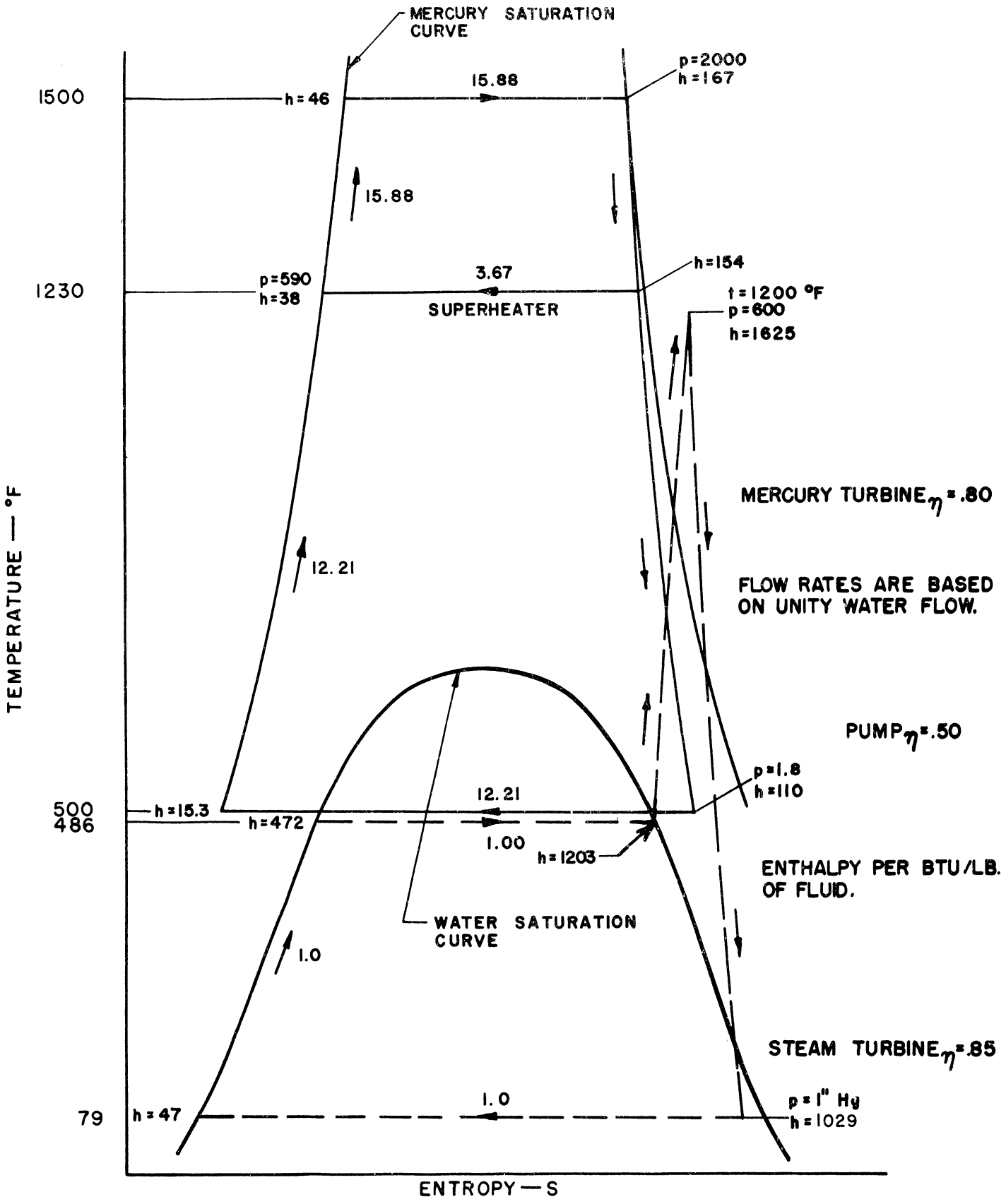

OVERALL EFFICIENCY = .550

FIG. 10 MERCURY-STEAM BINARY NON-EXTRACTION CYCLE TEMPERATURE-ENTROPY DIAGRAM

investigated in the course of the study. However, it was determined that the arrangement shown in Figure 9 is most suitable. Three extraction points for the mercury and also for the steam are assumed, with the lowest mercury extraction used to superheat steam. The calculated thermal efficiency (considering no reactor losses) is 59.0% for 1500 F inlet and 79 F condensate temperature. This can be compared to a similar cycle, which had been calculated without extractions (Figure 10) wherein it was determined that thermal efficiency under the same conditions is 55.0%. Thus, the improvement due to the extraction heaters is 1.07.

Two trinary sodium-mercury-steam cycles were calculated with three extractions in each phase but with slightly differing turbine efficiencies (Figures 6a and 6b; the thermal efficiencies were 60.0% and 58.8%). Using the extraction sodium cycle discussed above, cycles involving

1) sodium topping to steam cycle (Figure 7), and

2) sodium topping to gas turbine cycle (Figure 8)

were calculated. The resulting efficiencies for 1500 F inlet and 70 F cooling water (giving 80 F steam condensate and 90 F air compressor inlet) were .518 and .486 respectively. The latter cycle, when compared with the regenerative gas turbine cycle with reheat and intercooler shows an efficiency improvement of 8.4% (3.8 points). The former is about 2 points better than the corresponding super critical steam cycle and 7 points better than the gas turbine (14%).

To more clearly illustrate the basic relations involved, a simplified trinary cycle involving saturated Na, Hg, and H_2O portions with ideal turbines was calculated. This is shown on the T-S diagram of Figure 6c. The overall cycle efficiency was .694 compared to the Carnot efficiency of .725. However, if the individual portions are compared with the Carnot efficiency for that portion the results are as below:

Fluid	Ratio: Calculated to Carnot Efficiency
Na	1.024
Hg	.985
H_2O	.943

It is noted that the sodium portion shows an efficiency in excess of that of the ideal heat engine. The only possible conclusion is that the degree of refinement of the sodium thermodynamic data as plotted and listed (reference 6) is not adequate (linear extrapolation over large ranges were necessary for this calculation). It is assumed that the ratios of calculated to ideal efficiency for the mercury and steam cycle are probably typical. Therefore the sodium portion efficiency has been reduced by .985/1.024 = .962. On the basis that this correction should be applied to the heat input to the overall cycle, the efficiency becomes .671. This is a very conservative assumption since an equally defensible procedure would be reduction of Na work only by this ratio.

Estimates of the effect of turbine losses were made (method of calculation is shown in Section 7.4.2 of the Appendix). The results are shown in Table III.

It will be noted from Table III that losses in the sodium turbine have very little effect on the overall cycle. Losses in the mercury turbine have slightly more, and losses in the steam turbine are most important. This is explained by the fact that losses in the topping turbines result in additional heat to the lower turbines, and some of the loss is thus recouped. This factor is often used in steam turbine design where inefficient initial stages are employed to drop the pressure and temperature in a minimum number of stages to values which may be more economically handled. Therefore, an inefficient liquid metal turbine is not an important handicap to a cycle of this type.

The approximate results agree very closely with the superheat trinary cycle shown in Figure 6a where turbine efficiencies of 0.80, 0.83, and 0.85 (including reheat) were used for the sodium, mercury, and steam respectively. This cycle showed an overall efficiency of 60.0% as compared with 60.4% for the approximation in Table III. An additional cycle with efficiencies of .75, .80, and .85 was calculated (Figure 6b). The efficiency decreased by only 1.2 points to 58.8%. This confirms the expectation that the efficiency of the liquid metal turbines is not of great importance.

The effect of the irreversible heat transfer across the temperature drop between the various portions of the trinary cycle was estimated (Section 7.5 of Appendix). It is noted that the efficiency is decreased about 1.0 points on this account. The effect of a temperature differential in the extraction heaters also was estimated (Section 7.6 of Appendix). This involves an overall efficiency loss of only 0.4% (0.2 points) and is thus quite negligible (no temperature differential at this point was assumed in the calculations).

In the calculation of the sodium cycles it was assumed that the sodium did not dimerize to form Na_2. However, it is indicated in reference 6 that there is a likelihood of such an effect at high temperatures. It is shown that the number of moles of a given mass quantity of sodium will be decreased by about 15% at 1500 F equilibrium on account of this effect. If this is the case, there will be heat liberated during the expansion in the turbine, so that the process will not approach an isentropic, and the cycle efficiency will be somewhat reduced. This effect will be further investigated as the work progresses.

Sample calculations, analytical procedure, and assumptions for the one of sodium-mercury-steam extraction cycles are included in the Appendix (Section 7.3). The results of all these calculations are tabulated in Table II.

TABLE III. EFFECT OF TURBINE EFFICIENCY ON TRINARY CYCLES

	Cycle Conditions*	η	η_{Carnot}	η_{Corr}
1)	Na Turbine - 1.00 Hg Turbine - 1.00 H_2O Turbine - 1.00	.700	.725	.671
2)	Na Turbine - .80 Hg Turbine - 1.00 H_2O Turbine - 1.00	.679	.725	.652
3)	Na Turbine - .80 Hg Turbine - .83 H_2O Turbine - 1.00	.657	.725	.631
4)	Na Turbine - .80 Hg Turbine - .83 H_2O Turbine - .85	.630	.725	.604
	Trinary Cycle I - Superheat			
5)	Na Turbine - .80 Hg Turbine - .83 H_2O Turbine - .85	.626	.725	.600
	Trinary Cycle II - Superheat			
6)	Na Turbine - .75 Hg Turbine - .80 H_2O Turbine - .85	.613	.725	.588

* All cycles refer to inlet temperature of 1500 F and condensing temperature of 79 F. Cycles 1, 2, 3, and 4 do not employ superheat. The values were estimated as explained in Section 7.4.2 to show the effect of varying turbine efficiency.

3.0 COMPARISON OF VARIOUS CYCLES

The estimated attainable cycle efficiencies are plotted against temperature for the gas turbine cycle, steam cycle, and binary vapor cycle in Figure 11. In all cases, a cooling medium temperature of 70 F has been assumed. On this basis, the steam and binary vapor cycles, considering the good condensing for heat transfer coefficients, condense to 1" of Hg or 79 F, whereas for the gas turbine cycles, a minimum gas temperature of 90 F was assumed.

The efficiency values are based upon an effective "boiler efficiency" of 100%. In other words, no loss comparable to "stack loss" is assessed to the nuclear reactor plant.* This is not to say that 100% of the energy actually released in fission will find its way to the heat engine cycle. Actually, there will be heat losses in and through the shielding, the neutrino loss, and the conventional heat transfer losses in the primary loop, if the reactor is not cooled directly by the working fluid. However, this is a function of the particular design and can be applied to any desired case.

The assumed component efficiencies which enter into the overall cycle efficiency calculations are believed to be attainable in large power output installations where weight and space are not a factor per se. The quoted efficiencies for a given cycle temperature are thus somewhat in excess of the values applying to a transportation device where it may be desirable to compromise efficiency to some extent in exchange for size, weight, and perhaps cost advantages.

It will be noted from the curve of Figure 11 that the attainable efficiency of the gas turbine cycle, for a given temperature, is inferior to that of either the steam or the binary-vapor cycles over the entire temperature range. There is no doubt, however, that for the higher temperatures (1400 F to 1500 F and above) where the proper utilization of the available temperature requires extreme pressures and considerable auxiliary equipment for the steam cycle, that the gas turbine is the more suitable of the two in many applications. An obvious point in case is the aircraft powerplant. Thus, it appears that the developmental effort connected with producing a 1500 F gas turbine plant with an efficiency approaching that shown would be much less than that involved in producing a steam plant for these temperatures and efficiencies, except perhaps in extremely large output ranges.**

---

* It is for this reason that (by a factor of about .85) the values given for the steam and binary vapor cycles are higher than usually noted. This consideration does not affect the open cycle gas turbine since it is an internal combustion device.

** As shown in reference 4, the supercritical steam cycle is limited to fairly large power ranges because of the low volumetric steam flow rate in the high pressure positions. This difficulty does not affect the closed cycle gas turbine or the binary cycles to the same extent.

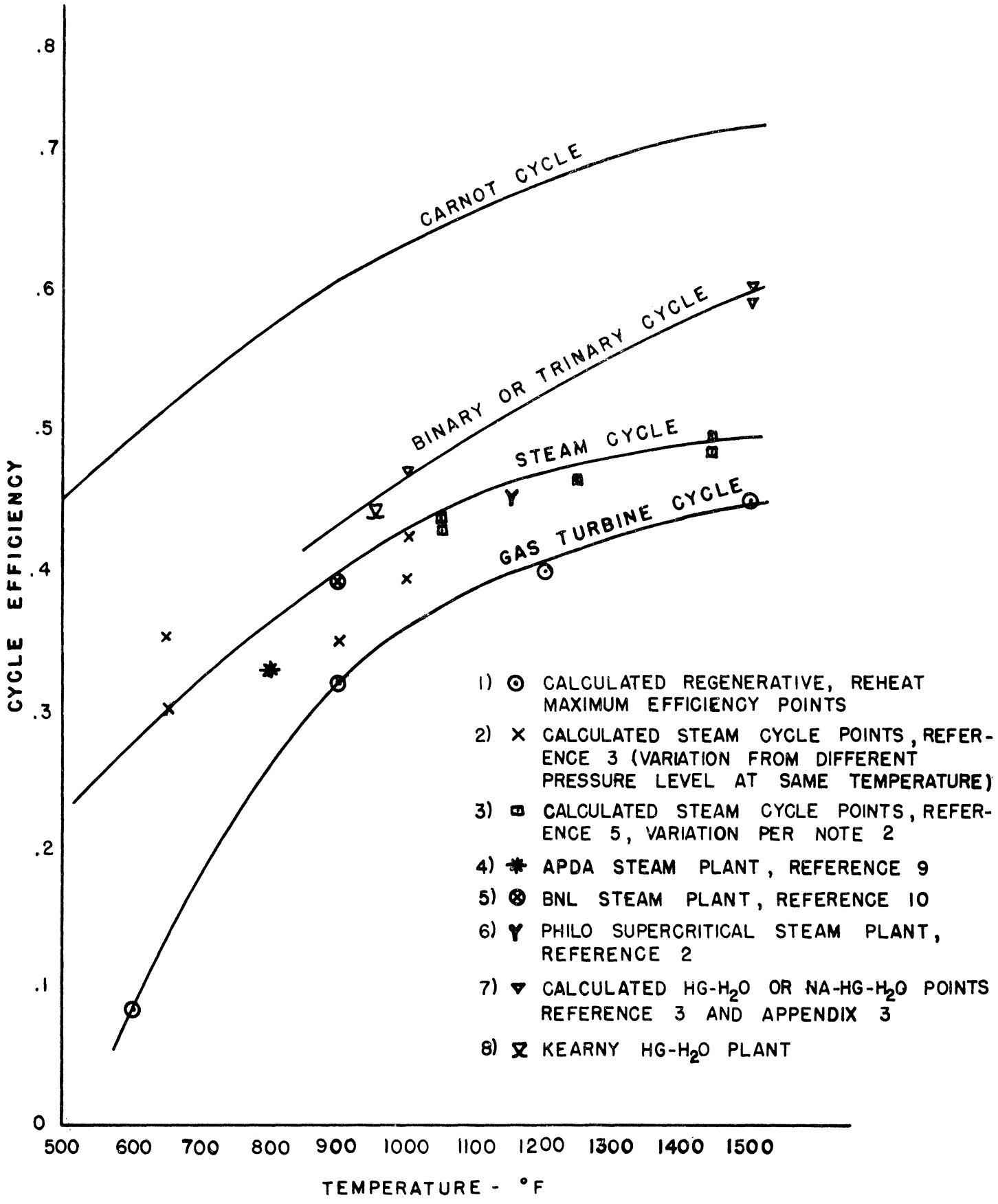

FIG. 11 MAXIMUM FEASIBLE EFFICIENCY VS TEMPERATURE

VARIOUS HEAT ENGINE CYCLES

COOLING WATER AT 70° F

The developmental effort involved in a binary type plant is no doubt large, but its true extent cannot well be estimated without more detailed engineering studies. In its favor, of course, is the absence of high pressure. As shown in the curve of Figure 11, the attainable efficiency from a binary or trinary cycle is considerably in excess of that for either the gas turbine or steam cycle, and follows quite closely to the Carnot efficiency which is plotted as a reference. It is apparent that this will be the case for any temperature if a fluid or fluids with a suitable liquid-vapor phase relation can be found, so that heat addition can be at an approximately constant temperature equal to the maximum temperature available. As higher reactor temperatures become feasible, it appears that the possibilities of cycles of this type must be given serious consideration, especially in view of the possibility of integrating the coolant and heat engine fluids, as in the previously discussed sodium boiler reactor. As previously shown, a sodium topping cycle of this sort may be combined with a low temperature gas turbine cycle to give an overall efficiency in excess of the ordinary gas turbine cycle over the same temperature range.

4.0 FUTURE WORK APPLYING TO PART I

Preliminary work on the basic thermodynamics of the various possible cycle arrangements has been completed, as here reported. Additional efforts, continuing from this basis, becomes desirable. Such work will include the following:

a) Investigation of various possible working fluids from the viewpoint of radioactivity effects; i.e. the degree of machinery shielding, accessibility considerations, etc. which are involved;

b) Further consideration to other possible working fluids in addition to those discussed in this report;

c) Further consideration of the binary type cycles from the viewpoint of evaluating probable developmental difficulties and costs;

d) Consideration of possible combinations other than those already investigated.

Considering the combined possibilities of a direct-boiling liquid metal reactor and the extremely high efficiencies of the binary-vapor cycle, this arrangement seems likely to represent one logical path for future developments.

5.0 CONCLUSIONS

A broad investigation of various conceivable heat engine cycles and working fluid combinations has been conducted. Their attainable thermal efficiencies as a function of temperature have been calculated. The results are plotted in Figure 11, and tabulated for 1500 F in Table II. These overall efficiency values are consistent with component efficiencies which are generally attainable in large scale plants where efficiency is of primary importance. They represent a maximum envelope curve for the given cycle and temperature.

The results show that the binary and/or trinary vapor cycles have an efficiency advantage of about 33% (15 points) over the optimum gas turbine and about 23% (11 points) over the steam cycle for an inlet temperature of 1500 F. The combined sodium-vapor-gas turbine cycle has an advantage of 8.5% over the simple gas turbine at 1500 F (3.8 points). Efficiency-wise the gas turbine is somewhat inferior to the other alternatives at any except extremely high temperatures. The gas turbine cycle efficiencies shown apply roughly to any diatomic gas as working fluid. Monatomic gases show a slightly reduced efficiency for equal component efficiencies.

It is believed that the high temperature highly efficient gas turbine is more easily attainable development-wise, especially in small sizes, than the alternatives presented. In many applications where weight and space are a factor, and capital cost of especial importance, it is no doubt the most suitable selection. However, there appears the strong possibility that a development of a boiling liquid metal reactor combined with a binary-vapor cycle or a vapor-gas-turbine combination cycle might achieve efficiencies and operating economies which are in excess of those attainable by other methods.

6.0 BIBLIOGRAPHY

1. Kasschou, Kenneth, Army Package Power Reactor, Preprint 30, Nuclear Engineering and Science Congress, December, 1955.

2. Fiala, S. N., First Commercial Supercritical Pressure Steam-Electric Generating Unit for Philo Plant, ASME Paper No. 55-A-137.

3. Kent's Mechanical Engineers Handbook, 12th Edition - Power Volume, Section 8, 1950, John Wiley and Sons, New York.

4. Downs J. E., Margins for Improvement of the Steam Cycle, ASME Paper No. 55-SA-76.

5. Sheldon, L. A., Thermodynamic Properties of Mercury Vapor, ASME Paper No. 49-A-30.

6. Inatomi, T. H., and Parrish, W. C., Thermodynamic Diagrams for Sodium, North American Aviation Report SR 62, 13 July 1950.

7. Atomic Energy Commission, Department of Navy, Liquid Metals Handbook, NAVEXOS-P-733 (Rev.), June, 1952.

8. Atomic Power Development Associates, Developmental Fast Breeder Power Reactor (Brochure).

9. Sengstakin, D. J., and Durham, E., The Liquid Metal Fuel Reactor Central-Station Power, Preprint 39, Nuclear Engineering and Science Congress, December, 1955.

10. Keenan, Joseph H. and Keyes, Frederick G., Thermodynamic Properties of Steam, 1936, John Wiley and Sons, New York.

11. Ohlgren, H. A., Weber, E., Hammitt, F. G., Initial Approaches to Systems Analyses of Nuclear Heat-Power Engines, Progress Report No. 5 to Chrysler Corporation, February, 1956.

7.0 APPENDIX - PART I

7.1 Assumptions for Steam Cycle Efficiencies (Figure 11).

7.1.1 Low and Moderate Temperature Steam Plants

Operating data for low and moderate temperature steam plants was abstracted from various portions of the literature. The data utilized and the sources are shown below.

7.1.1.1 Kent's Mechanical Engineers Handbook - Power, J. Kenneth Salisbury, 12th Edition, Reference 3.

Table XXIV, Section 8 (Part II) presents data calculated for various cycles under the following conditions:

1) Overall turbine efficiency 82%

2) Moisture at turbine exhaust (full load) 11%

3) Terminal difference on feedwater heaters of 5 to 20 F for feed temperatures of 100 to 525 F

4) Steam generator efficiency (including air preheater if used) 85%

5) Pressure drop between boiler and turbine, bleed points and heaters, reheater piping and reheater 10%

6) Radiation loss - Bleed point to heater 2%
Reheat lines 3%

7) Normal auxiliary power allowances, with 20 kw-hr/ton as power for pulverizing coal

8) Feed water heated in equal temperature steps to 75-80% saturation

9) Final vacuum 29" Hg

It was assumed that five feed water heaters would be used. It was also assumed that there were no heat losses between the reactor and the working fluid. This is not actually the case. Factors such as reactor shielding losses, heat transfer loop losses, etc. exist. However, they depend on the specific design and are usually not large. Thus, to provide an equal basis for the comparison of the various heat engine cycles it was determined to assume zero losses

of this type. Therefore, the nuclear plant efficiency is determined by dividing the conventional plant efficiency by the steam generator efficiency which is 0.85 for these cases.

Cycle Conditions	Heat Rate Btu/kw-hr	Conventional Plant Eff.	Nuclear Plant Eff.
400 psia, 800 F	12,400	.275	.323
600 psia, 900 F	11,590	.294	.346
1200 psia, 1000 F	10,220	.334	.393
3226 psia, 1000 F	9,550	.358	.422

7.1.1.2 Additional Sources

7.1.1.2.1 Liquid Metal Fuel Reactor steam plant. Reference 9. Calculated data is given for a steam plant designed in connection with an LMFR-type reactor which operates with steam at 1265 psia and 900 F.

Abstracting the heat balance of Figure 6, Reference 9.

$$\text{Heat Input to Cycle} = 1{,}915{,}080\ (1438.3 - 458.5)$$

$$= 1875 \times 10^6$$

$$\text{Work Output} = \frac{209{,}130 \times 3413}{.98} = 729 \times 10^6$$

(.98 is generator efficiency.)

$$\text{Efficiency} = \frac{729}{1875} = .389$$

7.1.1.2.2 Army Package Power Reactor - Reference 1
Cycle conditions call for 407 F, 200 psia, steam conditions. Anticipated overall efficiency is 19.25%.

7.1.1.2.3 Kent's Mechanical Engineering Handbook. Reference 3. Table 17, pp. 8-73.
This table gives the calculated non-extraction ideal turbine heat rates for various conditions. In the use of these points the following assumptions were made:

1) Improvement in heat rate due to five feed water heaters as given in Figure 43, Section 8 (Part II) of Reference 3;

2) Auxiliary losses are 5%;

3) Turbine efficiency is 0.85.

Then for an 800 psig, 650 F cycle:

Efficiency = 3413 x .85 x 1.115 x .95/8757 = .352.

For a 200 psig, 650 F cycle:

Efficiency = 3413 x .85 x 1.09 x .95/10140 = .296

7.1.2 Supercritical Steam Cycles

7.1.2.1 Reference 4 data.

Calculated data for supercritical steam cycles ranging from 1050 F to 1450 F, and from 4000 psia to 10,000 psia are given. It is shown that for large capacity plants (1000 MW, 300 MW, and 150 MW are discussed) the desirable pressure at a given temperature is greater. It is also shown that larger plants for the same temperature and for optimized pressure are capable of higher efficiencies. A steam generator efficiency of .89 was used in the calculations and thus the reported efficiency must be corrected by this ratio to give the corresponding value for a nuclear plant. All losses ascribable to an operating plant were considered and evaluated for the various cases. The data used in the plot of Figure 11 is shown and reduced below.

Cycle Conditions	Heat Rate Btu/kw-hr	Conventional Plant Eff.	Nuclear Plant Eff.
4,000 psia-1050 F, 150 MW	9050	.378	.425
4,000 psia-1050 F, 300 MW	8820	.387	.435
6,000 psia-1250 F, 300 MW	8320	.411	.462
7,000 psia-1450 F, 300 MW	7970	.429	.482
10,000 psia-1450 F,1000 MW	7770	.440	.494

In all cases condenser pressure is $1\frac{1}{2}$" Hg.

7.1.2.2 Philo Plant Operating Data (Reference 2).

This plant is to utilize steam at 1150 F, 4500 psia and to operate to 1" Hg condenser pressure. The full load output is 125 MW. The final anticipated heat balance shows an overall thermal efficiency, as a fossil-fueled unit of 3413/8530 = .400. Since the steam generator

efficiency is .896, the corresponding nuclear plant efficiency would be .400/.896 = .446.

7.2 Liquid Metal Turbine Design Characteristics

7.2.1 Successful turbine design for high efficiency operation requires that the Mach Number of the flow relative to the blading be subsonic. Thus, if the sonic velocity for a particular fluid is very low with respect to the conventional working fluids, turbine design might be seriously circumscribed. The approximate sonic velocities for various of the possible liquid metal vapors are listed in Table IV below. It will be noted that with the exception of mercury they do not differ tremendously from air. However, mercury turbines have been constructed and operated satisfactorily.

TABLE IV. SONIC VELOCITY OF LIQUID METAL VAPORS AT 1500 F

Fluid	Molecular Wt.	C ft/sec 1500 F
Na	23	2350
K	39	1800
Rb	85.5	1220
Hg	201	795
Air	29	2090
H_2O	18	2650

7.2.2 Sodium Turbine - Low Pressure Blading

Assume t = 1040 F in condenser. This is the value used in the calculations. Then p = .20 psi (Reference 6). This is the equivalent of about .4 in Hg. Sodium flow rates are about similar to steam rates for the same power output (see Figures 6 and 7). Thus the low pressure stage of such a turbine would be about comparable to the low pressure stage of a steam turbine in a plant of the same power rating, condensing at $\frac{1}{2}$" Hg, or twice the flow capacity of a steam turbine condensing to 1" Hg.

7.3 Trinary Na-Hg-H_2O Cycle. Sample Calculations and Assumptions

7.3.1 Sample Calculations and Assumed Values

Two Na-Hg-H_2O trinary cycles, a Na-H_2O, a Na-Air, and two Hg-H_2O cycles were computed. The results are shown in Figures 6, 7, 8, 9, and 10, and tabulated in Table II.

The calculating methods are the same for all the cycles. The trinary cycle of Figure 6 - Cycle II is chosen as an example for illustration.

The following assumptions were made for this cycle:

Turbine Efficiencies:

Na Turbine	.75
Hg Turbine	.80
H_2O Turbine	.85

Condenser Back Pressure:

H_2O	1" Hg

Maximum Temperature:

Na	1500 F

Cycle Arrangement:

Na: 3 extraction points. Saturated cycle.
Hg: 3 extraction points. Superheated by one of Na extractions.
H_2O: 3 extraction points. Superheated by one of Hg extractions.

Pump Work:

Pump efficiency .50
No credit for pump work input.

Extraction Feed Heaters:

Zero temperature and pressure differentials (see Section 7.4 for comment).

The thermodynamic points were computed from the data of references 5 and 6 for sodium and mercury respectively. No dimerization was assumed. Steam data was taken from Reference 10. The expansion lines were computed on the basis of the assumed efficiencies, considering the drops between extraction points individually. No further credit for turbine reheat was assumed.

For the steam expansion line, for example, the first drop (between the steam chest and first extraction) is computed in the following

manner:

$$S_1 = S_2' = 1.5214,\ t_1 = 780\ F,\ h_1 = 1362.35,\ p_1 = 1275$$

$$p_2' = 360$$

$$h_2' = 1228.9$$

$$\Delta h_{1-2}' = 1362.35 - 1228.9 = 133.45$$

$$\Delta h_{1-2} = .85 \times 133.45 = 113.43$$

$$h_2 = 1362.35 - 113.43 = 1248.92$$

$$t_2 = 497.9\ F$$

$$S_2 = 1.5426$$

The locations for the extraction points were selected on the basis of a more or less equal division of the feed water enthalpy rise.

The extraction quantities were computed on the basis of a simple heat balance. For example, the highest steam extraction becomes:

$$x\ (1248.92 - 412.67) = (1 - x)\ (412.67 - 269.59),$$

$$x = 143.08/979.33 = 0.1461.$$

In this manner the other extractions were computed and the corresponding flow rates through the turbine.

Then the work from the steam cycle becomes:

$$W = 113.43 + 0.8539 \times 118.382 + 0.7638 \times 102.483 + 0.6696 \times 144.15 = 113.43 + 101.086 + 78.274 + 96.520$$

$$= 389.31\ \text{Btu/lb-}H_2O.$$

The extraction quantities and work for the Na and Hg were computed in similar manner. The only difference in procedure involves the additional extraction flows for superheating of the subsequent fluids which must be included in these cases.

The matching of flow quantities between the various fluids is accomplished as a simple heat balance. The steam cycle flow was used as a basis, and it was assumed that 1.0 units H_2O was the quantity of flow through the H_2O steam generator. The Hg flow necessary to superheat

this steam was computed, as previously mentioned, along with one of the extraction flows. The quantity of Hg to boil the H_2O is computed in a heat balance as shown below.

$$\frac{\text{\# - Hg cond}}{\text{\# - } H_2O \text{ boil}} = \frac{1179.8 - 412.67}{128.437 - 18.513} = 6.979$$

The cycle points which correspond to the enthalpy values used may be noted from Figure 6b.

The same procedure was utilized to relate the flow quantities in the Na and Hg cycles. All work and heat units were then referred back to Btu/lb of water boiled.

On this basis the contributions to the total work from the Na, Hg, and H_2O portions of the cycle are:

Na	263	Btu/lb H_2O boiled
Hg	262.84	" " "
H_2O	389.31	" " "
Total	915	Btu/lb H_2O boiled

The heat input to the cycle is that quantity of heat necessary to heat the Na from the highest feedwater heater exit point to the saturated vapor condition corresponding to 1500 F. This quantity becomes

$$Q_{in} = 0.7877\ (2225 - 350) = 1480 \text{ Btu/lb } H_2O \text{ boiled.}$$

Then the cycle efficiency would be, considering pump work

$$\eta = \frac{\text{Work}}{\text{Heat In}} = \frac{908}{1480} = 0.613$$

As explained in Section 7.3, this result is reduced by a factor of .96 to account for an apparent discrepancy in the Na data. As is explained in that section, this is a very conservative assumption, since a factor of .99 would be equally defensible.

7.3.2 Comments on Assumptions

The cycle calculations were somewhat shortened by the following approximations:

1) No credit for pump work reducing heat input;

2) No temperature and pressure differentials in feed water heaters;

3) No allowance for pump suppression head following each heater;

4) No allowance for radiation losses;

5) Uniform but very low pump efficiency assumption applied to all cases;

6) Division of turbine expansion lines into four portions only, thus neglecting some of the existing reheat;

7) Use of only three feed heaters in each portion. A larger number would increase efficiency to some extent.

It will be noted that assumptions 1, 5, 6, and 7 tend to reduce cycle efficiency while the remainder cause it to increase. However, all of these effects are quite small and it is believed that they fairly closely cancel each other. The final application of a factor of 0.96 to the overall efficiency is very likely to be highly conservative. Thus the final cycle result, for turbines of the stated efficiency, is believed to be conservative.

7.3.2.1 Turbine Efficiencies

For trinary cycle II, turbine efficiencies of .75, .80, .85 (including reheat effect beyond the four divisions of the expansion line for each fluid) were selected for Na, Hg, and H_2O respectively. For cycle I, values of .80, .83, and .85 respectively were used.

For the Hg-H_2O cycles (Figures 9 and 10) turbine efficiencies of .80 and .85 for Hg and H_2O respectively were used (including reheat as above). In general the attainable efficiency is a function of the flow rate and hence depends on the size plants. No evaluation of attainable efficiency for given cases was made, but the values used apply generally to fairly large installations. The high temperature liquid metal turbine efficiency has been assumed lowest because of the unknown characteristics of the working fluid and the fact that it must operate with saturated vapor. The intermediate turbine in the trinary cycles has been assumed to be somewhat more efficient because it utilizes superheated vapor.

7.3.2.2 Liquid Metal Cycle Pump Designs

7.3.2.2.1 Mercury Cycles

Consider a 60,000 KW binary plant. As shown in these calculations the water flow rate is about 60 lb/sec and the mercury flow rate about 850 lb/sec. Then the respective flows are about 550 GPM for the mercury pump and 420 GPM for water. Thus

the pumping requirements will be of the same order of magnitude.

7.3.2.2.2 Sodium Cycle

The sodium flow rates are similar to those for the water portion of the cycle since the enthalpies and densities are similar. However, the total pressure rise in the sodium cycle is only about 15 psi. Thus the possibility of electromagnetic or jet pumps is strongly suggested.

7.4 Estimation of Effect of Turbine Efficiency on Ideal Trinary Na-Hg-H_2O Cycle. Corrections to Na Data.

7.4.1 Ideal Trinary Cycle

Utilizing the same temperatures, and thermodynamic data, which were used in the calculation for Trinary Cycle I explained in Section 2.3, a trinary cycle was computed using 100% turbine efficiency for the three turbines. The other assumptions and the calculations procedure was as per Section 7.3 except that superheat was not used for any of the fluids. The resulting efficiencies were compared to the Carnot efficiency for each portion. The results are as listed below.

Cycle	η	η_c	η/η_c	η/η_c corrected
Na	.2395	.234	1.024	.985
Hg	.280	.284	.985	--
H_2O	.452	.479	.943	--
Overall	.700	.725	.966	.928

7.4.1.1 Correction to Na Data

It is obvious that the Na data (reference 6) is not sufficient for these calculations. It is assumed that sodium and mercury should give cycle efficiencies about equally proportionate to the Carnot efficiency. Therefore, it has been assumed in all calculations that the heat input to the Na portion (which is of course the total input to the cycle) must be increased by .985/1.024 = 0.962. An equally defensible assumption would be that the heat input to the sodium cycle is correct but that the work output is reduced by this ratio. Then the effective reduction of the overall efficiency would be only about 0.99. The true situation probably lies between these extremes.

7.4.2 Effect of Changing of Turbine Efficiencies

The ideal trinary cycle discussed in Section 7.4.1 was used as a basis for the determination of the effect of changing of the various turbine efficiencies.

As a first step, the Na turbine efficiency was decreased from 100% to 80%. This has the effect of decreasing work output from the Na portion of the cycle, but increasing work outputs (i.e. flow rate/Na flow rate) of the Hg and H_2O portions since more heat becomes available in the Na condenser. On this basis, the heat/per unit Na flow rate to the Hg portion is increased by a factor of 1.06 and the Na turbine work decreased by .80.

Originally (all turbines at 100%) the work output was

$$\frac{\text{Na}}{10,880} + \frac{\text{Hg}}{9720} + \frac{H_2O}{11,700} = 32,300$$

and with the above corrections this becomes

$$\frac{\text{Na}}{10,880 \times .80} + 1.06\left(\frac{\text{Hg}}{9720} + \frac{H_2O}{11,700}\right) = 31,400$$

Thus, since heat input to the Na cycle is unchanged (Na flow rate unchanged), the cycle efficiency becomes (uncorrected for Na data)

$$.700\ (31,400/32,300) = .679$$

a reduction of only .021 for a turbine efficiency reduction of .20.

In addition, as a second step, the Hg turbine efficiency was reduced to .83. By a similar analysis, the cycle efficiency becomes .657, a further reduction of .022 for a Hg turbine drop of .17.

Finally, the steam turbine efficiency was reduced to .85. This has the effect of reducing overall cycle efficiency to .63, a drop of .027 for an H_2O turbine drop of .15. It will be noted that this final result, derived approximately, matches very closely the more exact result of Trinary Cycle II (Figure 6b) where the same turbine efficiencies were used, but where the Hg and H_2O cycles were superheated. This result is to be expected in that the superheat does not inherently improve the thermodynamic situation in this case since it is only a matter of intra-cycle heat transfer. The superheat is justified, actually, as a means of increasing attainable turbine efficiency.

7.5 Effect of Finite Temperature Differential Between Various Portions of Binary and Trinary Cycles

Consider as an example a binary Carnot cycle versus a simple Carnot cycle as sketched below.

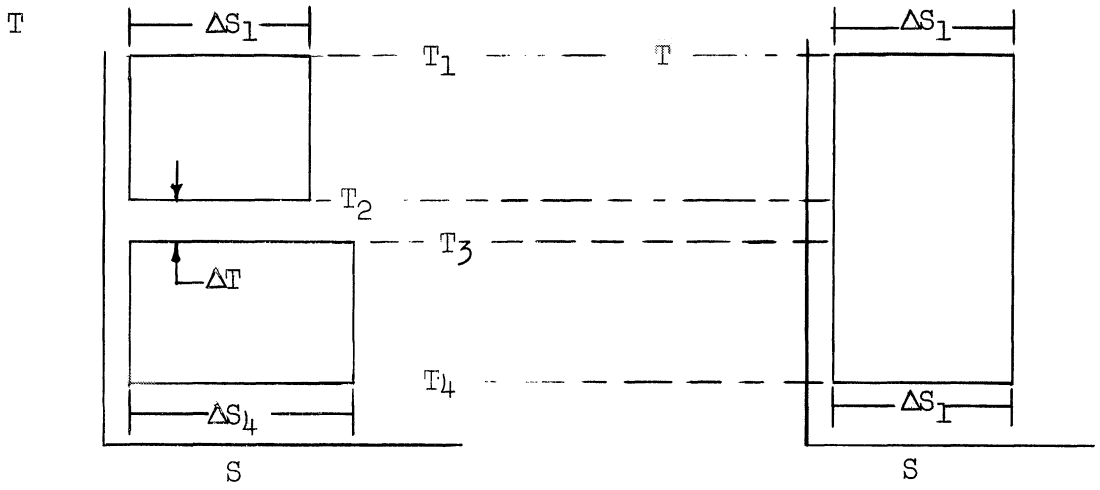

In either arrangement the heat input to the cycle is $T_1 \Delta S_1$. In the binary cycle, heat, in amount $T_2 \Delta S_1$, must be transferred across the temperature differential ΔT to become the heat input to the lower portion of the cycle, $T_3 \Delta S_4$.

By continuity, $T_2 \Delta S_1 = T_3 \Delta S_4$. Since $T_2 > T_3$, $\Delta S_4 > \Delta S_1$. Heat in amount $T_4 \Delta S_4$ is rejected from the binary cycle and $T_4 \Delta S_1$ from the simple cycle. The heat rejected from the binary cycle is greater than that rejected from the simple cycle by the ratio $\Delta S_4 / \Delta S_1 = T_2/T_3$. Since heat inputs to the cycles were equal, the work output and efficiency of the binary cycle are less than for the simple cycle.

The amount of this reduction can be estimated for a typical example. Suppose $\eta_{Carnot} = .60$, $T_2 = 1500$ R, and $\Delta T = 30$ F. Then $T_2 = 1500/1470 = 1.02$

$$\eta = \frac{\text{Heat In - Heat Out}}{\text{Heat In}} = 1 - \frac{\text{Heat Out}}{\text{Heat In}}$$

In this case

$$\frac{\text{Heat Out}}{\text{Heat In}} = .40$$

If Heat Out is increased in proportion to T_2/T_3 (i.e. 1.02), $\frac{\text{Heat Out}}{\text{Heat In}}$ is increased by the same factor. Thus

η becomes $1 - .40 \times 1.02 = .592$

Thus, for this type of cycle, there is an efficiency loss of about 1 point for every 30 F additional temperature differential between the portions. Inherently, then, the trinary cycle is perhaps 1 point less efficient than a comparable binary arrangement.

7.6 Effect of Temperature Differential in Extraction Feed Heaters

As stated in Section 7.3, no temperature differential was assumed for the feed heaters. Practically, this case might be attained for the sodium cycle by the use of sodium ejectors rather than feed pumps, since the pressure differential is very low. However, for the mercury and steam cycles it is only an approximation. A rough estimate of the magnitude of the discrepancy introduced by this approximation is made in this section.

Suppose we assume a 20 F differential for each feed heater. Roughly we may assume that the effect is similar for any of the portions of the trinary cycle. This effect is the reduction of turbine work caused by a removal of a portion of the working fluid at a temperature 20 F greater than implied by the zero temperature differential assumption which was made.

Say we consider the portion of one of the Hg cycles in a trinary cycle between the second and third extractions as typical. In this region of the turbine expansion line there is a Δh of approximately 1.7 Btu/lb corresponding to a Δt of 20 F. The flow extracted at this point for feed water heating is .189 out of a total flow of 8.89 or .021 of the total. Since the total turbine enthalpy drop is about 37 Btu/lb, the loss on this account is proportionately

$$\frac{1.7 \times .021}{37} = .00096$$

Since there are three extractions per fluid the total proportionate loss is about 0.003 and is thus quite negligible.

PART II. GAS TURBINE DETAILED STUDIES FOR NUCLEAR POWERPLANTS

1.0 GENERAL THERMODYNAMIC FEATURES OF GAS TURBINE CYCLE

1.1 Approach to Ideal Efficiency

For the appraisal of any thermodynamic heat engine cycle, it is first desirable to investigate its degree of approach to the ideal heat engine cycle efficiency which, according to the Second Law of Thermodynamics, sets the maximum possible efficiency for given temperature limits. This situation is examined in some detail in Part I.

It is concluded that the gas turbine type cycle can approach the ideal efficiency limitation either through the utilization of the "simple cycle" (Figure 2 of Part I) with a pressure-ratio approaching infinity or through an ideal regenerative cycle (Figure 3 of Part I) which approaches the Ericsson cycle. This latter involves an infinite number of reheat and also intercooler stages in the ideal case. Practically, of course, a compromise somewhere between these two extremes is required.

In past practice with fossil-fueled gas turbine plants, the first possibility, i.e. the use of a high pressure ratio with no heat exchanging equipment, has been applied to cases where size and weight of plant were of more importance than efficiency. A case in point is the aircraft gas turbine plant. However, where efficiency assumes proportionately more importance, as for most land-based and marine applications, plants utilizing highly effective heat transfer equipment and a rather low pressure ratio seem more suitable. If practically attainable component efficiencies and effectivenesses are assumed, it may be shown that plants designed according to the latter philosophy can achieve considerably higher thermal efficiency values for any imposed temperature limitations. This fact is illustrated graphically by a comparison of Figures 6e and 6d. Figure 6e is a plot of thermal efficiency against pressure ratio for a plant including regenerator, intercooler, and reheater, as well as the universally required heat sink and source. It is noted that, in this case, the maximum thermal efficiency values for source temperatures of 900, 1200, and 1500 F respectively are 25.0, 34.7, and 41.5. On the other hand, Figure 6d shows the maximum efficiency against pressure ratio for a plant with no regenerator, intercooler, or reheater. Here it is noted that the maximum efficiency values occur for considerably higher pressure ratios (about 5.5 instead of 3.5 for 1200 F). However, the maximum efficiency values are only 12.8, 19.3, and 24.6, at the same temperatures.

1.2 Selection of Basic Cycle

High efficiency appears essential for any but perhaps airborne

nuclear powerplants. Therefore, it was decided to base the study on the cycle arrangement which is capable of the higher efficiency. As explained in the last section, the choice of the regenerative type cycle is dictated. A basic arrangement (see Figure 1) is assumed which includes regenerator, intercooler, and heat source and sink, as well as turbine and compressor. (Thermodynamically the decision as to whether the turbine would be divided into a power and compressor drive turbine and the decision as to whether the cycle is open or closed is of no significance.) This cycle was used as a basis from which the effects of the possible variations in component arrangement, efficiencies, and effectiveness could be evaluated. For this "basic cycle", the assumptions listed in Table I were made.

TABLE I. ASSUMED COMPONENT EFFICIENCIES FOR THE BASIC GAS TURBINE CYCLE

Turbine Efficiency	85%
Compressor Efficiency	85%
Regenerator Effectiveness	93%
Ratio of Compressor Pressure Ratio to Turbine Expansion Ratio	1.07
Cooling Medium Temperature	70 F
Minimum Fluid Temperature	90 F

These values are believed to be attainable in large scale plants where efficiency is of considerable import compared to capital cost. The relations between the relative importances of capital cost and efficiency depend on the particular application and no general statements may be made. For a nuclear plant these relations may differ considerably from a fossil-fueled plant. They depend very strongly on the type of reactor because of the influences of fabrication and reprocessing costs for the fuel elements, as well as the price of uranium. A further study of this situation seems a logical extension to the work which has been already accomplished.

A closed cycle type installation is assumed in the selection of these component efficiencies. This is apparent in the case of the regenerator. It is believed that, for a fairly large plant operating at elevated pressure, that considering the consequent increase in heat transfer coefficients, a regenerator effectiveness of 0.93 is reasonable. This is particularly the case for plants utilizing helium instead of air, where there is a further improvement in heat transfer.

In general, the turbine efficiency will exceed to some extent the compressor efficiency, and each of these values will increase for large flow rates. This increase is somewhat obviated with the closed-cycle, elevated-pressure plant, since the turbomachinery volume flow rates may be too low for optimum efficiency in an optimized plant. This is the case because the pressure level selection for an optimum plant design may be influenced more strongly

by the regenerator requirements than by the turbo-machinery. It is believed that the selection of a rather high regenerator effectiveness with more moderate turbomachinery efficiencies may represent a reasonable compromise for the closed-cycle plant. Therefore, an assumption of 0.85 for turbine and compressor efficiency has been made for the "basic cycle." It is not implied that the turbine and compressor efficiencies are equal at 0.85, but that they achieve values (turbine somewhat higher than compressor) which are the equivalent, so far as the overall cycle efficiency is concerned.

1.3 General Relations with Perfect Gas

The calculations reported in this section are based on the assumption of a perfect gas. There is no question of a mixture of combustion products with the working fluid for a nuclear plant as in the case of the conventional open-cycle fossil-fueled gas turbine. Therefore, the perfect gas assumptions are believed to be fairly close to the actual case. The relations for the thermal efficiency of the basic cycle and for the various permutations of this cycle which were studied are derived in the Appendix (Section 8.1) and listed in Table II.

It will be noted from the expressions for the thermal efficiency listed in Table II that the thermal efficiency is not a function of the working fluid. The only characteristic of a perfect gas working fluid which is involved in the expression for the theoretical cycle thermal efficiency is the ratio of specific heats. Thus, as far as the perfect gas assumption is applicable, a certain thermal efficiency is attainable with any diatomic ($k = 1.4$), and another with any monatomic ($k = 1.66$) gas, assuming no change in the attainable component efficiencies and effectivenesses. This is, of course, not the general case since the optimum heat exchanger designs for a given application strongly depend on many characteristics of the gas not considered in this type of analysis, and the optimum turbomachine design depends on such factors as the Mach number and Reynold's number.

Under the assumption of a perfect gas working fluid and constant component efficiencies and effectivenesses, it can be shown that for any given temperature limits the attainable thermal efficiency increases as the ratio of specific heats decreases. This is illustrated in Figure 11 where thermal efficiency at optimum pressure ratio is plotted against the ratio of specific heats. The same effect is also evident from an examination of Figure 6, where in all cases the maximum thermal efficiency for the $k = 1.4$ value exceeds by one or two points that of the $k = 1.66$ value. Thus, under the assumptions of this study, gases such as air or nitrogen are inherently capable of higher cycle thermal efficiencies than helium or argon. On this basis, gases with a still lower k value such as carbon dioxide would be even more suitable. As far as actual machinery design is concerned this may not be the case. The machinery required to extract the required efficiencies and effectivenesses from the heavier gases may be more extensive than that required for helium, so that the optimized plant for a given application may well show a higher

TABLE II. GAS TURBINE CYCLE THERMAL EFFICIENCY RELATIONS

Cycle Arrangement	Thermal Efficiency Equation
Basic Cycle	$\eta_{th} = \dfrac{TR\eta_T \left[1 - (\eta_p PR)^{-\gamma} \right] - \frac{2}{\eta_c} \left(PR^{\gamma/2} - 1 \right)}{TR\left\{ 1 - \eta_R + \eta_R \eta_T \left[1 - (\eta_p PR)^{-\gamma} \right] \right\} + \frac{\eta_R - 1}{\eta_c} \left(PR^{\gamma/2} + \eta_c - 1 \right)}$
Basic Cycle Without Recuperator	$\eta_{th} = \dfrac{TR\eta_T \left[1 - (\eta_p PR)^{-\gamma} \right] - \frac{2}{\eta_c} \left(PR^{\gamma/2} - 1 \right)}{TR - \frac{1}{\eta_c} \left(PR^{\gamma/2} + \eta_c - 1 \right)}$
Basic Cycle Without Intercooler	$\eta_{th} = \dfrac{TR\eta_T \left[1 - (\eta_p PR)^{-\gamma} \right] - \frac{1}{\eta_c} \left(PR^{\gamma} - 1 \right)}{TR \left\{ 1 - \eta_R + \eta_R \eta_T \left[1 - (\eta_p PR)^{-\gamma} \right] \right\} + \frac{\eta_R - 1}{\eta_c} \left(PR^{\gamma} + \eta_c - 1 \right)}$
Basic Cycle Without Intercooler and Recuperator	$\eta_{th} = \dfrac{TR\eta_T \left[1 - (\eta_p PR)^{-\gamma} \right] - \frac{1}{\eta_c} \left(PR^{\gamma} - 1 \right)}{TR - \frac{1}{\eta_c} \left(PR^{\gamma} + \eta_c - 1 \right)}$
Basic Cycle With Reheat	$\eta_{th} = \dfrac{2\eta_T TR \left[1 - (\eta_p PR)^{-\gamma/2} \right] - \frac{2}{\eta_c} \left(PR^{\gamma/2} - 1 \right)}{TR\left\{ 1 - \eta_R + \eta_R \eta_T \left[1 - (\eta_p PR)^{-\gamma/2} \right] \right\} + \frac{\eta_R - 1}{\eta_c} \left(PR^{\gamma/2} + \eta_c - 1 \right) + TR\left[1 - \left(\frac{1}{\eta_p PR} \right)^{\gamma/2} \right]}$

Note: Symbols are defined in Section 6.

overall efficiency with helium as working fluid than air. It is felt that this situation deserves further examination and will be considered at greater length in a continuing investigation.

2.0 OPERATING PARAMETER VARIATION EFFECTS ON EFFICIENCY FOR PERFECT GAS

2.1 Basic Cycle

As was explained in Section 1.0, a "basic cycle" was postulated, consisting of a compressor with a single intercooler, a turbine, a regenerator, and a heat source and sink (Figure 1). Along with the "basic cycle", four other cycles, including the elements as listed below, were considered.

a. Compressor with single intercooler, turbine, heat source and sink, (i.e. no regenerator). (Schematic Figure 2, performance Figure 6b).

b. Compressor, turbine, regenerator, heat source and sink, (i.e. no intercooler). (Schematic Figure 3, performance Figure 6c).

c. Compressor, turbine, heat source and sink, (i.e. no intercooler or regenerator). (Schematic Figure 4, performance Figure 6d).

d. Compressor with single intercooler, turbine with single reheater, regenerator, heat source and sink. (Schematic Figure 5, performance Figure 6e).

The "basic cycle" is also used as a basis for the determination of the effect on thermal efficiency of changing each of the significant cycle parameters individually with all other factors held constant. From the data presented it is possible to estimate the efficiency of any gas turbine cycle. The estimate is obtained by correcting the "basic cycle" efficiency value by the proportionate efficiency change caused by each of the cycle parameter variations involved. The data is plotted in all cases as a function of pressure ratio, and thus the optimum pressure ratio for given conditions can be selected from the curves. Also, the proportionate loss of efficiency to be expected from operation (as perhaps at part load) at pressure ratios other than the optimum may be estimated. In all cases, data is presented for both a monatomic and a diatomic gas (i.e. for k values of 1.66 and 1.4 respectively) and for inlet temperatures of 1500 F, 1200 F, and 900 F. The cycle diagrams are presented in Figures 1 through 5, and the performance curves in Figures 6 through 9. Listed in Table III are the various cycle conditions which are presented in this report.

2.2 Results of Theoretical Performance Calculations

Several important points are apparent from this study. At 900 F, 25% is approximately the maximum obtainable efficiency. This value corresponds to the cycle with a reheater. Without a reheater, the approximate maximum is 23.5%. At 1200 F the maximum thermal efficiency with reheater approaches 35% and without reheater 34%.

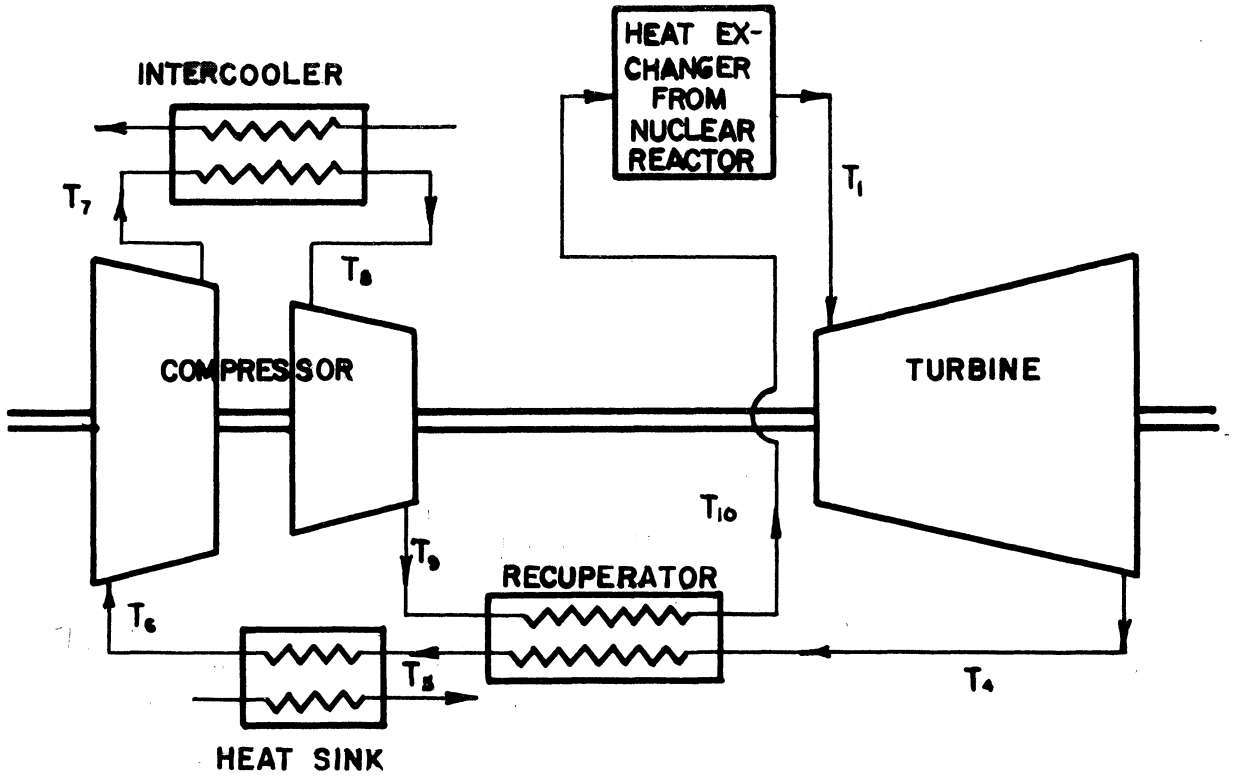

FIG. 1 SCHEMATIC FLOW DIAGRAM OF THE BASIC GAS TURBINE CYCLE

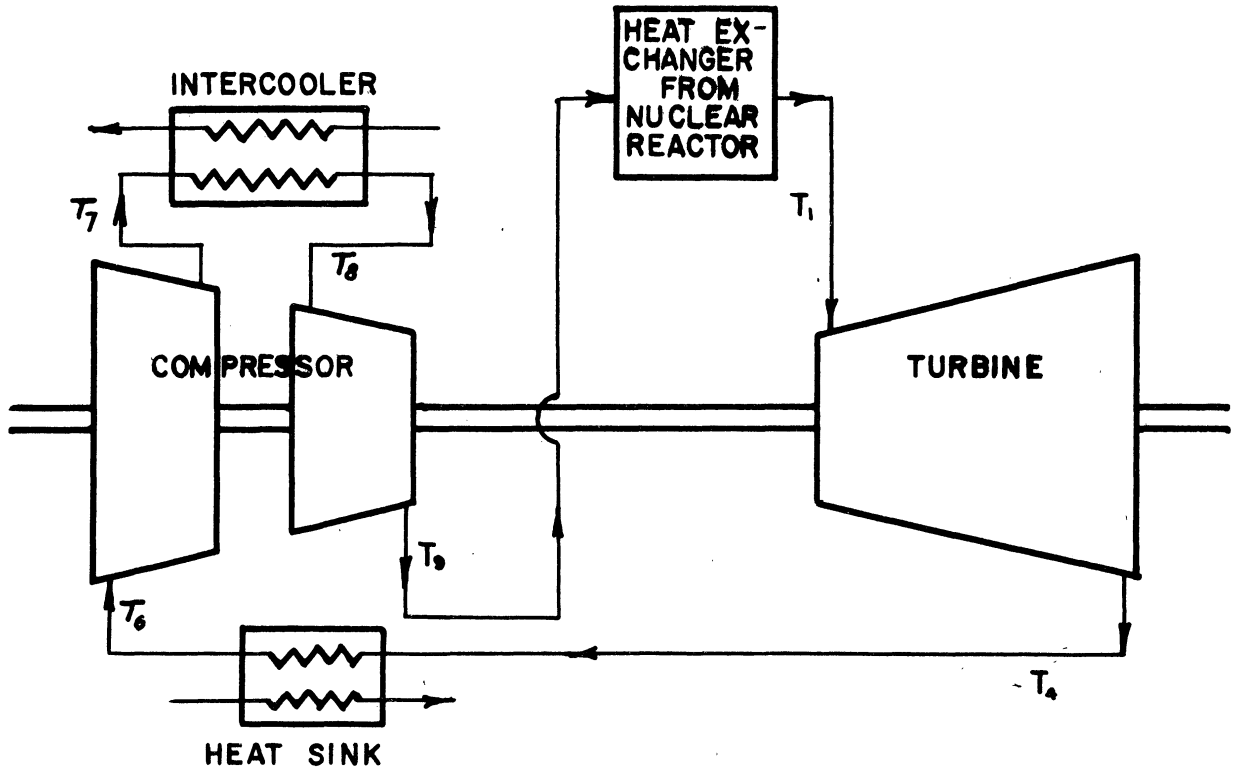

FIG. 2 SCHEMATIC FLOW DIAGRAM OF THE BASIC GAS TURBINE CYCLE WITHOUT RECUPERATOR

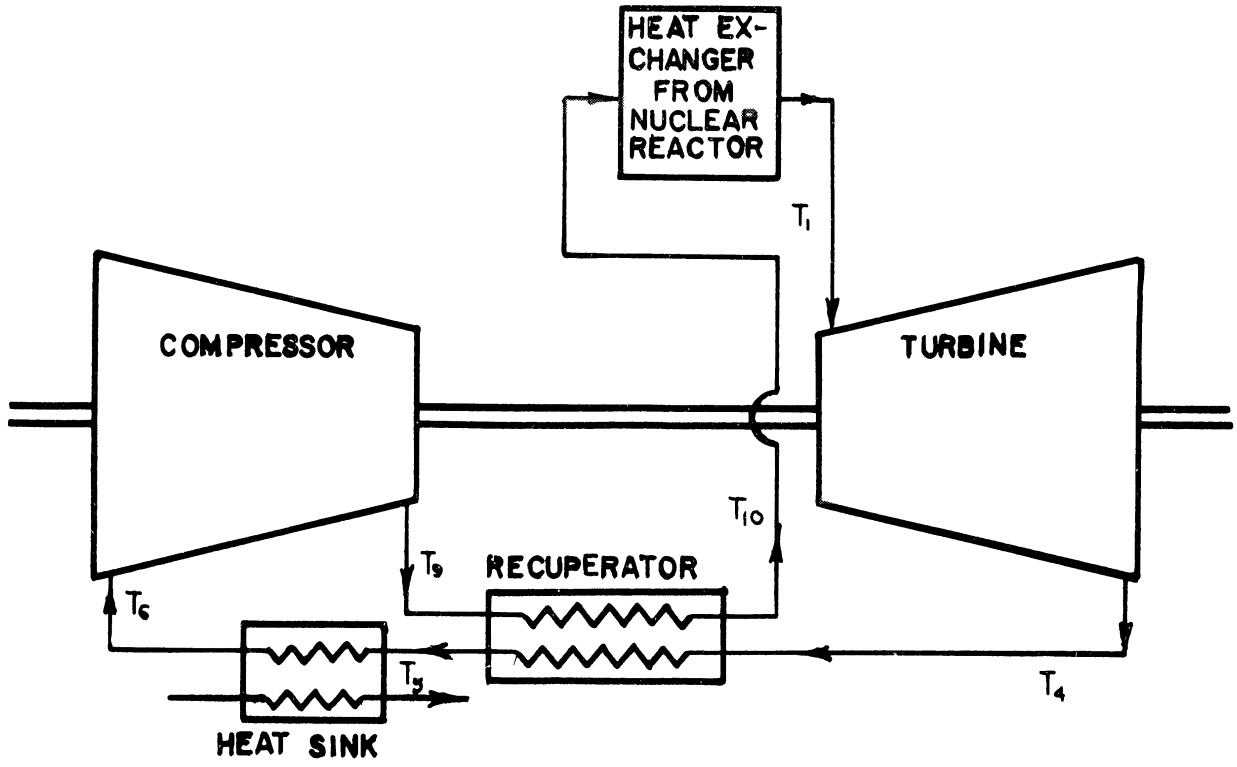

FIG.3 SCHEMATIC FLOW DIAGRAM OF THE BASIC GAS TURBINE CYCLE WITHOUT INTERCOOLER

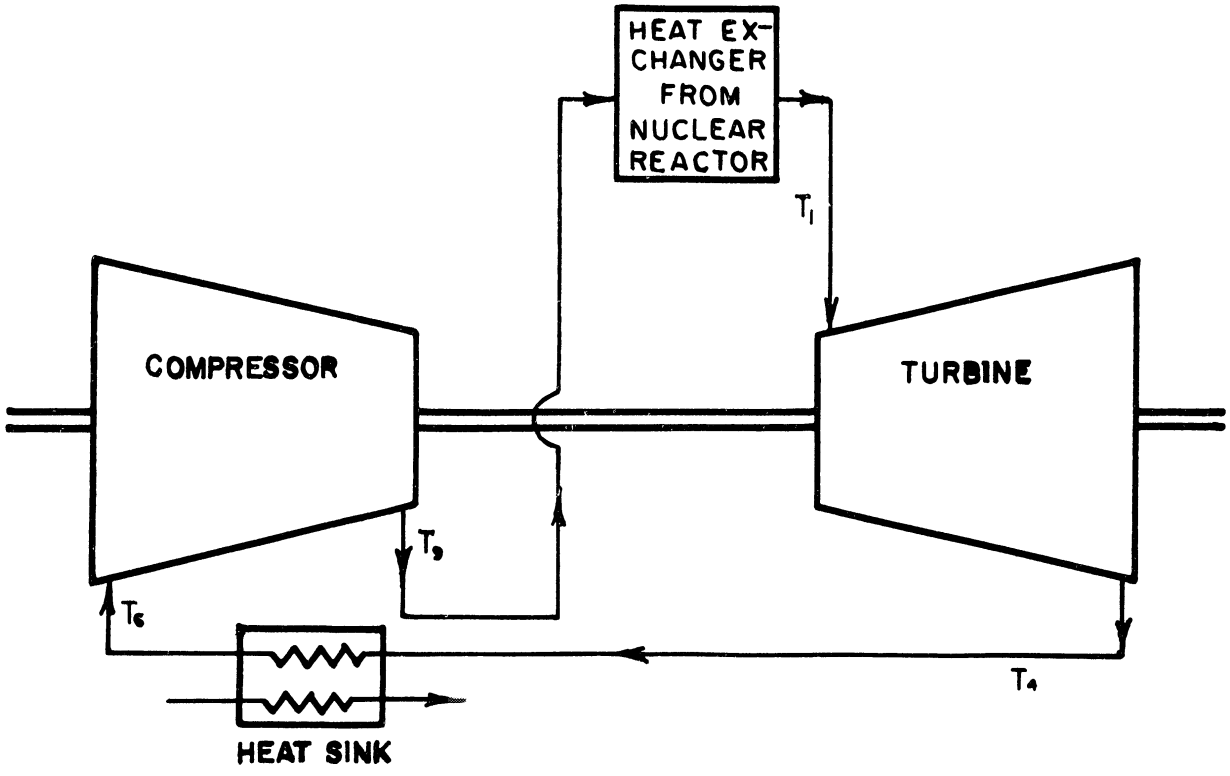

FIG. 4 SCHEMATIC FLOW DIAGRAM OF THE BASIC GAS TURBINE CYCLE WITHOUT RECUPERATOR OR INTERCOOLER

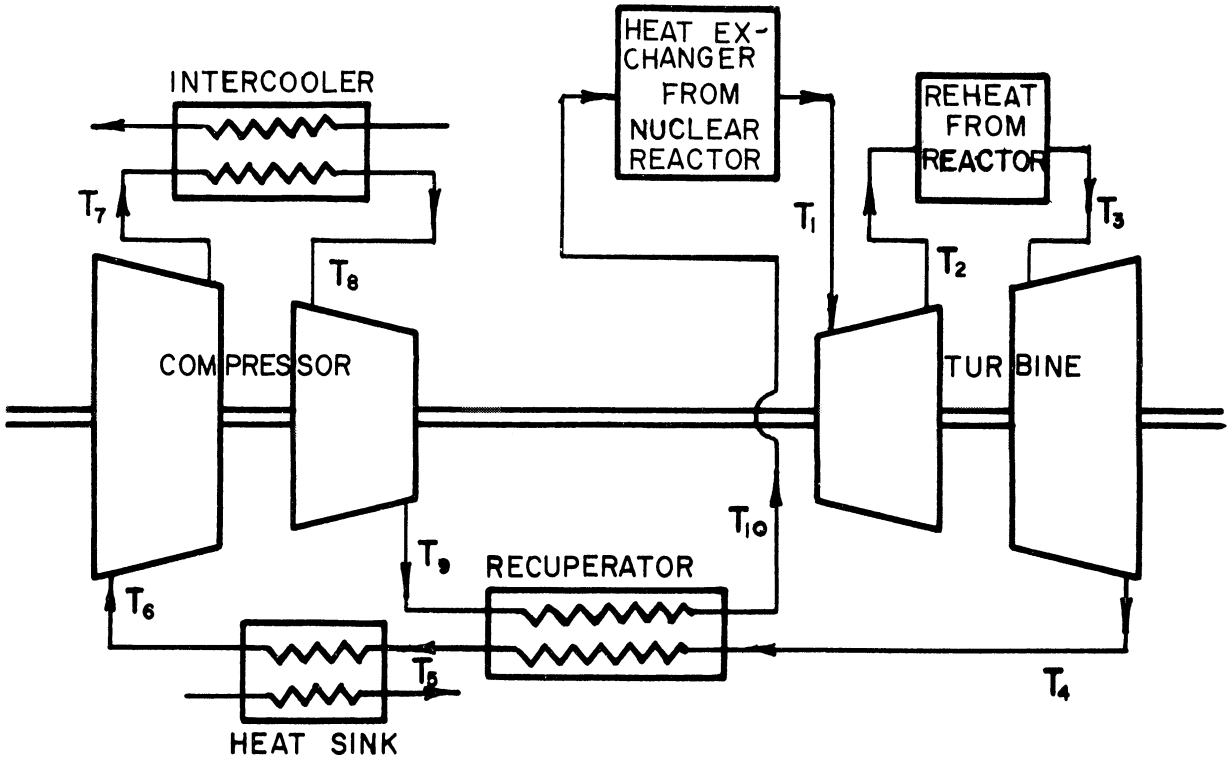

FIG. 5 SCHEMATIC FLOW DIAGRAM OF THE BASIC GAS TURBINE CYCLE WITH REHEATER

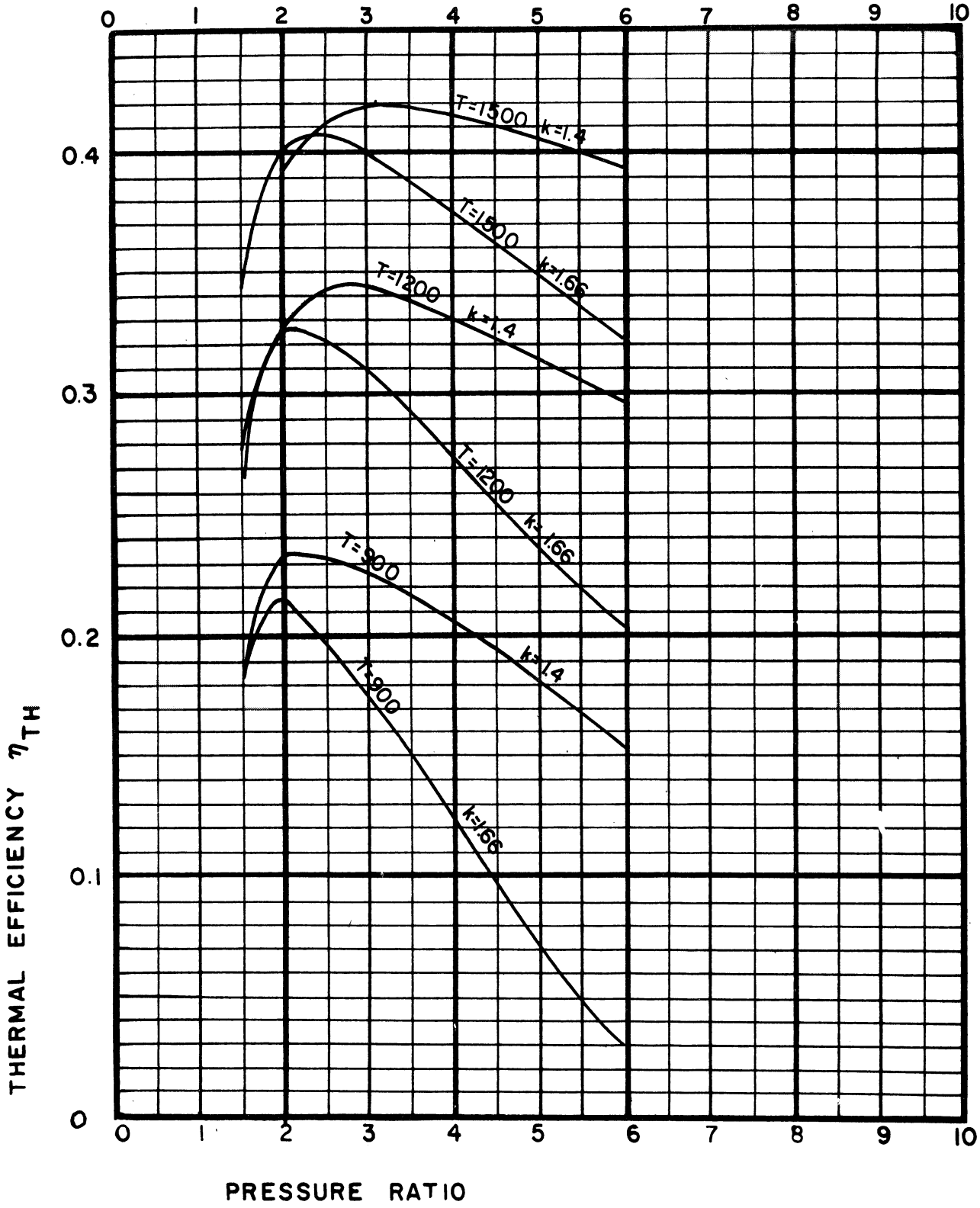

FIG. 6a. THERMAL EFFICIENCY OF A GAS TURBINE CYCLE WITH VARIOUS CYCLE ARRANGEMENTS.

"BASIC"* CYCLE

*SEE TABLE 3, PART II

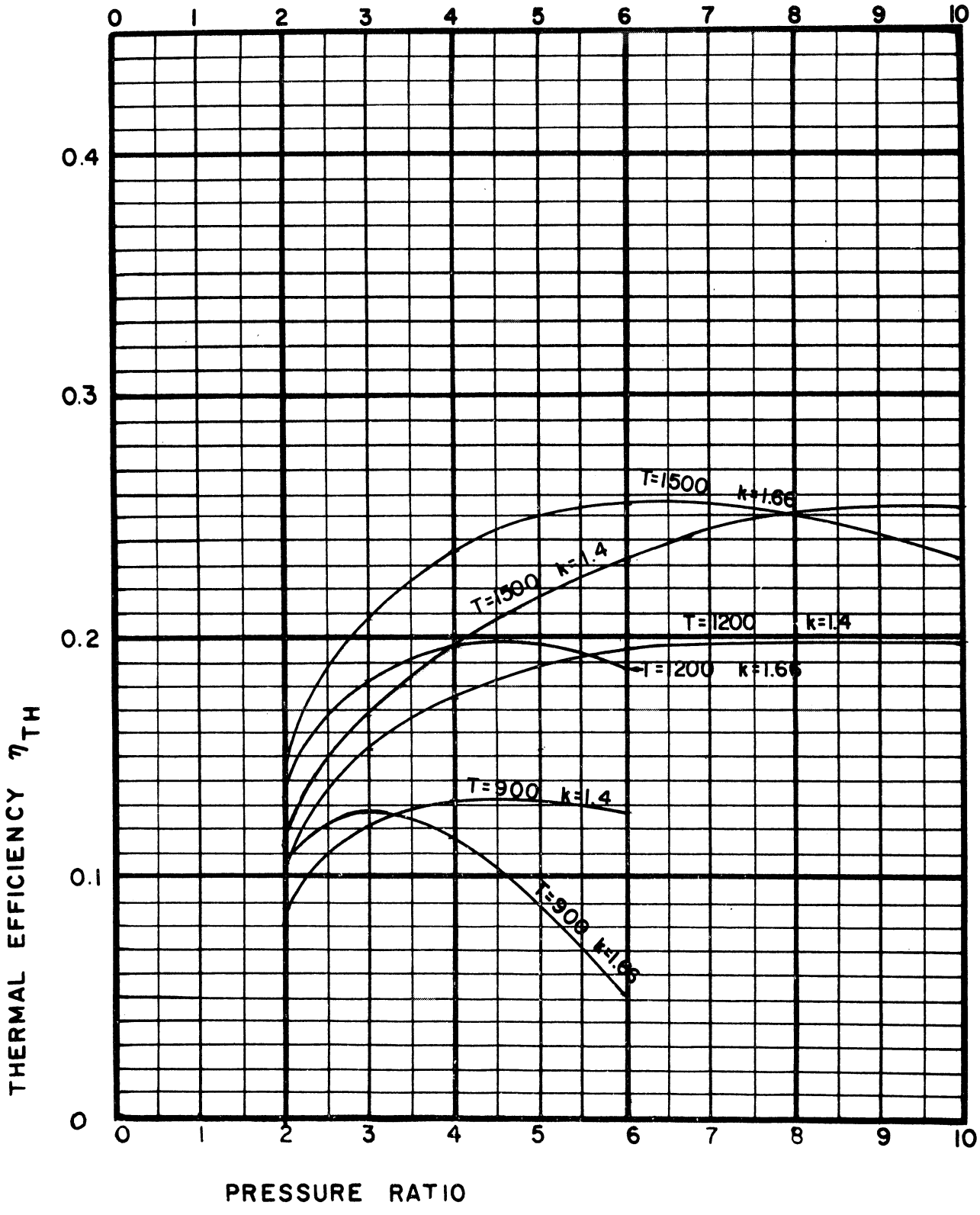

FIG. 6b. THERMAL EFFICIENCY OF A GAS TURBINE CYCLE WITH VARIOUS CYCLE ARRANGEMENTS.

"BASIC"* CYCLE WITHOUT RECUPERATOR

* SEE TABLE 3, PART II

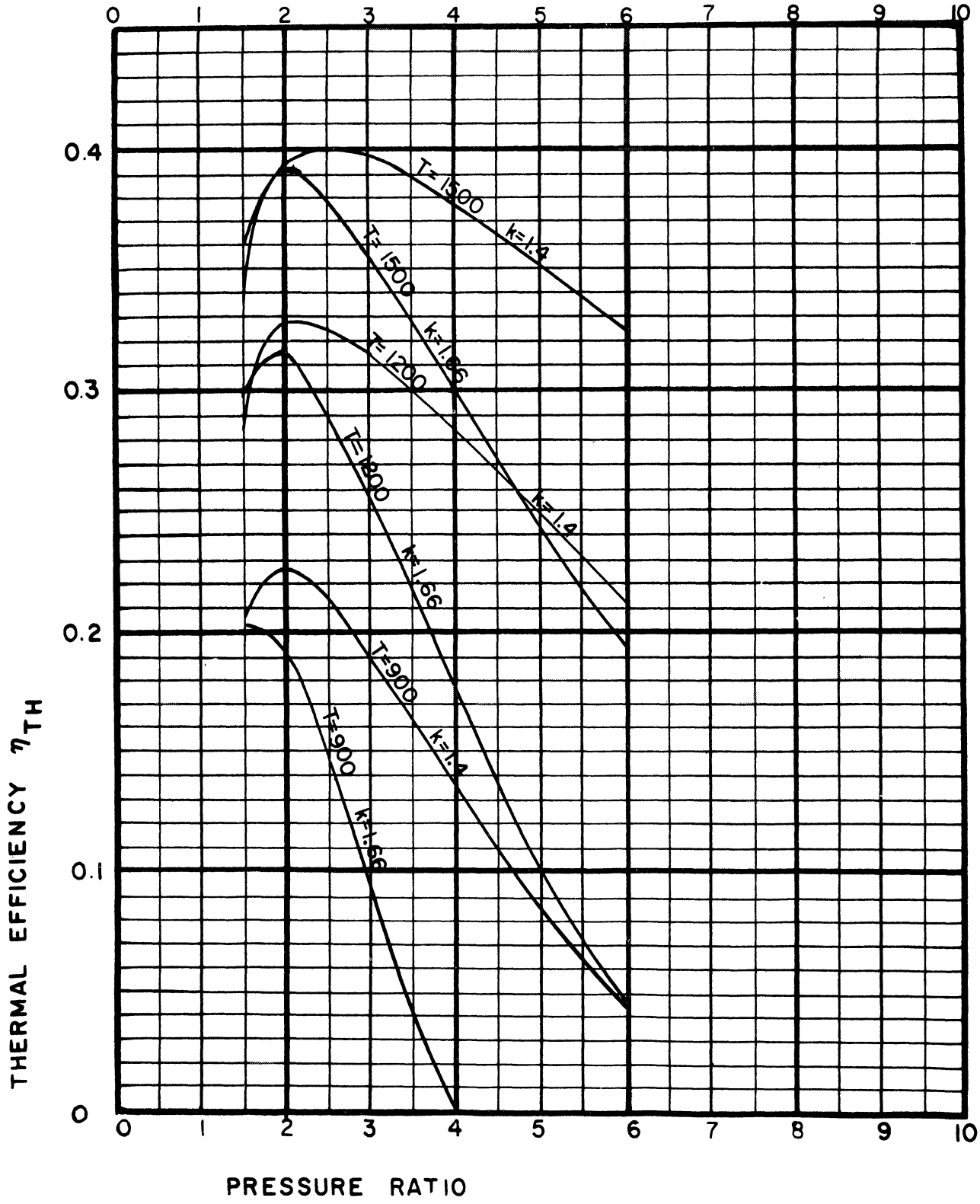

FIG. 6c. THERMAL EFFICIENCY OF A GAS TURBINE CYCLE WITH VARIOUS CYCLE ARRANGEMENTS

"BASIC"*CYCLE WITHOUT INTERCOOLER

*SEE TABLE 3, PART II

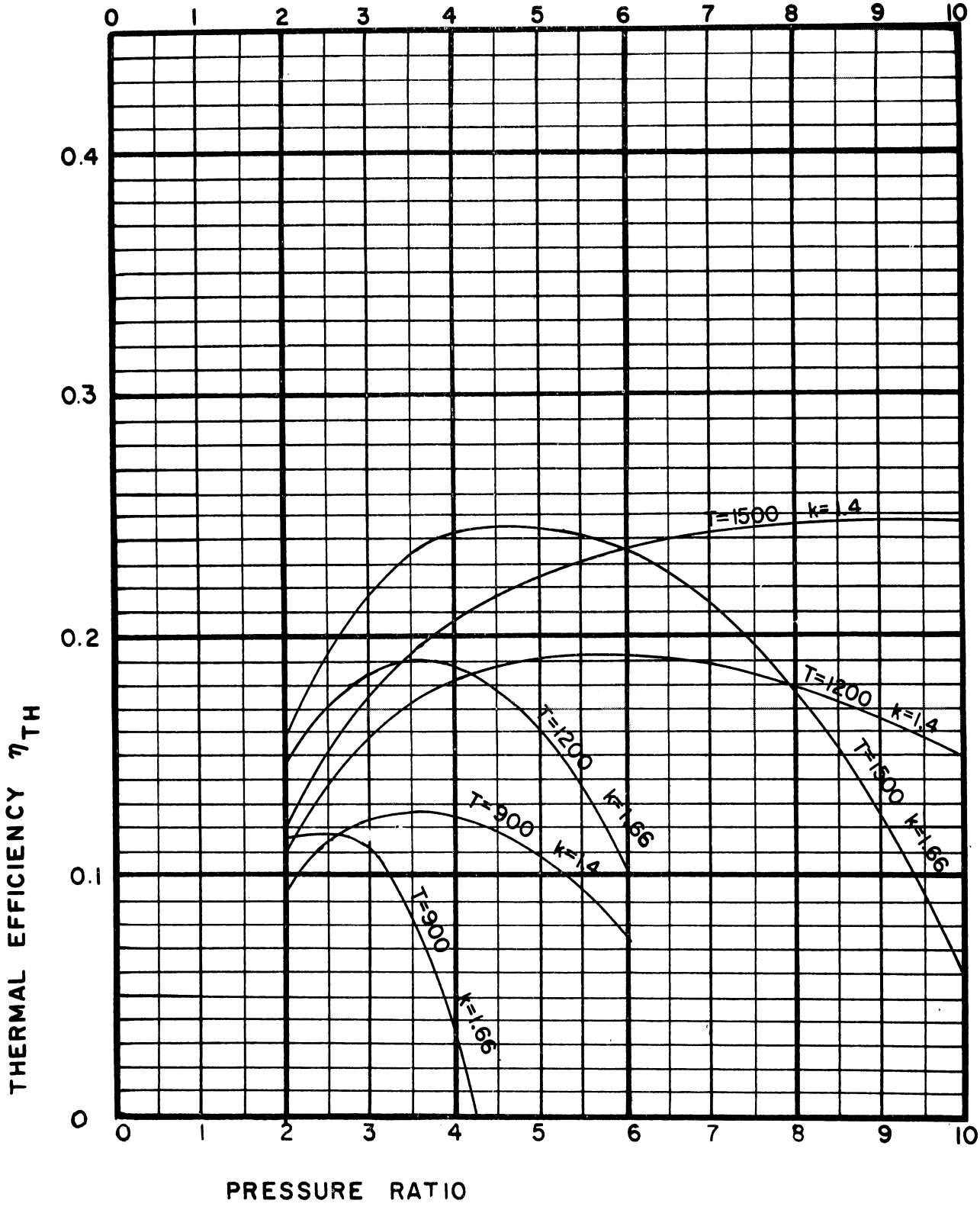

FIG. 6d. THERMAL EFFICIENCY OF A GAS TURBINE CYCLE WITH VARIOUS CYCLE ARRANGEMENTS.

"BASIC"* CYCLE WITHOUT RECUPERATOR AND INTERCOOLER

*SEE TABLE 3, PART II

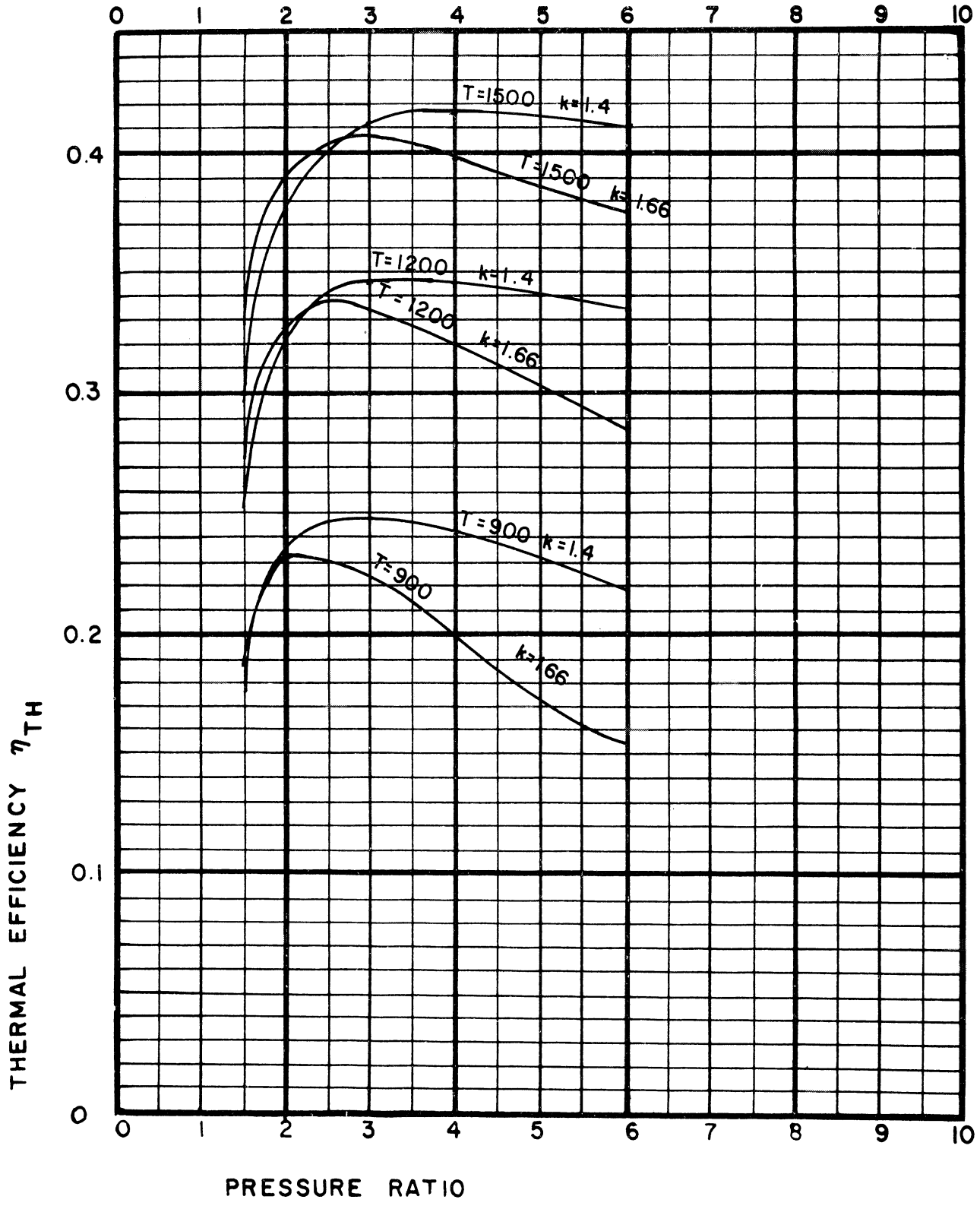

FIG. 6e. THERMAL EFFICIENCY OF A GAS TURBINE CYCLE WITH VARIOUS CYCLE ARRANGEMENTS.

"BASIC"* CYCLE WITH REHEATER

* SEE TABLE-3, PART II

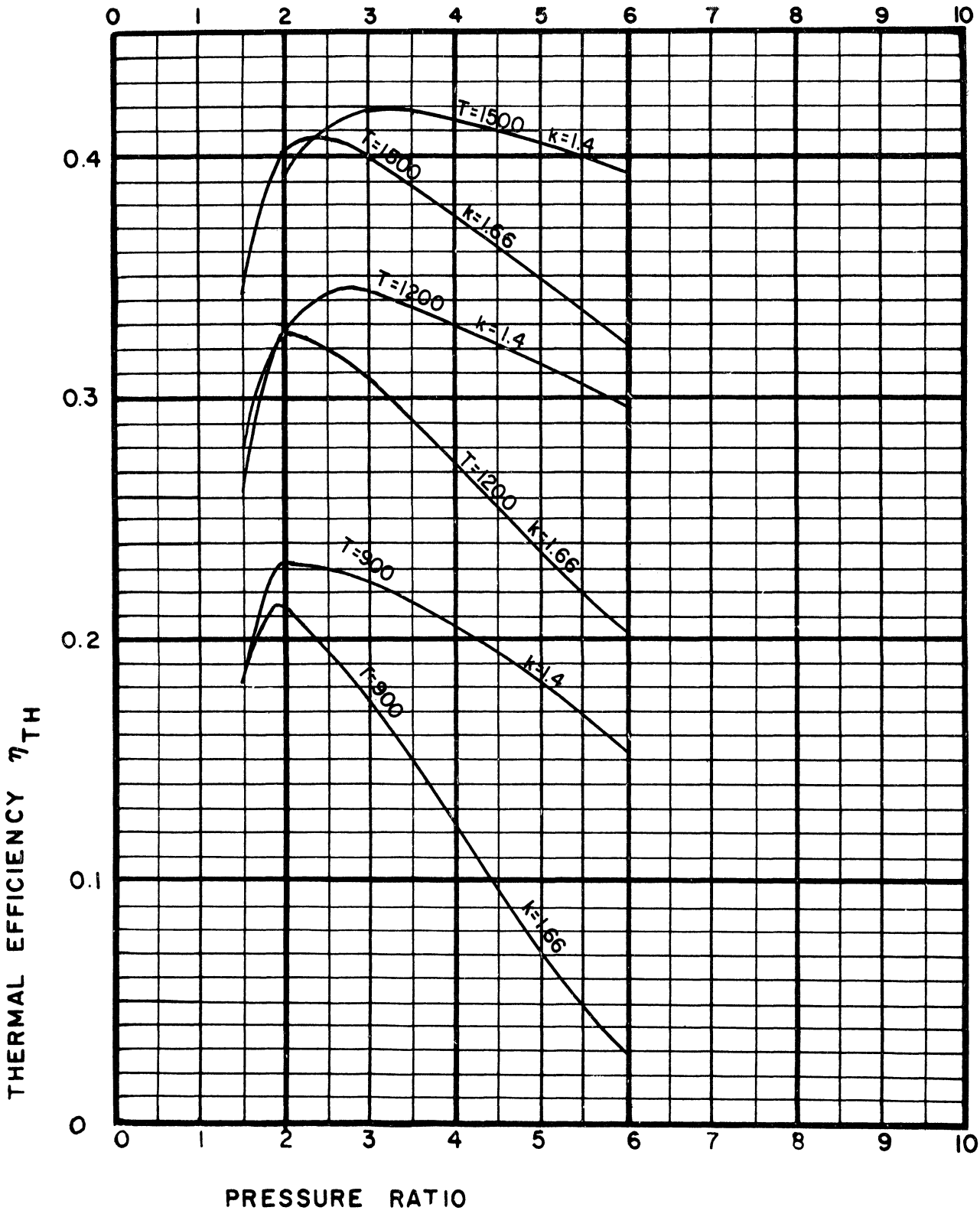

FIG. 7a. THERMAL EFFICIENCY OF A "BASIC"* GAS TURBINE CYCLE WITH RECUPERATOR EFFECTIVENESS = 0.93

* SEE TABLE 3, PART II

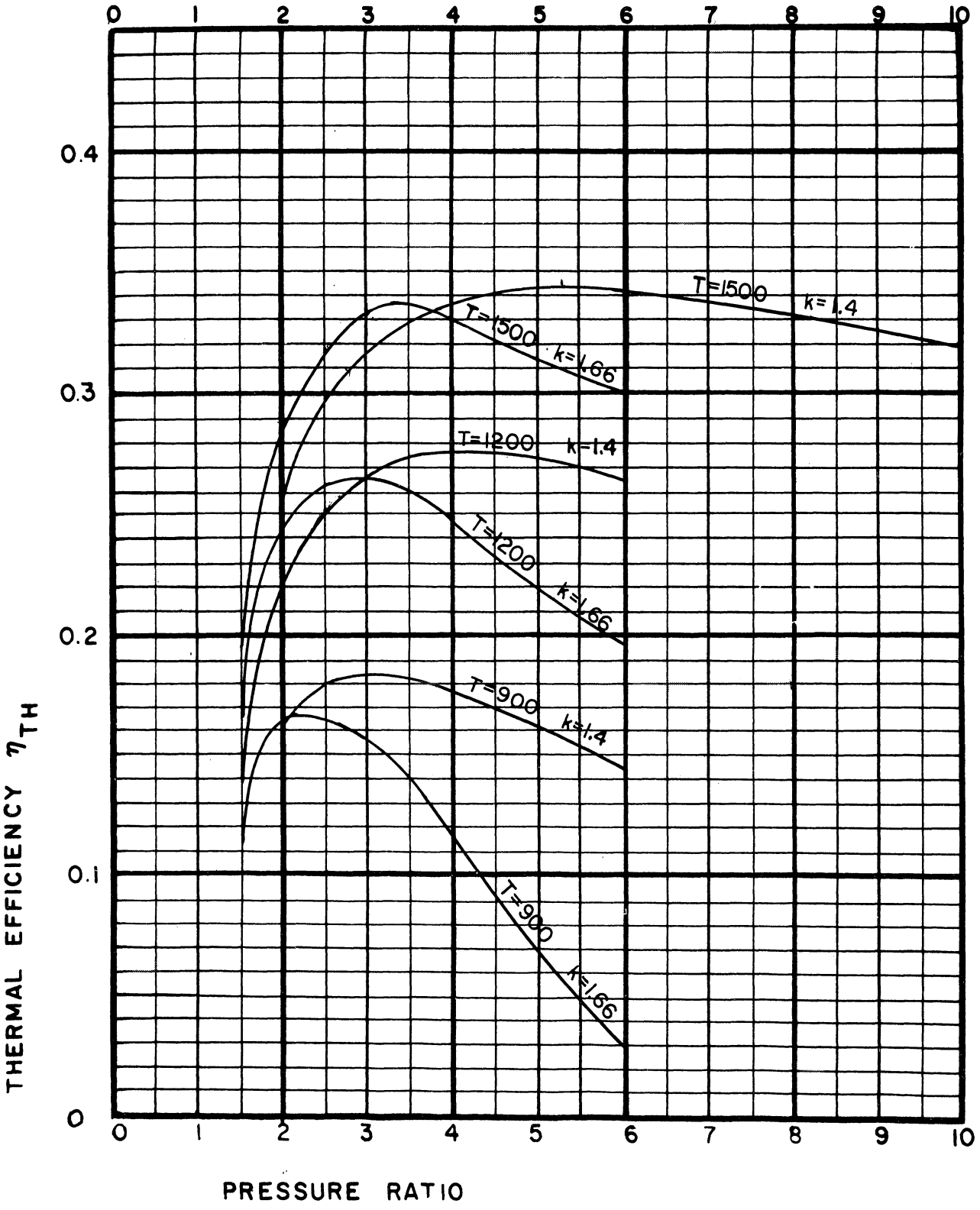

FIG. 7b. THERMAL EFFICIENCY OF A "BASIC"* GAS TURBINE CYCLE WITH RECUPERATOR EFFECTIVENESS = 0.75

*SEE TABLE 3, PART II

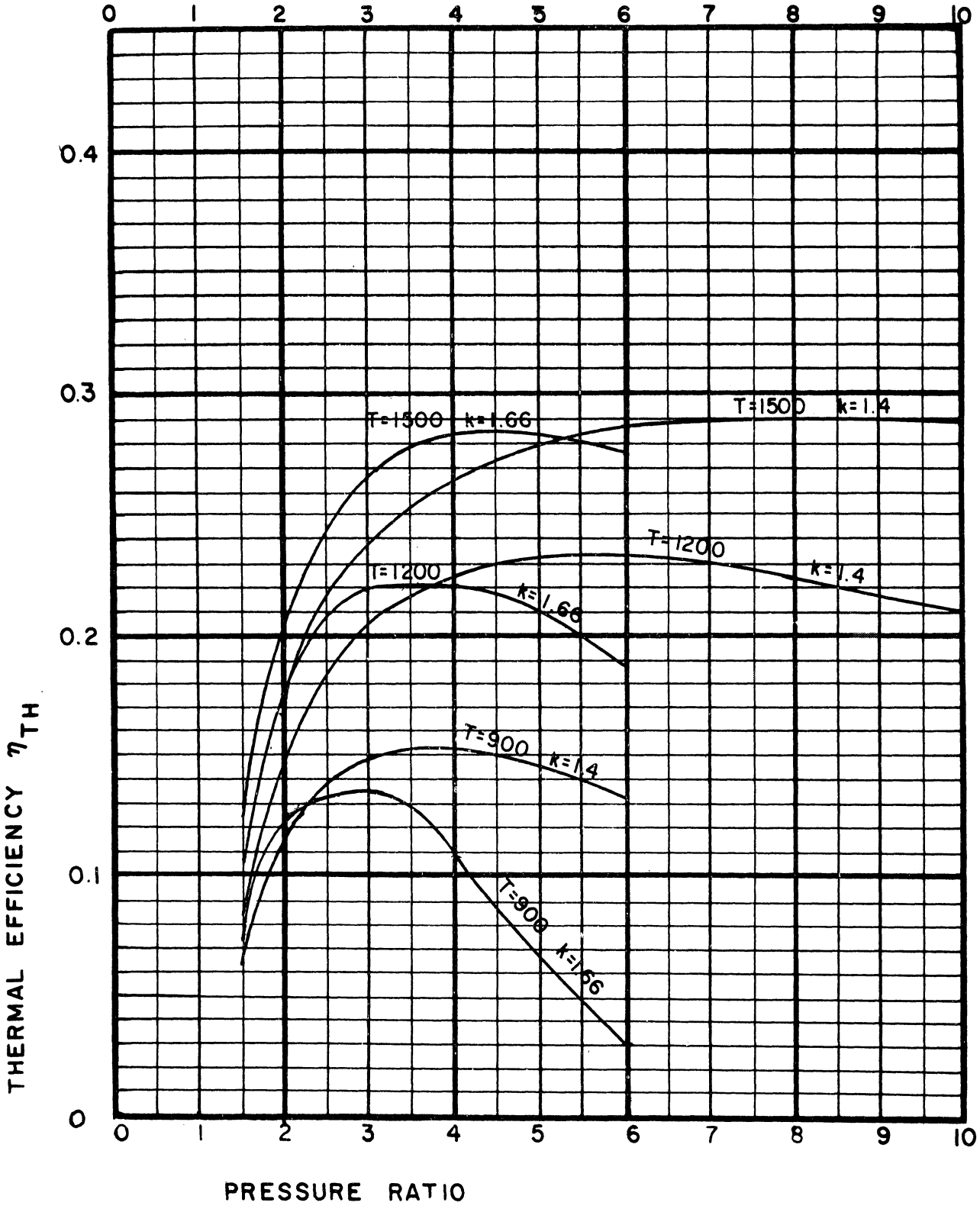

FIG. 7c. THERMAL EFFICIENCY OF A "BASIC"* GAS TURBINE CYCLE WITH RECUPERATOR EFFECTIVENESS=0.50

* SEE TABLE 3, PART II

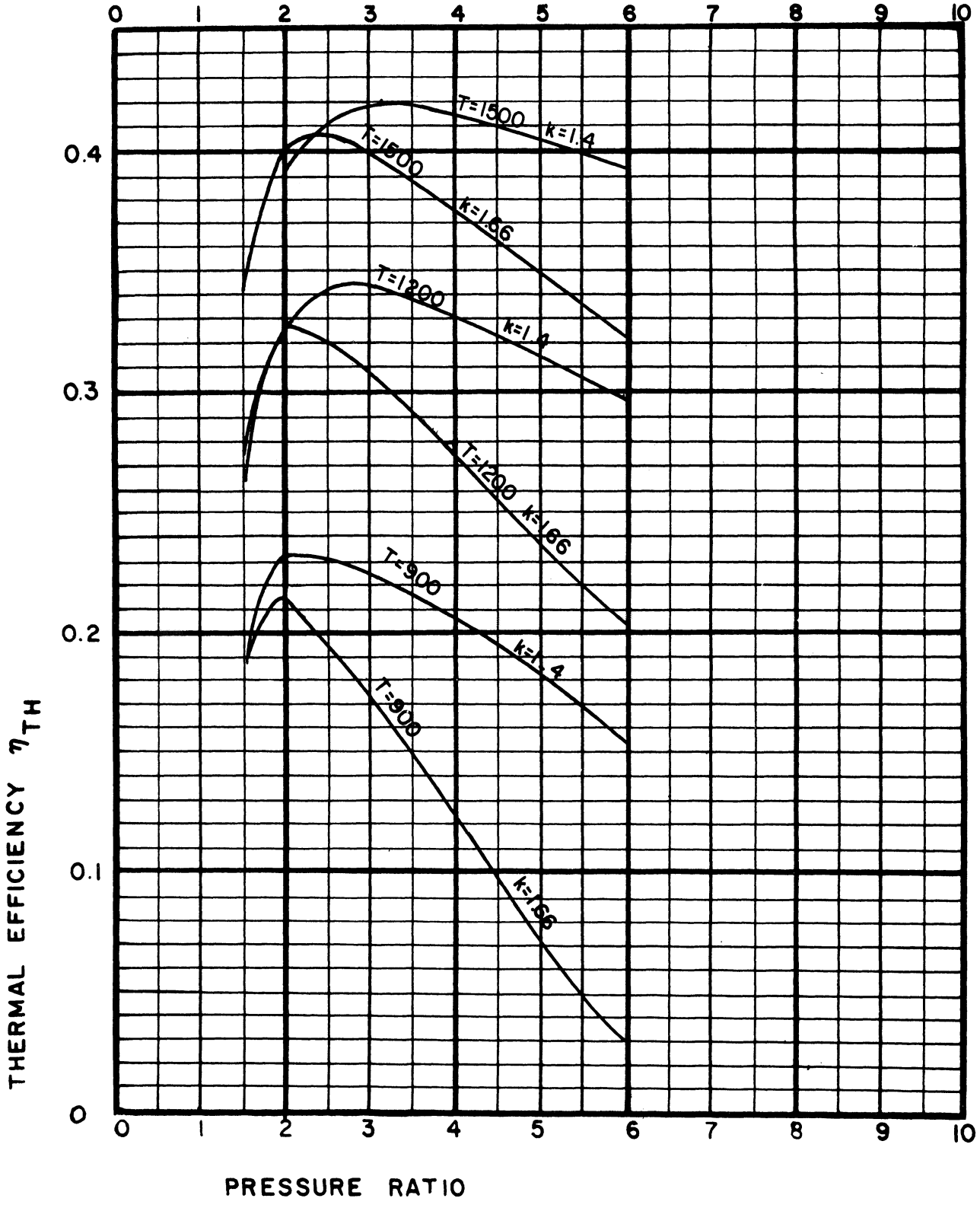

FIG. 8a. THERMAL EFFICIENCY OF A "BASIC"* GAS TURBINE CYCLE WITH FRICTIONAL PRESSURE LOSSES=0.07

*SEE TABLE 3, PART II

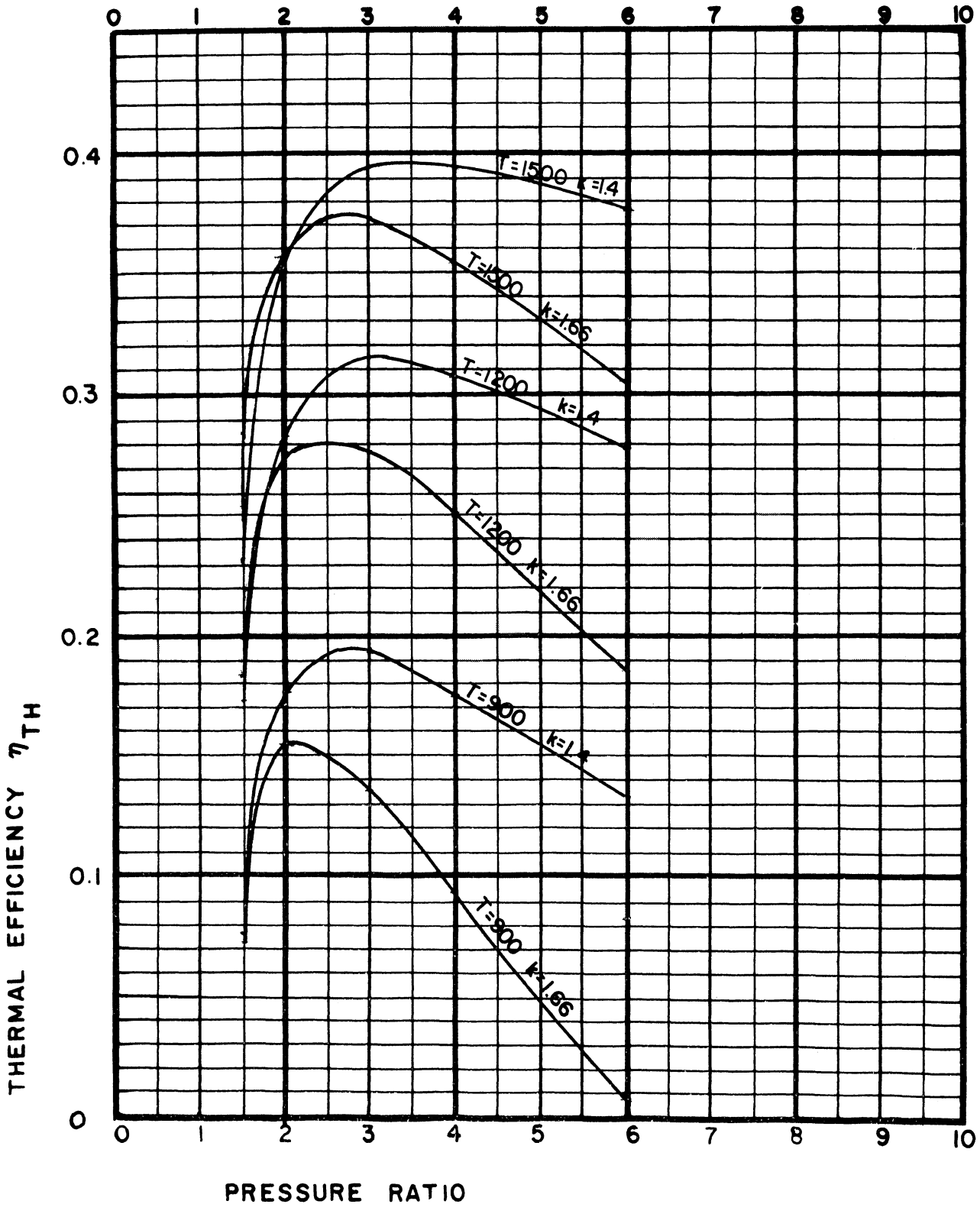

FIG. 8b. THERMAL EFFICIENCY OF A "BASIC"* GAS TURBINE CYCLE WITH FRICTIONAL PRESSURE LOSSES = 0.12

*SEE TABLE 3, PART II

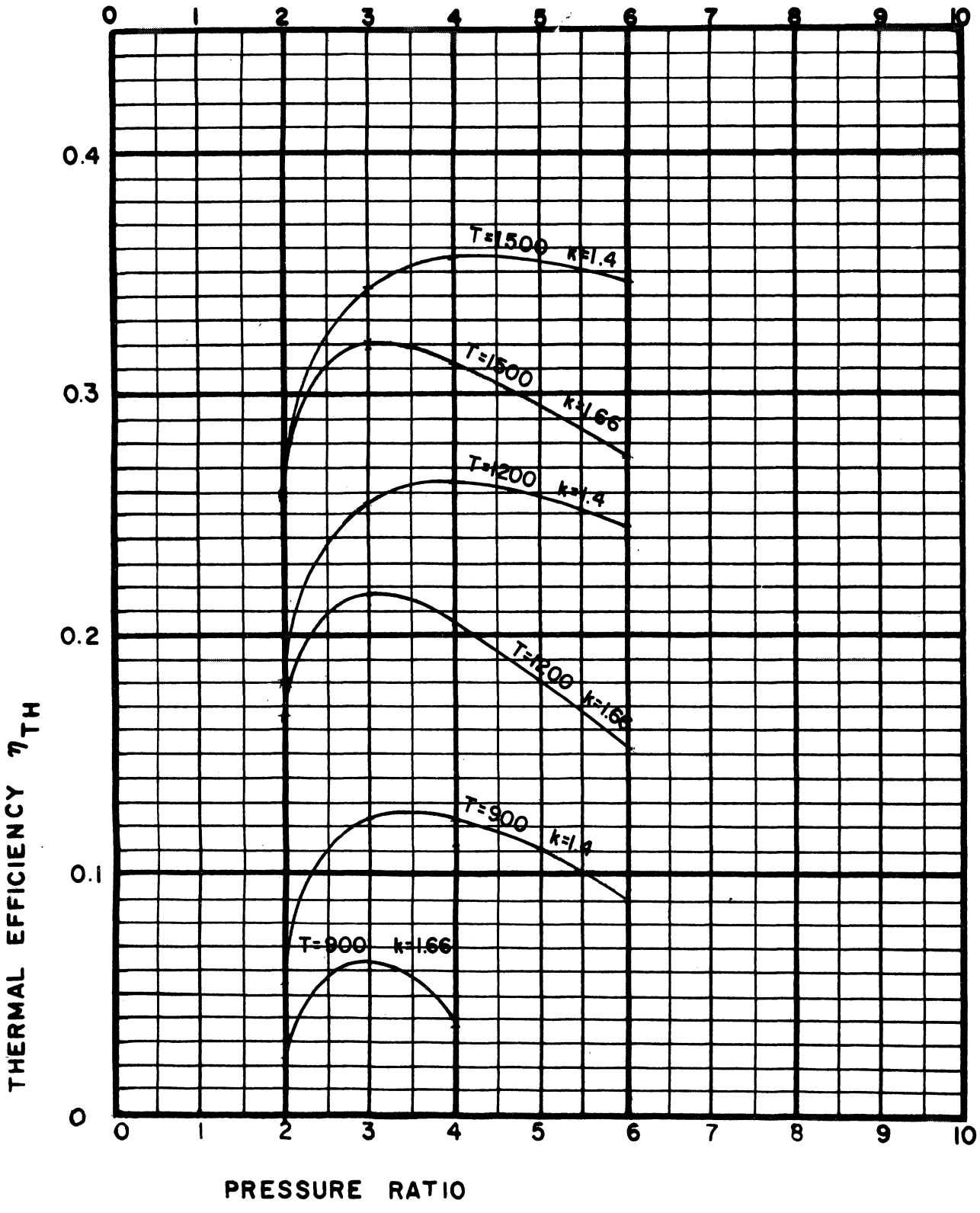

FIG. 8c. THERMAL EFFICIENCY OF A "BASIC"* GAS TURBINE CYCLE WITH FRICTIONAL PRESSURE LOSSES=0.20

*SEE TABLE 3, PART II

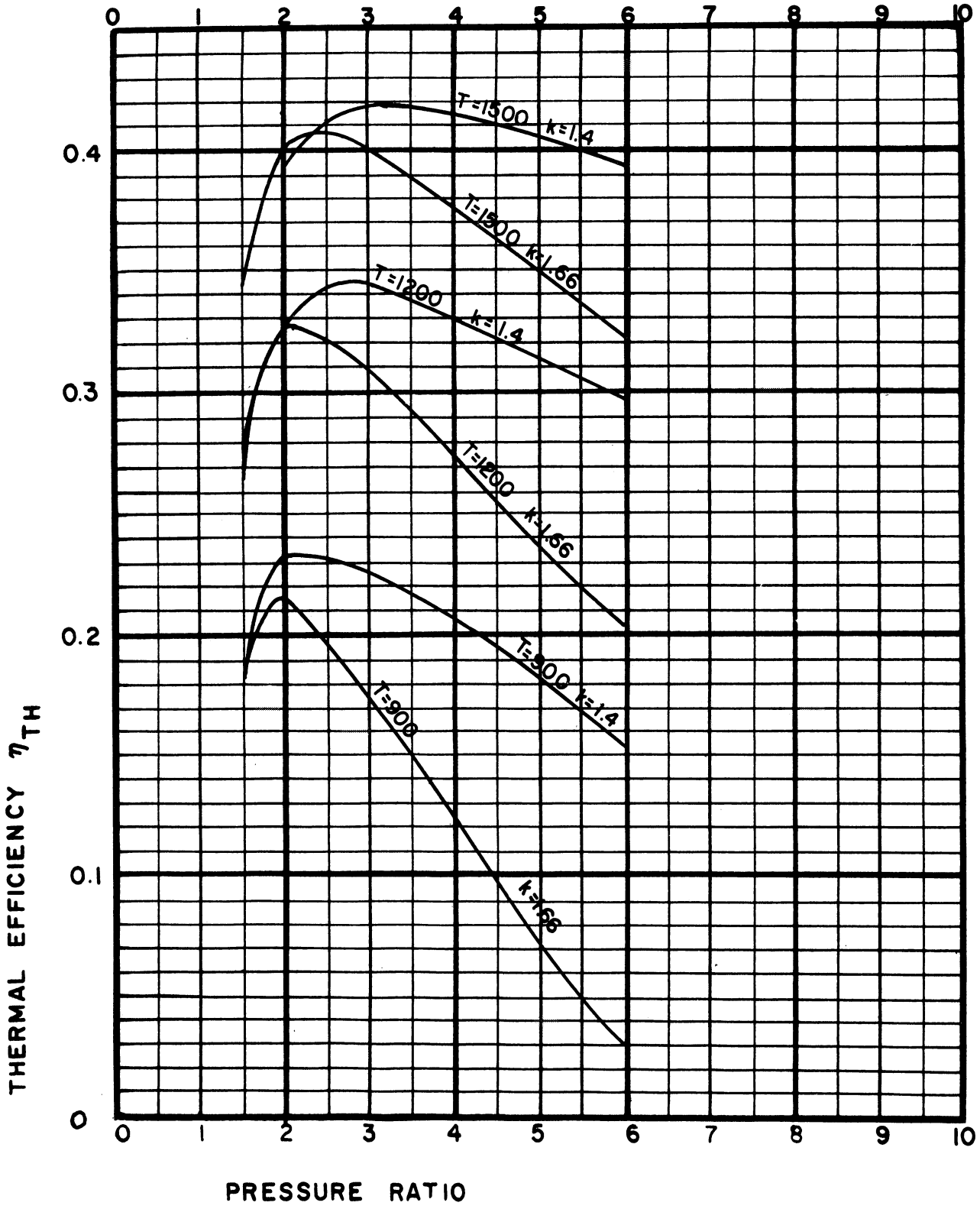

FIG. 9a THERMAL EFFICIENCY OF A "BASIC"* GAS TURBINE CYCLE WITH TURBINE EFFICIENCY= COMPRESSOR EFFICIENCY=0.85

* SEE TABLE 3, PART II

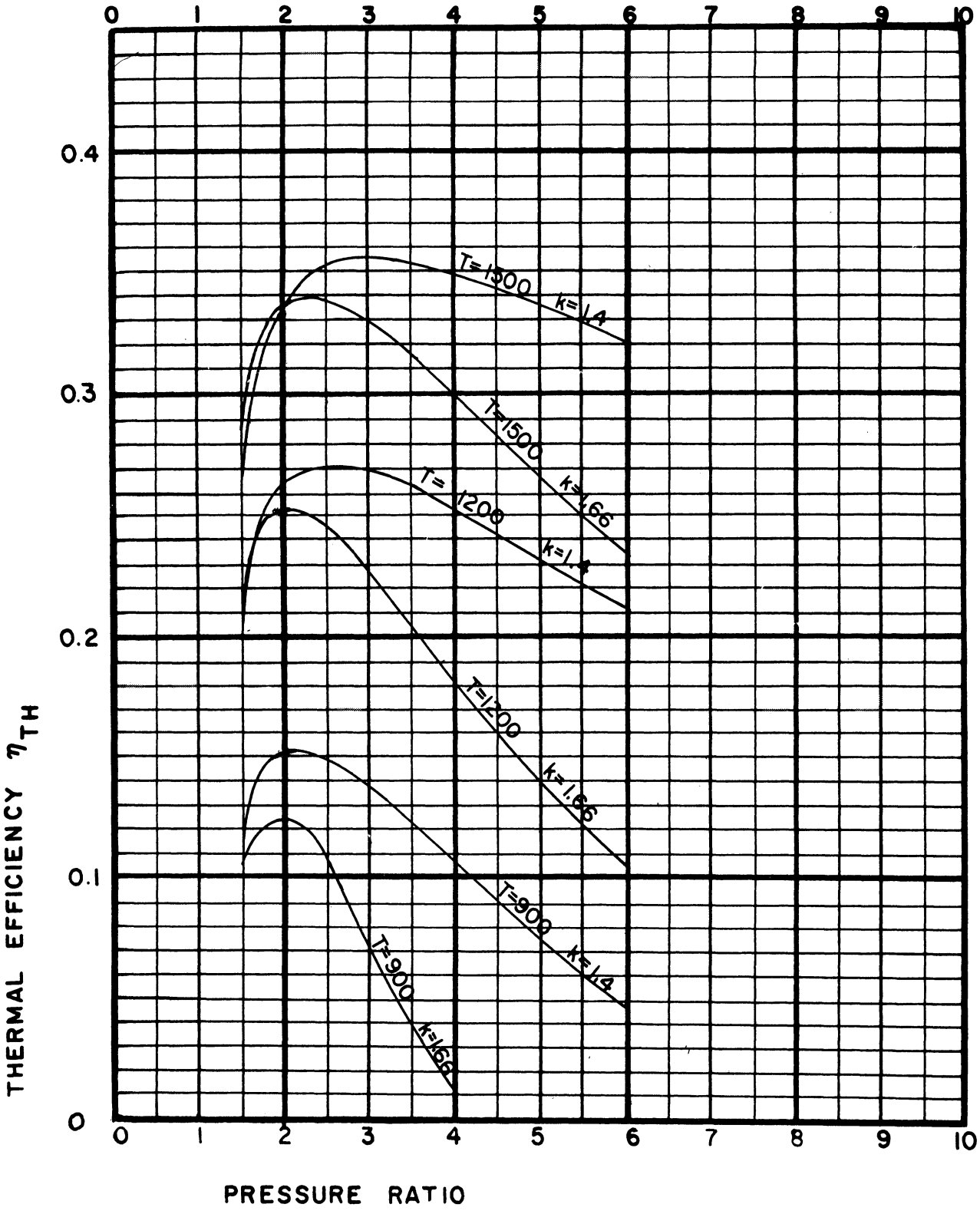

FIG. 9b THERMAL EFFICIENCY OF A "BASIC"*GAS TURBINE CYCLE WITH TURBINE EFFICIENCY=COMPRESSOR EFFICIENCY=0.80

*SEE TABLE 3, PART II

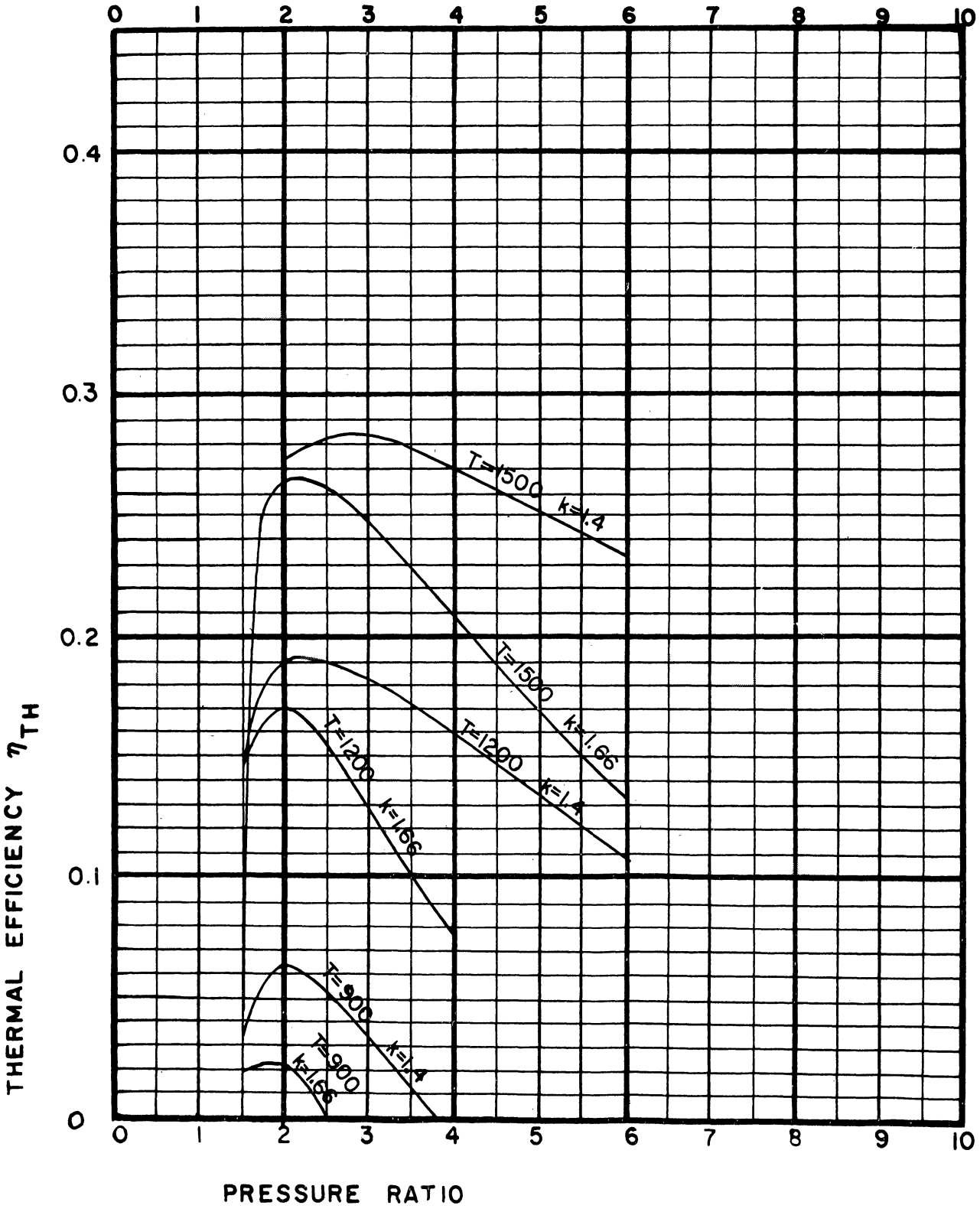

FIG. 9c. THERMAL EFFICIENCY OF A "BASIC"* GAS TURBINE CYCLE WITH TURBINE EFFICIENCY= COMPRESSOR EFFICIENCY= 0,75

* SEE TABLE 3, PART II

TABLE III. TABULATION OF CYCLE CONDITIONS PRESENTED IN REPORT

Cycle Diagram	Component Efficiency and Effectiveness							Results in Figure
	Turbine	Compressor	Recuperator	Intercooler	Duct & Heat Exch. Losses	Reheat	k	
Basic Cycle - Figure 1	.85	.85	.93	Yes	.07	No	1.4 1.66	6a
Basic Cycle - without Recuperator - Figure 2	.85	.85	No	Yes	.03	No	1.4 1.66	6b
Basic Cycle - without Intercooler - Figure 3	.85	.85	.93	No	.05	No	1.4 1.66	6c
Basic Cycle - without Intercooler & Recuperator- Figure 4	.85	.85	No	No	.01	No	1.4 1.66	6d
Basic Cycle - with Reheat Figure 5	.85	.85	.93	Yes	.09	Yes	1.4 1.66	6e
Basic Cycle - Figure 1	.85	.85	.93 .75 .50	Yes	.07	No	1.4 1.66	7
Basic Cycle - Figure 1	.85	.85	.93	Yes	.07 .12 .20	No	1.4 1.66	8
Basic Cycle - Figure 1	.85 .80 .75	.85 .80 .75	.93	Yes	.07	No	1.4 1.66	9
Basic Cycle - Figure 1	.75	.75	.93	Yes	.07	No	1.33 1.4 1.5 1.66	10

At 1500 F however, the relation is reversed and the efficiency is 42% with reheat and 44% without.* It will be noted that these values are greatly in excess of those for the cycles without a regenerator. For example, with an intercooler but without regenerator or reheater, the approximate obtainable maximum efficiencies at 900 F, 1200 F, and 1500 F, respective inlet temperatures are 13.5, 20.0, and 25.0. These values are obtained at a much greater pressure ratio than is optimum for the regenerative cycles. The optimum pressure ratios for the cycles with regenerator are in the order of 2.5 to 4.0 whereas for the non-regenerative cycle they are in the order of 5-10.

In all the cycles which are plotted, it is seen that a greater increase in thermal efficiency is realized for the temperature increase from 900 F to 1200 F than for the increase from 1200 F to 1500 F. This result is to be expected since it will be noted from the tabulated thermal efficiency functions in Table II that thermal efficiency is a function of temperature ratio across the cycle and not simply of temperature difference.

In considering the suitability of various gases for working fluids in such a cycle it has been noted in Section 1 that the molecular weight of the gas does not enter into the determination of the efficiency. The only effect of using various "perfect gases" with fixed component efficiencies is through the ratio of specific heats. This is relatively minor. Consequently, all diatomic gases are equal in efficiency and also all monatomic gases. The monatomic gas optimum efficiency is always a few points less than that of the diatomic gas. In fact, (Figure 10), optimum thermal efficiency increases consistently with decreasing ratio of specific heats. Of course, as was previously mentioned, these results may be misleading, since for a given physical heat exchanger component, the effectiveness may be higher with helium, for example, than with air, because of superior heat transfer properties. Then, for this case, the cycle efficiency with the monatomic gas may be superior to that with the diatomic gas.

The advantage of a diatomic over a monatomic gas decreases as the inlet temperature is increased. At 900 F, the thermal efficiency decreases from 23.5% with a diatomic gas in one case (Figure 6a) to 21.5% for the monatomic, and at 1500 F, from 42% for diatomic to 41% for monatomic gases.

The optimum pressure ratio increases as the maximum thermal efficiency increases. However, the extent of the increase is greater with a diatomic gas than with a monatomic gas. The cycle efficiency for a monatomic gas also tends to decrease more rapidly at pressure ratios above the optimum than for a diatomic gas. Thus the monatomic gas cycle does not allow as broad an operating range at high efficiency as does the diatomic.

---

* However, in all cases, reheat will considerably reduce mass flow rates.

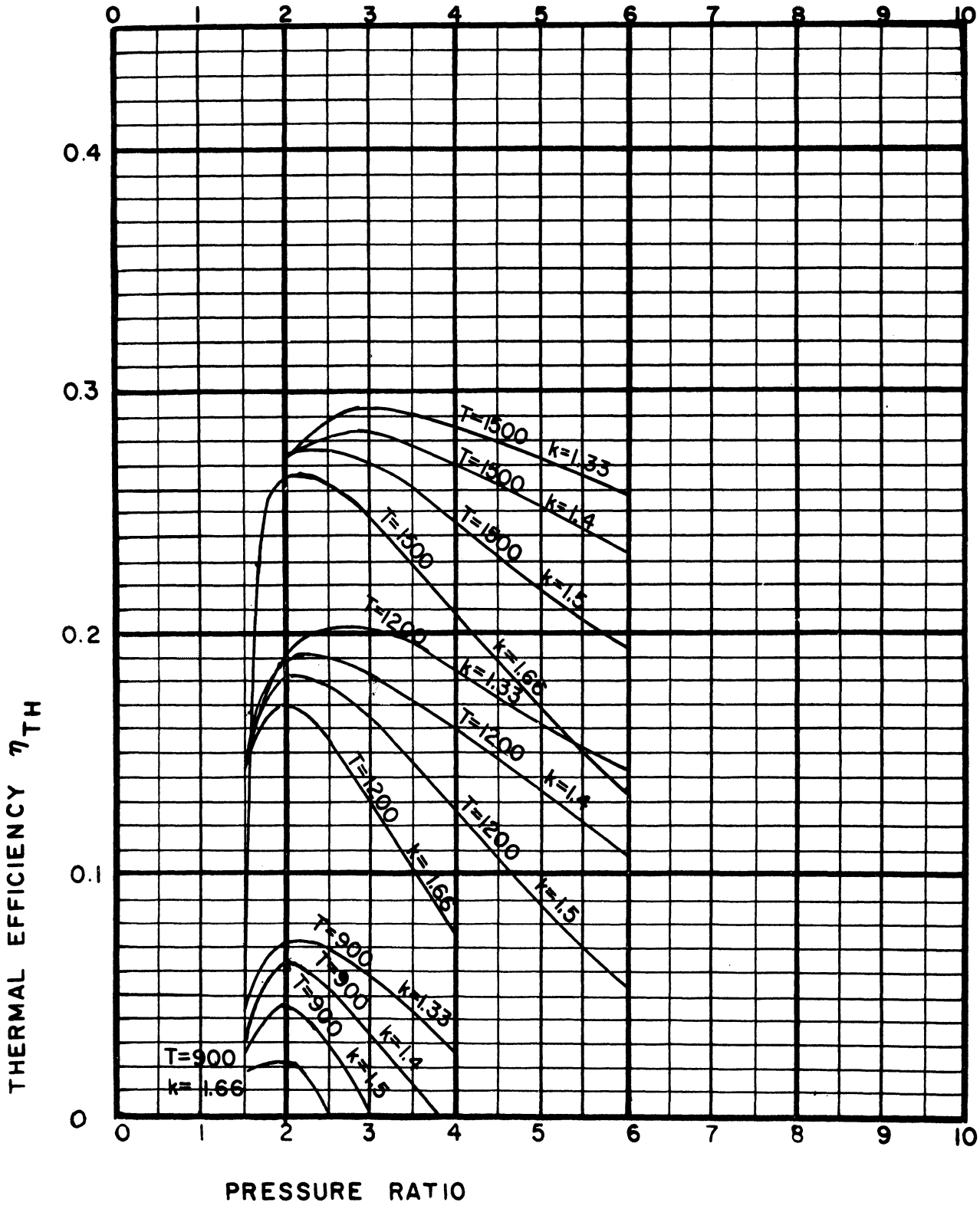

FIG. 10 THERMAL EFFICIENCY OF A "BASIC"* GAS TURBINE CYCLE WITH RATIO OF SPECIFIC HEATS VARIED.

* SEE TABLE 3, PART II

FIG. 11 THERMAL EFFICIENCY AT OPTIMUM PRESSURE RATIO AS A FUNCTION OF THE RATIO OF SPECIFIC HEATS. BASIC GAS TURBINE POWERPLANT WITH REGENERATOR AND INTERCOOLER.

RATIO OF SPECIFIC HEATS FOR WORKING FLUIDS VARIED.
INLET TEMPERATURE = 1500 F, 1200 F, and 900 F
REGENERATOR EFFECTIVENESS = .93
DISCHARGE TEMPERATURE = 90 F
DUCT AND HEAT EXCHANGER PRESSURE LOSSES = .07

CODE: ——— TURBINE AND COMPRESSOR EFFICIENCY = .85
– – – – – TURBINE AND COMPRESSOR EFFICIENCY = .80
——– ——– TURBINE AND COMPRESSOR EFFICIENCY = .75

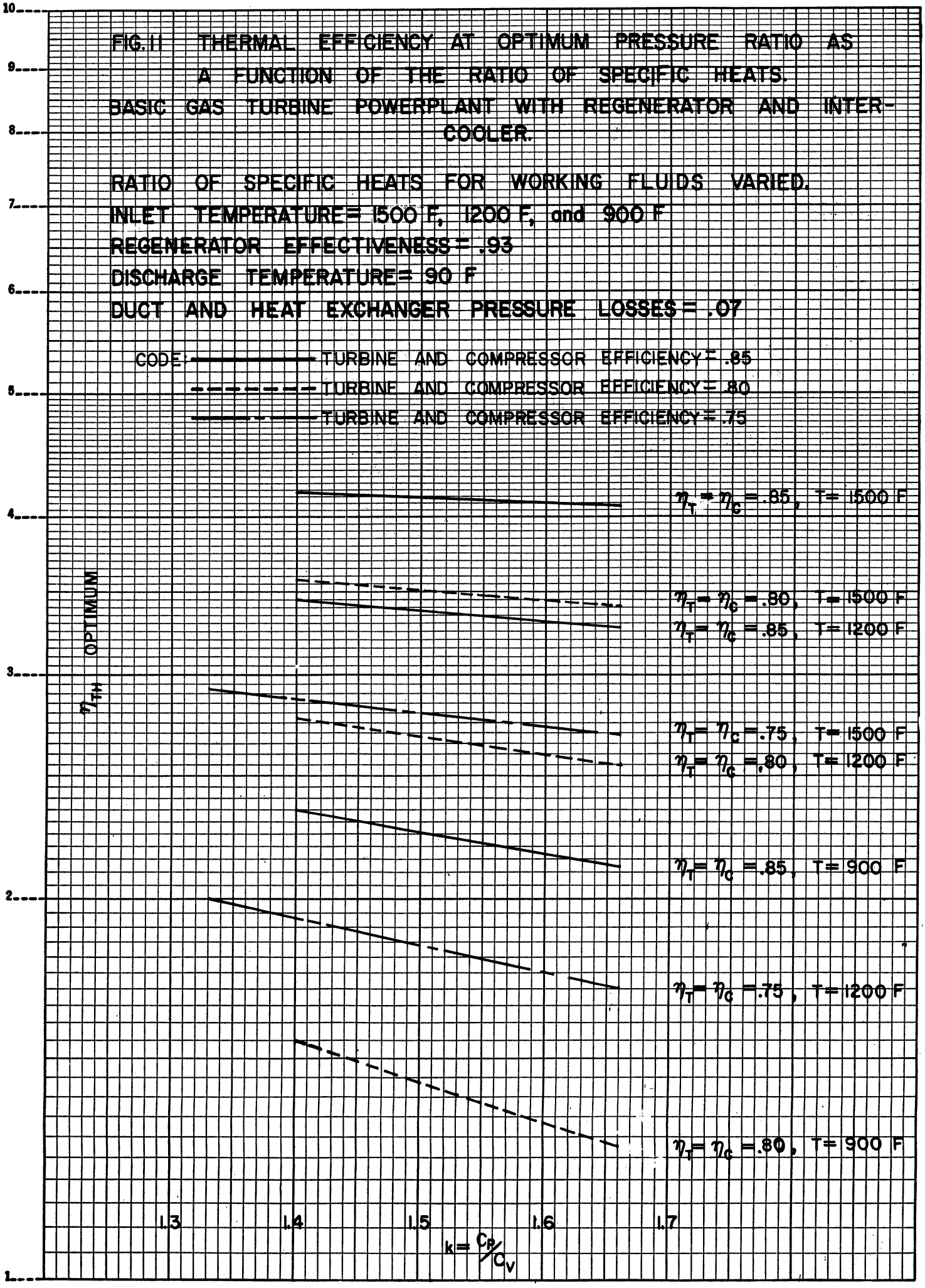

It would appear for this reason that the monatomic cycle would be at a somewhat greater disadvantage compared to the diatomic in off-design conditions (as part load) than for the design condition; i.e. if part load were to be achieved by reducing machinery speed rather than the alternate possibility for a closed cycle plant of reducing the operating pressure level by removing gas from the system.

It will be noted that the optimum pressure ratio also increases with reduced heat exchanger effectiveness. Figure 7 shows the effect as regenerator effectiveness is reduced from .93 to .75 to .50. In fact the optimum pressure ratio for the 1500 F cycle without regenerator (Figure 6b) is over 10, while it is only 4.2 for the 1500 F regenerative cycle with reheat and 3.2 for the regenerative cycle without reheat. It is only 2.3 for this cycle at 900 F (Figure 6a).

3.0 EFFECT OF PLANT SIZE AND REAL WORKING FLUID ON OTHER PLANT PARAMETERS

3.1 General Considerations

The data presented in Figures 1 through 10 and discussed in detail in Sections 1 and 2, Part II of this report are based on perfect gas relations and certain component efficiencies and effectivenesses. These are assumed to be typical regardless of plant size or actual working fluid. They are then arbitrarily varied to ascertain the corresponding change in overall plant thermal efficiency.

It is the purpose of the work reported in this section to attempt to evaluate the actual efficiency values which may most probably be obtained under various conditions of plant size, working fluid, operating pressure level, and available source and sink temperature. To date this work has been concerned mainly with the variation of turbine and compressor efficiency as a function of the above parameters and the corresponding effect on the overall plant efficiency. It appears useful to examine the heat exchanger components in the same way, including the interrelations of capital cost and operating cost for specific applications. Such an investigation will involve the cost of uranium processing, fuel rod fabrication, etc.

The present work has assumed given effectiveness levels for the heat exchangers. It is obviously possible to attain any desired effectiveness for such a component, the only question being one of the balance of capital cost, weight and "fuel" cost. The situation is somewhat different with respect to the turbomachinery. There is an approximate ceiling on the efficiency for a given application depending on flow rates, Mach numbers, Reynold's numbers, and the state of the art for this type of machinery. It is desirable in almost all cases to approach this ceiling value fairly closely; i.e. to utilize a sufficient number of stages at proper speeds, etc. Possible exceptions are air-borne devices where size and weight may be of especially overbearing importance compared to efficiency. This latter is particularly true of a nuclear plant, since in many cases, a reduction in thermal efficiency of the heat engine device will not increase the size of the reactor, or decrease the range of the vehicle or missile. It will only result in an increase in the replacement fuel costs. In many cases this would be of no importance whatsoever.

Efforts have been made to evaluate the ceiling value for turbomachinery efficiencies as it is affected by size of plant, working fluid, temperature, and pressure. The evaluation has been conducted for a closed cycle arrangement ("basic cycle"), which includes a compressor with a single intercooler, a turbine, a regenerator, and a heat source and sink. To the present time the evaluation has included air and helium as working fluids for plants ranging in size from 600 to 60,000 horsepower, for inlet

temperatures from 1500 F to 600 F, and for operating pressure levels, i.e. compressor discharge pressure, from 45 to 1000 psia. In the future the study will expand to include carbon dioxide. Air, helium, and carbon dioxide were chosen for the initial work since they cover a wide range of molecular weight with the corresponding variation of the other applicable quantities (sonic velocity, specific heat, ratio of specific heats, density, viscosity, etc.)

In order to simplify the calculations to some extent, a pressure ratio of 3.0 was selected for all the conditions. This is fairly close to the optimum for the "basic cycle" with high heat exchanger component effectivenesses for the entire range of temperatures for both diatomic and monatomic gases, as illustrated in Figure 6a. The other cycle constants which were assumed for the study are listed in Table IV.

TABLE IV. THERMODYNAMIC ASSUMPTIONS FOR PLANT DESIGN CALCULATIONS

Regenerator Effectiveness	0.93
Ratio of Compressor Pressure Ratio to Turbine Expansion Ratio	1.07
Cooling Medium Temperature	70 F
Minimum Working Fluid Temperature	90 F
Compressor Pressure Ratio	3.0
Insulation and Auxiliary Losses	3%

The results of the study may be used to estimate the probably efficiency of plants in which the cycle constants differ somewhat from those chosen. This can be accomplished through the use of Figures 7 through 9, where the loss of efficiency from the "basic cycle" optimum, chargeable to various changes in the cycle parameters considered separately, is illustrated.

3.2 Gas Properties

The air properties utilized in the study are as given in reference 1. References 1 and 2 were used for the viscosity data. These data consider the variation in the specific heat with temperature, but assume that the properties are constant with pressure. If the variations with pressure as presented in references 3 and 4 are considered, it is found that over the range of interest to this study the effect is negligible, i.e. the thermal efficiencies which are computed from the air properties as corrected for pressure variation are very close to those computed directly from the tables of reference 1.

For helium, perfect gas data was used. Extreme-case cycle efficiencies computed on this basis were compared with efficiencies computed from

the data given in reference 5 and it was found that the difference was negligible. Viscosity data for helium was taken from reference 2.

3.3 Turbomachinery Types Considered

The type of turbomachinery to be selected for a given application depends on:

1) flow rate,

2) efficiency desired,

3) temperature,

4) type of fluid (corrosive, lubricating qualities, abrasive qualities, necessity for seal integrity, etc.)

5) pressure level,

6) variation from design point.

In the selection of components for a gas turbine plant, flow rate and off-design performance are of the greatest importance. For a nuclear gas turbine plant, there may be introduced complications involving the necessity for absolute sealing if the fluid is radioactive, the necessity of preventing any admixture of lubricant and fluid, and the necessity for remote maintenance. In any closed cycle plant, if the fluid is other than air, there is the necessity for a very good sealing arrangement on the basis of the replacement cost of the fluid. For air, it becomes simply a matter of auxiliary power to operate the make-up compressor.

For the present, only the fluid-dynamic flow path design has been considered. The study will be expanded to consider the mechanical difficulties which will be involved if radioactive working fluids are to be utilized. However, the fluid-dynamic flow-path considerations dictate the choice of axial flow machinery for the large sizes, both for compressors and turbines for the attaining of optimum efficiency values. In general as the volume flow is decreased, because of low power requirements or high pressure levels at moderate power, the possibility of a centrifugal compressor and/or turbine exists. (For sufficiently small output, the centrifugal compressor efficiency surpasses that of the axial flow machine.) Because of its more stable operating conditions over a broader range, it may become the logical choice for small plants. If very small flow rates are to be considered, there is in fact the possibility that positive displacement machinery may show to advantage in certain applications. If weight and space are not important, it is certainly true that the efficiencies in small sizes of such a device (reciprocating or rotating) may be superior to the centrifugal or axial machines. However, in a closed cycle nuclear plant there may be

added difficulties of sealing and of preventing any contamination of the working fluid from lubrication.

The same considerations of applicable type of machine versus flow rate may be applied also to the turbine. However, due to the favorable direction of the pressure gradient in the boundary layer, turbine design is not nearly so sensitive a matter as is compressor design. Hence, it is believed that an axial flow type can be used for the entire range. This is not to say that centripedal or centrifugal turbines, or even positive displacement expanders, may not be more applicable for certain situations, but only that the axial-flow turbine efficiency will be typical, and not too far from the optimum.

For the cycle evaluations herein reported, axial-flow, centrifugal, and positive displacement (as the Lysholm type) compressors were considered in the applicable flow range. Axial-flow turbine designs were considered throughout. It was assumed that a turbine of this type, with 100% arc of admission, was feasible to a wheel diameter of 5 inches with a 5/8 inch blade height. Because of the necessity of high efficiency in this type of plant, no partial admission designs were deemed suitable. Thus the operating pressure level for the minimum output plant considered is based on reasonable volume flow requirements for such a turbine.

3.4 Methods of Efficiency Estimation

Efficiencies were estimated for the compressors and turbines primarily on the basis of correcting the handbook values as quoted for given flow rates with air at nominal pressures, according to the Reynold's number and Mach number effect. This takes account of both pressure and working fluid variation from the air machines. For the relatively large machines the data was abstracted from reference 6 for axial, centrifugal, and positive displacement Lysholm type compressors. This data was plotted as shown in Figure 12 and extrapolated into the low ranges according to data available from private sources. It is assumed that the efficiency of air compressors, with the fixed pressure ratio of 3 and drawing suction from atmospheric air follows the curve shown. While there are no doubt examples of numerous machines which vary substantially from these values, it is believed that the curve is typical and certainly illustrates the correct trend. A division between the ranges of axial, centrifugal, and positive displacement machines was made. This is more or less arbitrary but follows the information of reference 6. It is assumed that the actual efficiencies obtainable with axial and centrifugal machines of a given size is a function of the Reynold's number and the Mach number but that these parameters have no effect on the efficiency of the positive displacement machine. It is believed that the assumptions are well substantiated by experimental results.

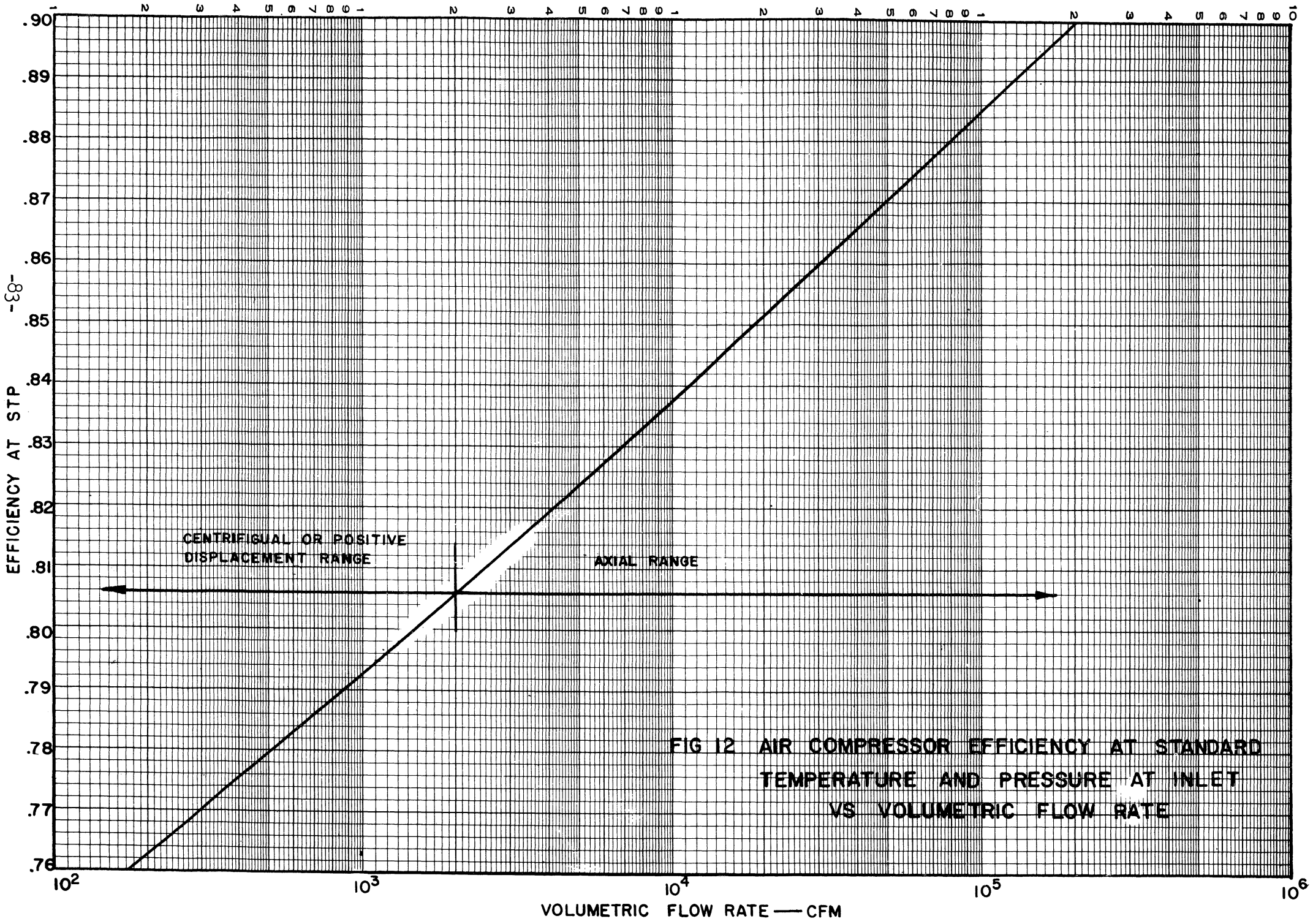

FIG 12 AIR COMPRESSOR EFFICIENCY AT STANDARD TEMPERATURE AND PRESSURE AT INLET VS VOLUMETRIC FLOW RATE

3.4.1 Axial Flow Compressors

To correct the efficiencies from the values applying to air at standard temperature and pressure suction, the Reynold's number and Mach number for the standard air case as well as the actual case under consideration must be computed and compared. To accomplish this, certain assumptions with respect to the compressor design must be made. It is assumed that symmetrical staging will be used as a typical although not necessarily optimum solution, with a pressure ratio per stage of 1.082 for air. The vector diagram is illustrated in Figure 13. Using typical blading angles, the axial velocity becomes 200 ft/sec, which is again a reasonably typical value. It is assumed that the hub/tip diameter ratio is 0.75 and that the ratio of blade height to blade spacing measured perpendicular to the flow stream is 0.500 of the blade height. Then the hydraulic diameter of the blading flow path becomes 0.667 x blade height. (On the basis that the guidance of flow need not be as close in the turbine as in the compressor, a blade height to passage width ratio of 0.48 was assumed for the turbine. This is believed to be in the direction of optimization since the frictional loss becomes less with the reduced blading surface area.)

From these relations the compressor wheel dimensions were computed and are tabulated for the various plants in Tables V through IX. The Reynold's numbers for each condition (all dimensions and computations refer to the first stage for both compressor and turbine), based on relative blading velocity and passage hydraulic diameter perpendicular to the flow, were computed. These also are tabulated. On the same basis, Reynold's number values for the standard temperature and pressure air machines were computed and listed.

To estimate the actual efficiency of an axial flow compressor for given conditions with a given working fluid, the efficiency for a machine of the same volumetric capacity pumping air at standard temperature and pressure suction conditions is first noted from the curve of Figure 12. It is then necessary to consider those changes in condition between the air fluid and that under consideration, and to apply suitable correction factors.

It is usually considered that the efficiency of an axial flow compressor will be affected by mechanical losses, leakage losses (both shaft seals and blade tip leakage), and by fluid dynamic losses associated with the blading. The mechanical losses are usually quite small compared to the overall power. These are assumed as a constant proportion for the investigation. Leakage losses are mainly a matter of dimensional control (i.e. a certain portion of the prescribed flow path area through the blading is available for leakage flow around the tips; shaft sealing losses are also a function of the clearances) and so, for

AIR - 14 STAGES
PRESSURE RATIO PER STAGE = 1.082

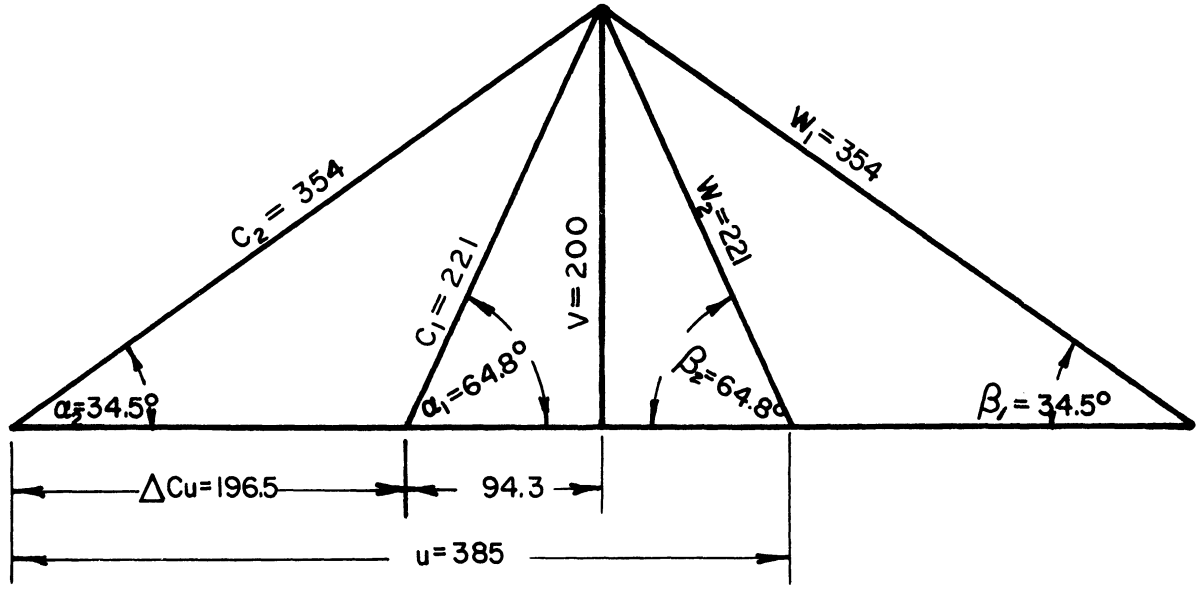

HELIUM - 16 STAGES
PRESSURE RATIO PER STAGE = 1.071

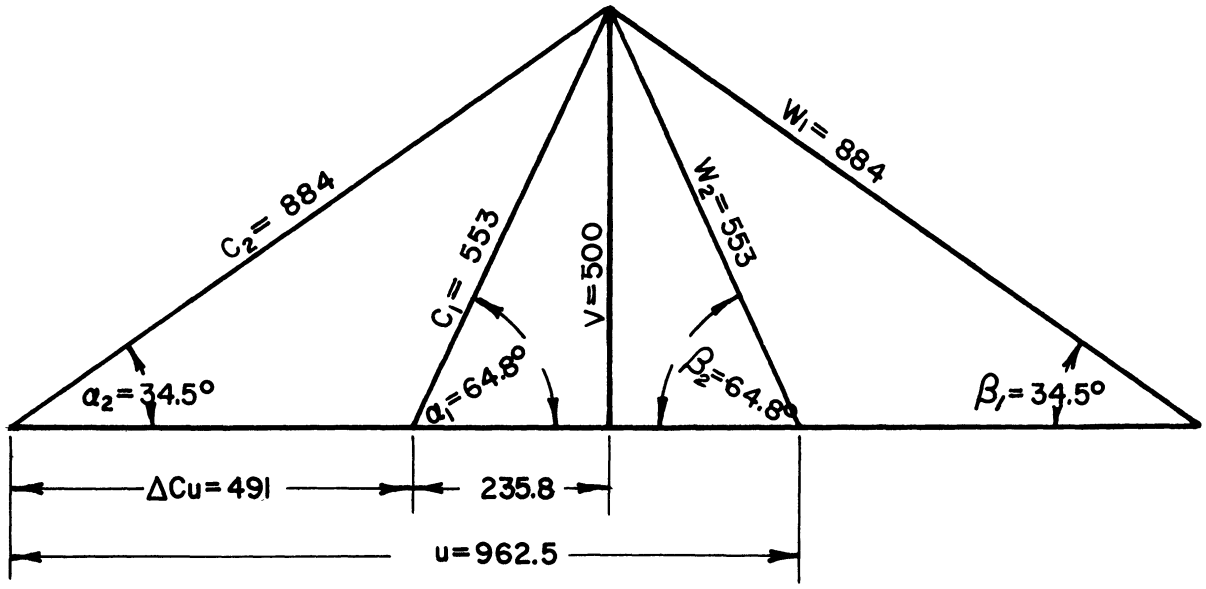

FIG. 13 VELOCITY VECTOR DIAGRAMS FOR AIR AND HELIUM.
a. COMPRESSOR DIAGRAM

AIR - 9 STAGES
PRESSURE RATIO PER STAGE = 1.121

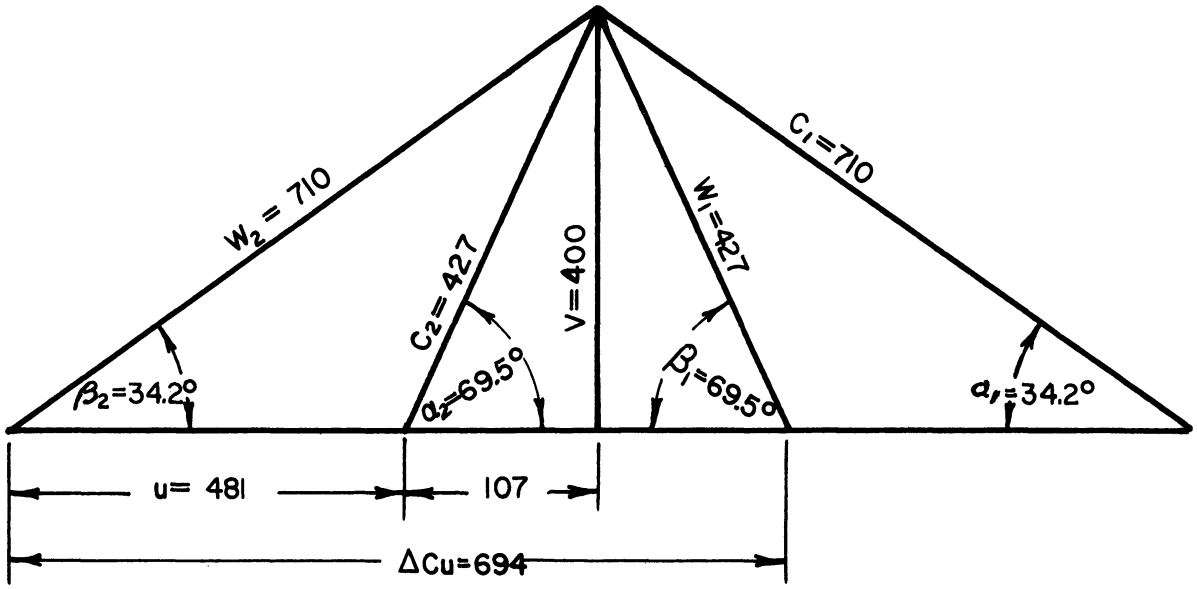

HELIUM - 21 STAGES
PRESSURE RATIO PER STAGE = 1.050

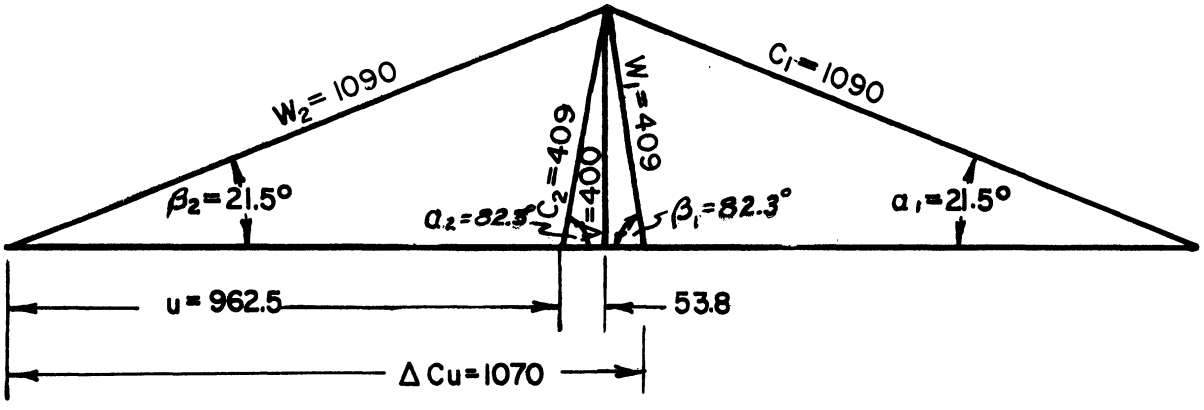

FIG. 13 VELOCITY VECTOR DIAGRAMS FOR AIR AND HELIUM.
b. TURBINE DIAGRAMS

(1) T_1 (°F) & $\Delta h'_T$ BTU/#	(2) P_1 PSIA	(3) W #/sec	(4) G_T CFM $\times 10^{-3}$	(5) A_T Sq. In.	(6) h_{bd_T} inches	(7) $D_{T_{tip}}$ inches	(8) G_c CFM $\times 10^{-3}$	(9) A_C Sq. In.	(10) h_{bd_c} inches	(11) $D_{hyd.}$ inches	(12) μ_c #/hr.ft	(13) Re_c $\times 10^{-4}$	(14) Re_c STP $\times 10^{-4}$	(15) η_c STP	(16) $\Delta \eta_c$ Corr.	(17) η_c Final	(18) HP_T HP $\times 10^{-3}$	(19) η_{TH}
1500°	1000	759	33.0	198	1.75	37.4	27.8	334	3.90	2.60	.0436	870	35.0	.857	.020	.877	114	.433
"	700	759	47.6	286	2.10	44.6	39.9	478	4.66	3.10	.0436	727	45.0	.865	.018	.883	115	.491
1218	400	759	82.6	496	2.75	59.0	69.9	838	6.15	4.10	.0436	546	60.4	.877	.014	.891	116	.498
1200°	1000	1085	40.0	240	1.75	44.6	39.8	478	4.66	3.10	.0436	1040	45.0	.865	.020	.885	139.5	.378
"	700	1085	57.1	343	2.15	53.5	56.9	684	5.59	3.72	.0436	867	54.5	.872	.016	.888	140.0	.382
1028	400	1085	100.0	600	2.90	70.8	100	1200	7.38	4.92	.0436	656	72.5	.885	.013	.898	141.8	.392
900	1000	1895	57.3	344	1.85	59.1	69.5	834	6.16	4.11	.0436	1370	60.0	.877	.019	.896	201	.291
"	700	1895	81.7	491	2.25	70.6	99.4	1192	7.36	4.91	.0436	1143	72.5	.885	.016	.900	202	.298
83.65	400	1895	143	860	3.00	93.6	174.5	2092	9.75	6.50	.0436	866	96.5	.897	.012	.900	202	.298

TABLE V – CALCULATIONS FOR GAS TURBINE POWERPLANT

Working Fluid – *Air* , T_6 = 90°F , Output = 60,000 HP

$P.R._T$ = 2.79, $P.R_c$ = 3.00, D_h / D_t = .75, η_R = .93

NOTE: $\Delta h'_c$ = 45

(1) T_1 (°F) & $\Delta h'_T$ BTU/#	(2) P_1 PSIA	(3) W #/sec	(4) G_T CFM $\times 10^{-3}$	(5) A_T Sq. In.	(6) h_{bd_T} inches	(7) $D_{T_{tip}}$ inches	(8) G_c CFM $\times 10^{-3}$	(9) A_C Sq. In.	(10) h_{bd_c} inches	(11) $D_{hyd.}$ inches	(12) μ_c #/hr.ft	(13) Re_c $\times 10^{-4}$	(14) Re_c STP $\times 10^{-4}$	(15) η_c STP	(16) $\Delta \eta_c$ Corr.	(17) η_c Final	(18) HP_T HP $\times 10^{-3}$	(19) η_{TH}
1500°	1000	253	11.0	66.0	1.05	21.4	9.3	111.4	2.23	1.49	.0436	504	21.5	.833	.022	.855	37.2	.416
¢	700	253	15.75	94.5	1.25	25.7	13.3	159.4	2.68	1.79	.0436	420	26.5	.841	.019	.860	37.4	.421
121.8	400	253	27.5	165	1.60	34.1	23.3	280	3.56	2.37	.0436	317	35.0	.853	.015	.868	37.8	.427
	100	253	110	660	3.15	68.5	93	1114	7.13	4.75	.0436	159	70.0	.883	.006	.889	38.8	.444
	45	253	245	1470	4.80	101.8	206	2472	10.6	7.06	.0436	106	104.2	.900	—	.900	39.2	.456
1200°	1000	361	13.35	80.0	1.05	25.7	13.3	159.2	2.68	1.79	.0436	598	26.5	.841	.021	.862	45.1	.348
¢	700	361	19.0	114	1.25	30.8	19.0	228	3.20	2.13	.0436	500	32.0	.849	.018	.867	45.4	.356
102.8	400	361	33.3	200	1.60	40.9	33.2	400	4.26	2.84	.0436	379	40.5	.861	.015	.876	46.0	.370
	100	361	133.5	800	3.25	81.6	133	1592	8.51	5.68	.0436	190	84.0	.891	.0055	.897	47.1	.391
	45	361	296	1775	4.90	121.9	294	3530	12.7	8.47	.0436	127	124.2	.900	—	.900	47.2	.394
900°	1000	632	19.1	114.5	1.10	34.2	23.2	278	3.56	2.37	.0436	794	35.0	.853	.020	.873	65.4	.261
¢	700	632	27.2	163.5	1.30	40.9	33.2	400	4.26	2.84	.0436	664	40.5	.861	.020	.881	66.0	.271
83.65	400	632	47.8	287	1.75	54.3	58.2	698	5.64	3.76	.0436	500	55.0	.873	.014	.887	66.4	.283
	100	632	191	1145	3.40	107.3	232	2780	11.2	7.47	.0436	250	109.5	.900	—	.900	67.3	.297
	45	632	424	2540	5.20	161	515	6180	16.8	11.2	.0436	168	164.5	.900	—	.900	67.3	.297

TABLE VI – CALCULATIONS FOR GAS TURBINE POWERPLANT

Working Fluid – *Air* , T_c = 90°F , Output = *20,000 HP*

$P.R._T$ = 2.79, $P.R_c$ = 3.00, D_h / D_t = .75, η_R = .93

NOTE: $\Delta h'_c$ = *45*

(1) T_1 (°F) & $\Delta h'_T$ BTU/#	(2) P_1 PSIA	(3) W #/sec	(4) G_T CFM $\times 10^{-3}$	(5) A_T Sq. In.	(6) h_{bd_T} inches	(7) $D_{T_{tip}}$ inches	(8) G_c CFM $\times 10^{-3}$	(9) A_C Sq. In.	(10) h_{bd_c} inches	(11) $D_{hyd.}$ inches	(12) μ_c #/hr.ft.	(13) $Re_c \times 10^{-4}$	(14) Re_c STP $\times 10^{-4}$	(15) η_c STP	(16) $\Delta \eta_c$ Corr.	(17) η_c Final	(18) HP_T HP $\times 10^{-3}$	(19) η_{TH}
1500°	1000	75.9	3.30	22.0	.625	11.8	2.78	33.4	1.23	.820	.0436	275	12.1	.812	.023	.835	10.90	.389
&	700	75.9	4.76	28.6	.675	14.2	3.98	47.8	1.48	.987	.0436	240	15.15	.819	.021	.840	10.95	.395
1218	400	75.9	8.26	49.6	.875	18.7	6.99	83.8	1.95	1.30	.0436	173.5	19.0	.830	.017	.847	11.08	.404
	100	75.9	33.0	198	1.75	37.4	27.8	334	3.90	2.60	.0436	86.8	36.0	.857	.006	.863	11.25	.423
	45	75.9	73.4	491	2.60	55.6	61.9	744	5.80	3.87	.0436	58.4	57.0	.874	—	.874	11.4	.431
1200°	1000	108.5	4.00	27.0	.625	14.1	3.98	47.8	1.47	.987	.0436	328	14.5	.819	.023	.842	13.30	.326
&	700	108.5	5.71	34.3	.675	16.9	5.69	68.4	1.76	1.17	.0436	275	17.35	.826	.021	.847	13.35	.332
1028	400	108.5	10.00	60.0	.900	22.4	10.0	120	2.34	1.56	.0436	208	22.5	.836	.017	.853	13.43	.340
	100	108.5	40.0	240	1.85	44.8	39.8	478	4.66	3.11	.0436	104	45.0	.864	.006	.870	13.71	.360
	45	108.5	89.0	534	3.07	66.6	88.5	1062	6.94	4.63	.0436	69.5	68.0	.882	—	.882	13.9	.373
900°	1000	189.5	5.73	35.5	.625	18.7	6.95	83.4	1.95	1.30	.0436	435	19.0	.829	.022	.851	19.0	.225
&	700	189.5	8.17	49.1	.750	22.3	9.94	119	2.32	1.55	.0436	362	22.4	.836	.020	.856	19.2	.234
83.65	400	189.5	14.3	86.0	.950	29.5	17.45	209	3.08	2.05	.0436	274	30.5	.847	.015	.862	19.3	.242
	100	189.5	57.3	344	1.85	59.1	69.5	834	6.16	4.11	.0436	137	60.5	.877	.006	.883	19.8	.274
	45	189.5	127.0	763	4.12	88.0	154.5	1852	9.16	6.11	.0436	92.0	91.0	.897	—	.897	20.1	.292

TABLE VII – CALCULATIONS FOR GAS TURBINE POWERPLANT

Working Fluid – *Air* , T_c = 90°F , Output = 6,000 HP

$P.R._T$ = 2.79, $P.R_c$ = 3.00, D_h / D_t = .75, η_R = .93

NOTE: $\Delta h'_c$ = 45

(1) T_1 (°F) & $\Delta h'_T$ BTU/#	(2) P_1 PSIA	(3) W #/sec	(4) G_T CFM $\times 10^{-3}$	(5) A_T Sq. In.	(6) h_{bd_T} inches	(7) $D_{T_{tip}}$ inches	(8) G_c CFM $\times 10^{-3}$	(9) A_C Sq. In.	(10) h_{bd_c} inches	(11) $D_{hyd.}$ inches	(12) μ_c #/hr.ft.	(13) Re_c $\times 10^{-4}$	(14) Re_c STP $\times 10^{-4}$	(15) η_c STP	(16) $\Delta \eta_c$ Corr.	(17) η_c Final	(18) HP_T HP $\times 10^{-3}$	(19) η_{TH}
1500°	1000	30.2	1.315	8.60	.625	5.00	1.11	13.3	*	*	.0436	173.6	7.66	.796	—	.796	4.26	.359
¢	700	30.2	1.88	8.60	.625	5.00	1.59	19.0	*	*	.0436	144.5	9.11	.803	—	.803	4.30	.364
121.8	400	30.2	3.28	21.8	.625	11.7	2.78	33.4	1.22	.814	.0436	109.5	12.10	.813	.018	.831	4.32	.385
	100	30.2	13.15	78.9	1.10	23.6	11.1	133	2.46	1.64	.0436	54.8	24.2	.839	.007	.846	4.40	.402
	45	30.2	29.2	175	1.75	33.4	24.6	296	3.58	2.39	.0436	35.9	36.3	.854	—	.854	4.45	.411
1200°	1000	41.0	1.515	19.4	.625	5.00	1.50	18.1	*	*	.0436	202	8.93	.801	—	.801	4.91	.289
¢	700	41.0	2.16	26.0	.625	10.5	2.16	25.8	1.09	.727	.0436	168.5	10.6	.808	.022	.830	4.95	.302
102.8	400	41.0	3.78	53.2	.625	13.7	3.75	45.0	1.43	.954	.0436	127	14.0	.819	.018	.837	4.99	.320
	100	41.0	15.15	90.9	1.10	27.7	15.0	181	2.88	1.92	.0436	63.9	28.2	.845	.006	.850	5.07	.336
	45	41.0	33.7	202	1.60	41.3	33.4	402	4.30	2.87	.0436	42.8	42.2	.861	—	.861	5.14	.346
900°	1000	64.4	1.945	20.0	.625	10.9	2.36	28.4	1.14	.760	.0436	253	11.2	.810	.024	.834	6.36	.197
¢	700	64.4	2.78	24.5	.625	13.1	3.38	40.6	1.36	.907	.0436	212	13.4	.817	.021	.838	6.40	.207
83.65	400	64.4	4.86	33.8	.625	17.9	5.94	71.2	1.86	1.24	.0436	160	17.8	.828	.017	.845	6.45	.216
	100	64.4	19.45	116.8	1.10	34.6	23.6	284	3.60	2.40	.0436	80	35.5	.854	.006	.860	6.56	.241
	45	64.4	43.3	260	1.70	51.4	52.5	630	5.35	3.57	.0436	53.6	53.0	.871	—	.871	6.66	.26

TABLE VIII – CALCULATIONS FOR GAS TURBINE POWERPLANT

Working Fluid – Air , T_6 = 90°F , Output = 2,000 HP

$P.R._T$ = 2.79, $P.R_c$ = 3.00, D_h / D_t = .75, η_R = .93

NOTE: $\Delta h'_c$ = 45

*CENTRIFUGAL COMPRESSOR

(1) T_1 (°F) & $\Delta h'_T$ BTU/#	(2) P_1 PSIA	(3) W #/sec	(4) G_T CFM $\times 10^{-3}$	(5) A_T Sq. In.	(6) h_{bd_T} inches	(7) $D_{T_{tip}}$ inches	(8) G_c CFM $\times 10^{-3}$	(9) A_C Sq. In.	(10) h_{bd_c} inches	(11) $D_{hyd.}$ inches	(12) μ_c #/hr.ft.	(13) Re_c $\times 10^{-4}$	(14) Re_c STP $\times 10^{-4}$	(15) η_c STP	(16) $\Delta \eta_c$ Corr.	(17) η_c Final	(18) HP_T HP $\times 10^{-3}$	(19) η_{TH}
1500°	1000	10.46	.430	8.60	.625	5.00	.383	4.60	*	*	.0436			.776	—	.776	1.45	.332
"	700	10.33	.642	8.60	.625	5.00	.543	6.50	*	*	.0436			.782	—	.782	1.49	.342
121.8	400	10.00	1.09	8.60	.625	5.00	.921	10.86	*	*	.0436			.792	—	.792	1.405	.353
	100	9.32	4.06	24.5	.625	13.1	3.42	41.0	1.37	.914	.0436	30.5	13.5	.817	.007	.824	1.322	.376
	95	9.00	8.71	52.4	.900	19.2	7.35	88.0	2.00	1.33	.0436	20.0	19.7	.832	—	.832	1.290	.386
1200°	1000	16.4	.605	8.60	.625	5.00	.601	7.22	*	*	.0436			.784	—	.784	1.935	.264
"	700	15.7	.825	8.60	.625	5.00	.825	9.90	*	*	.0436			.790	—	.790	1.865	.270
102.8	400	15.0	1.38	8.60	.625	5.00	1.38	16.6	*	*	.0436			.800	—	.800	1.790	.281
	100	13.6	5.02	30.2	.625	16.0	4.99	59.8	1.66	1.11	.0436	36.7	16.2	.824	.007	.831	1.640	.310
	45	13.13	10.8	64.6	.950	22.8	10.70	128	2.38	1.59	.0436	23.8	23.3	.838	—	.838	1.598	.320
900°	1000	30.9	.935	8.60	.625	5.00	1.13	13.6	*	*	.0436			.796	—	.796	3.02	.156
"	700	29.2	1.26	8.60	.625	5.00	1.535	18.4	*	*	.0436			.802	—	.802	2.86	.161
83.65	400	27.7	2.09	21.5	.625	11.3	2.55	30.6	1.18	.787	.0436	104.6	11.5	.812	.018	.830	2.72	.193
	100	24.6	7.49	44.6	.690	21.3	9.02	108	2.22	1.48	.0436	49.5	21.8	.835	.007	.842	2.45	.213
	45	23.6	15.85	95.1	1.00	31.1	19.25	230	3.24	2.16	.0436	32.5	31.8	.850	—	.850	2.37	.225

TABLE IX — CALCULATIONS FOR GAS TURBINE POWERPLANT

Working Fluid — Air , T_6 = 90°F , Output = 600HP

$P.R._T$ = 2.79, $P.R_c$ = 3.00, D_h/D_t = .75, η_R = .93

NOTE: $\Delta h'_c$ = 45

* CENTRIFUGAL COMPRESSOR

a given physical size of machine they are approximately a constant proportion of the through flow. Such an assumption is utilized for the study.

The fluid dynamic losses through the blading are a function of the blading geometry as well as Mach number and Reynold's number. The influence of the geometry is evident through such factors as aspect ratio loss, friction loss*, and blading form, involving the concepts of angle of attack, lift, and drag. The blading form is intimately concerned with the required pressure ratio per stage.

For the purposes of this investigation it is assumed that the blade width to height ratio, the pressure ratio per stage, and the blade forms are always optimized. In this connection a pressure ratio per stage of 1.082 is assumed. Such a value is believed to be reasonably typical of high efficiency designs. Therefore the only factors which cause a variation in efficiency from the standard air machine are Reynold's number and Mach number. If closed-cycle air gas turbine plants are considered, there is no substantial variation of sonic velocity at compressor inlet from that obtained in the conventional open-cycle, since the sonic velocity is not a function of pressure. If the same velocity triangles are assumed, there is no Mach number effect. It will be noted that the maximum Mach number, based on relative velocity, is about .308. If closed cycle helium plants are considered, and the same velocity magnitudes are used, the Mach number at compressor inlet will be reduced from the air case by a factor of about 2.9 and compressibility effects will be negligible if the air velocities are used. Thus, it appears that a high efficiency helium compressor can be safely designed for considerably greater gas velocities than an air compressor. The limit would then be one of wheel stresses. The ratio of the number of helium stages required to obtain a given pressure ratio to the number of air stages, if identical fluid velocities are assumed, is about 7. (See Appendix Section 8.5.) However, if the Mach number were held constant between the machines, the number of stages would be roughly the same(except for variation in k). See Appendix, Section 8.3 for derivation. The air compressor wheel speed assumed for the study is about 385 fps (see the velocity diagram of Figure 13). In view of the low temperature of the fluid in the compressor, it seems reasonable to assume a wheel speed for helium of about 2-1/2 times the value for air or 962 fps. From this viewpoint, the number of stages for the helium compressor for a given pressure ratio does not greatly exceed that for air and the diameter for a given volumetric flow is considerably less.

---

* Controlled by blade width. There is an optimum between increasing blade width to reduce sharpness of turning and decreasing it to reduce friction loss.

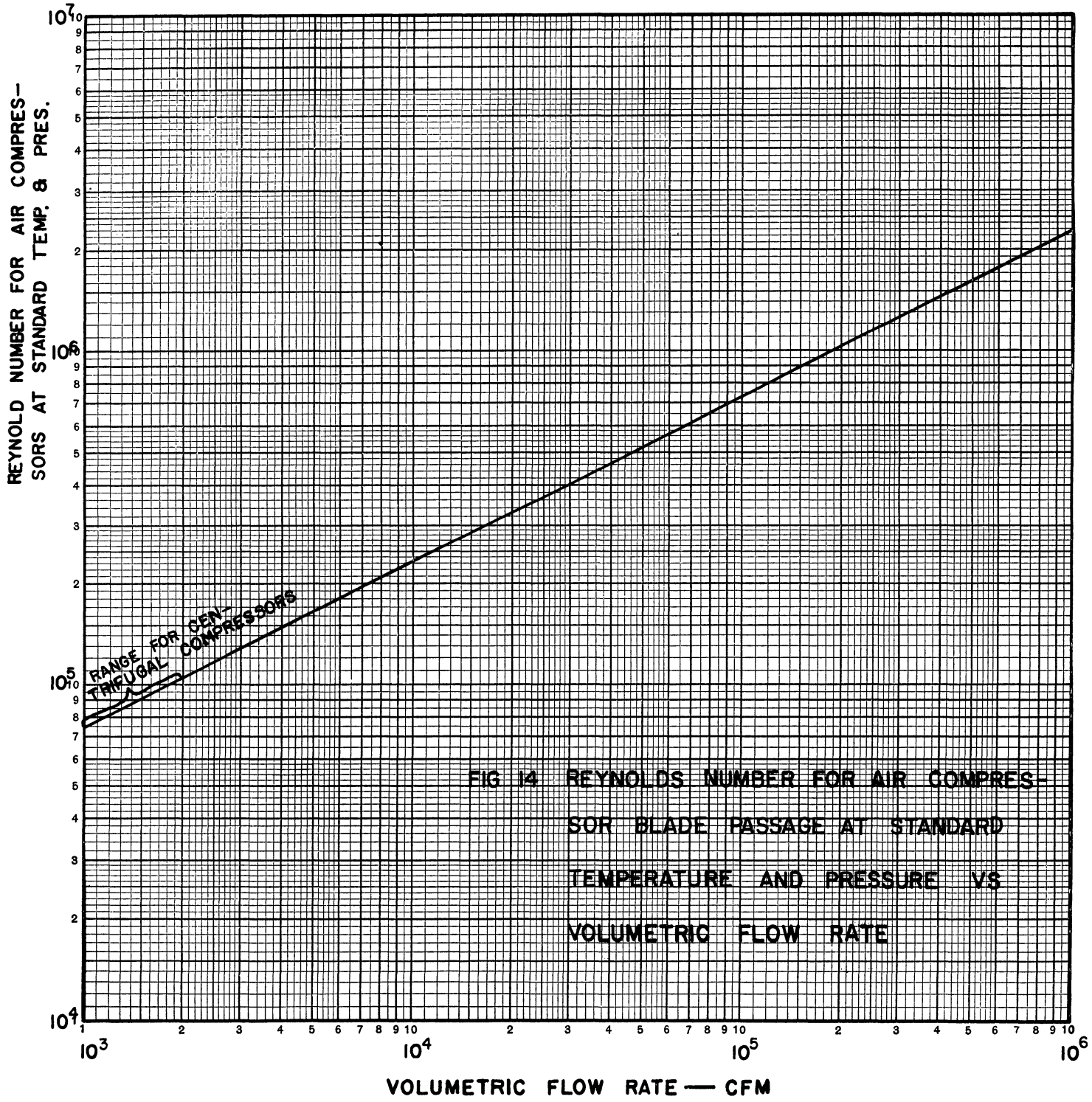

FIG 14 REYNOLDS NUMBER FOR AIR COMPRESSOR BLADE PASSAGE AT STANDARD TEMPERATURE AND PRESSURE VS VOLUMETRIC FLOW RATE

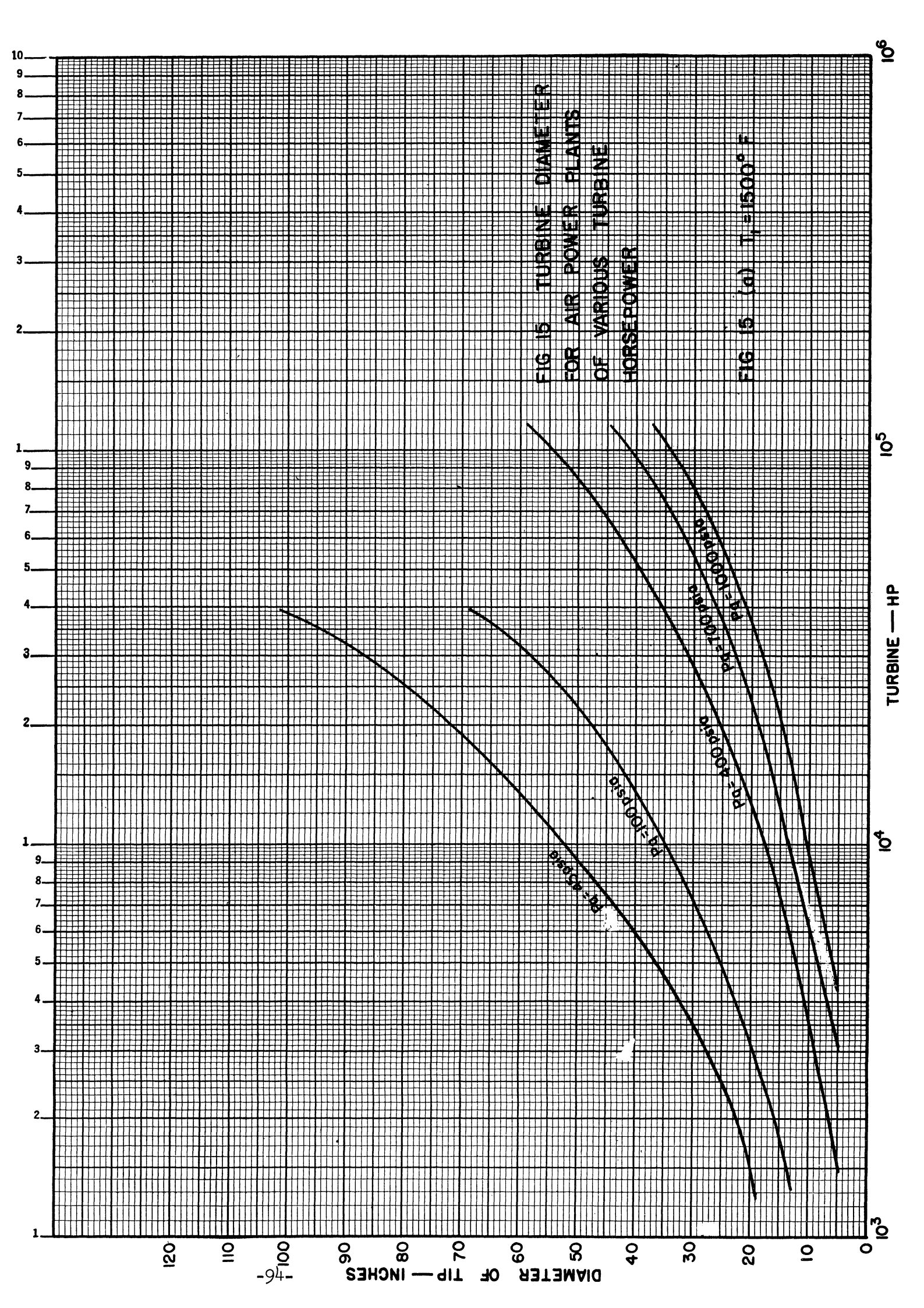
FIG. 15 TURBINE DIAMETER FOR AIR POWER PLANTS OF VARIOUS HORSEPOWER
FIG. 15 (a) $T_1 = 1500°F$
$P_2 = 100 P_{sid}$
$P_2 = 200 P_{sid}$
$P_2 = 400 P_{sid}$
$P_2 = 1000 P_{sid}$
$P_2 = 2000 P_{sid}$
$P_2 = 4000 P_{sid}$
TURBINE — HP
DIAMETER OF TIP — INCHES

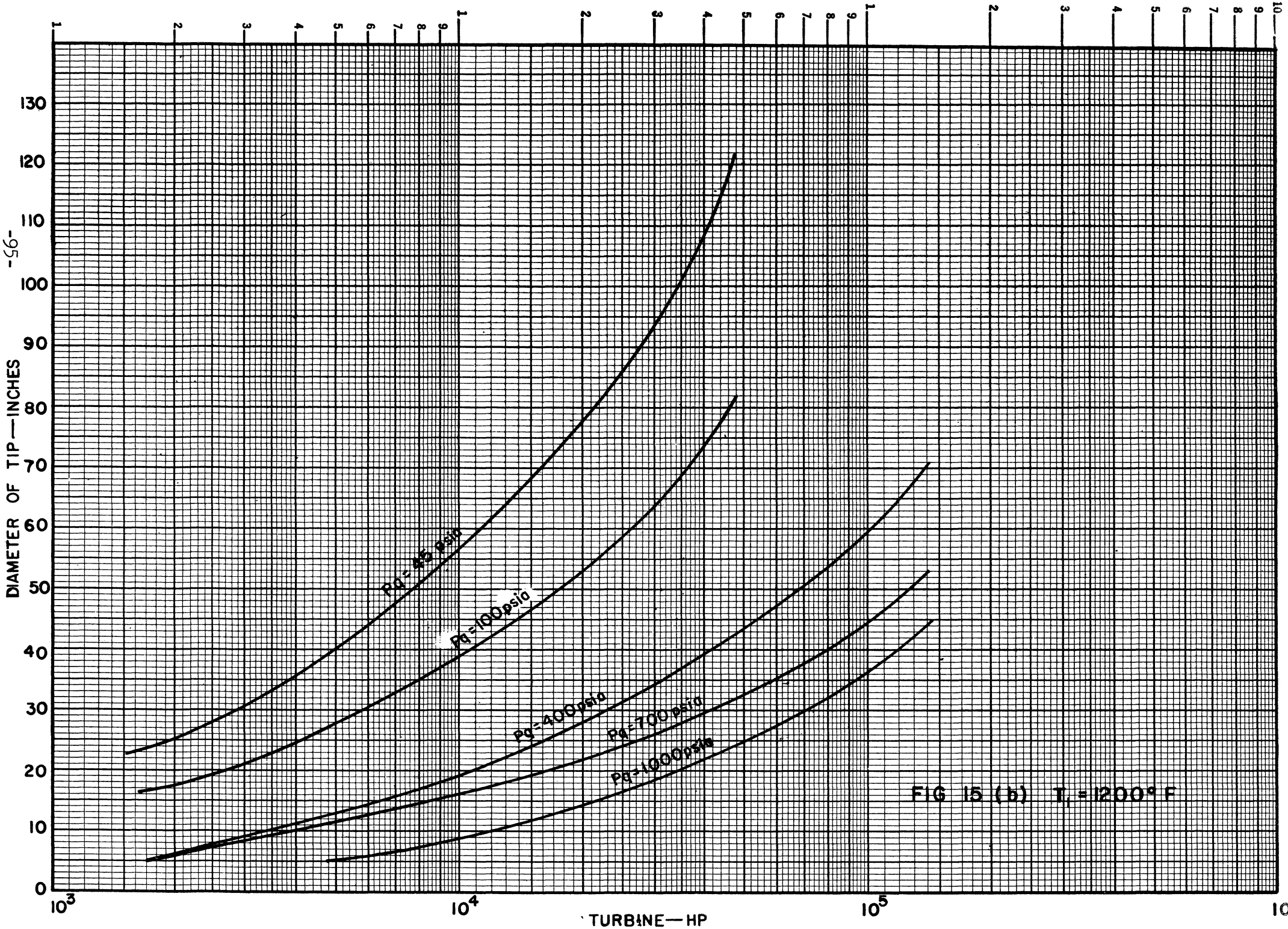

FIG 15 (b) $T_1 = 1200°F$

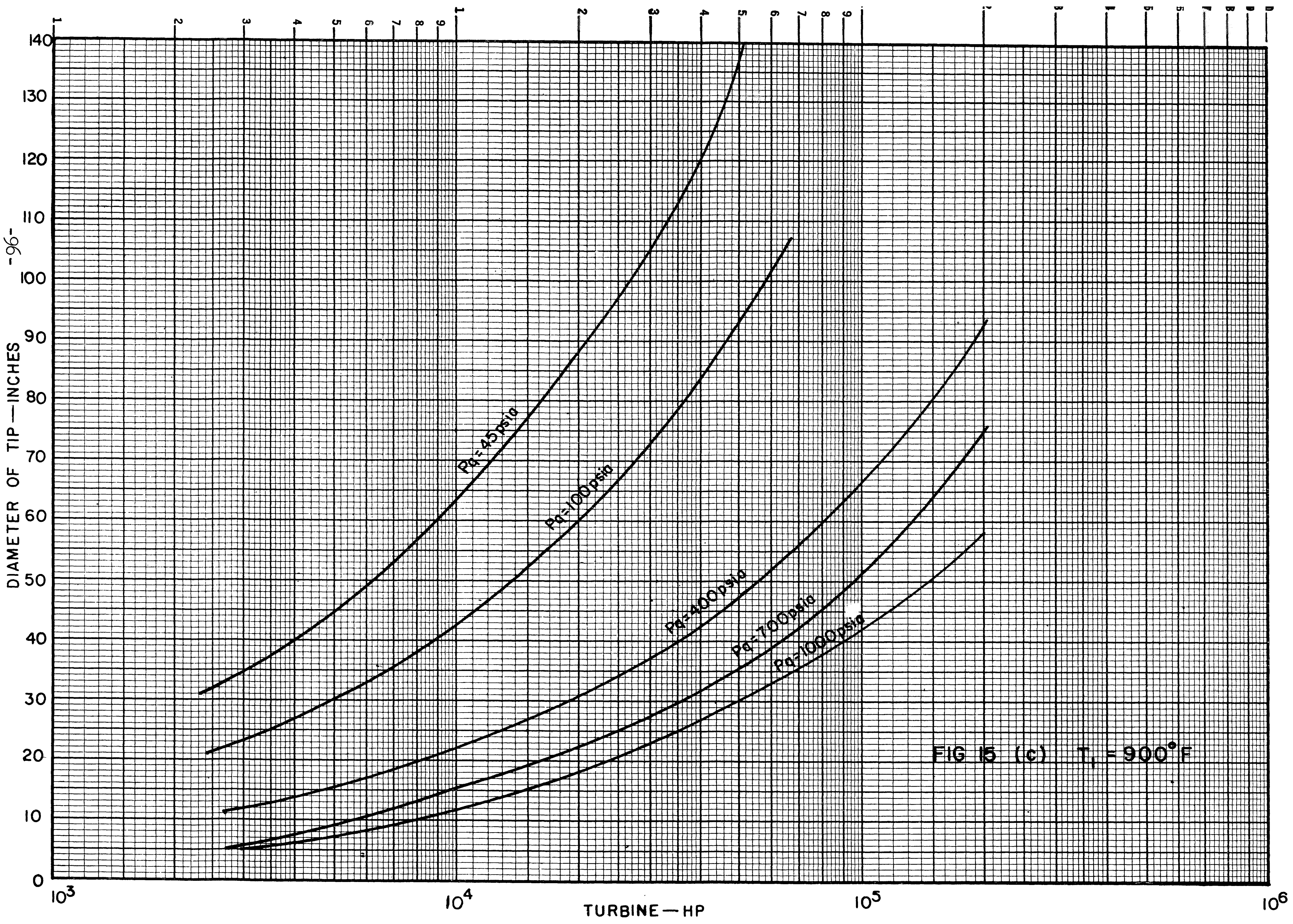

FIG 15 (c) $T_1 = 900°F$

This increase of velocity results in a very substantial reduction in turbomachinery size for a given application. However, in substituting a smaller machine there is a consequent efficiency reduction (Figure 19). Thus the efficiency "ceiling" is not approached as closely for helium as for air. However, it seems a reasonable assumption that the large saving in cost and size should more than overbalance the loss in efficiency. The diameters are tabulated in Tables X through XIV and plotted in Figure 16. The number of compressor and turbine stages (turbine assumptions are considered later) for various pressure ratios are tabulated in Table XV.

For carbon-dioxide, the Mach number effects (as compared with air) are in the opposite direction from helium. If the air velocity diagram were assumed for a carbon-dioxide compressor, the Mach number would be increased over the value with air by a factor of about 1.248. Thus for carbon-dioxide the velocities should be reduced by this factor if the efficiencies are to be compared. For a given volumetric flow rate and pressure ratio, the diameters and blade heights for the carbon-dioxide compressor will be somewhat greater than for the air unit. The calculations for this fluid are not presently complete and will be reported at a later date.

It is assumed in these estimations, that the Mach numbers must be limited to those of present day conventional practice if the high efficiencies, reported in the literature, are to be obtained. It is believed that the assumption of a drop of efficiency with increase of Mach number is well substantiated by present experience, but may well be a function of the state of the art and not an inherent limitation. For example, it is known that a certain degree of success has been obtained with transonic and supersonic compressors, although the operating characteristics and efficiencies for the preliminary attempts have not been as favorable as was hoped.

To summarize the estimating procedure to this point, the compressor flowpath designs are assumed to be arranged in such a way that the Mach numbers, blading designs, leakage areas and vector diagrams are the same as those for a "typical" series of air designs for which the efficiencies as a function of flow rate are known. The only remaining variable parameter is the Reynold's number. This has been computed as explained previously for the "typical" air designs and is plotted in Figure 14 as a function of inlet volumetric flow rate (which of course determines the physical size of the machine under the stated assumptions). Now, to estimate the efficiency of an axial flow compressor with given flow, temperature, pressure, and fluid, it is necessary to rough out the design of the machine under the assumptions

(1) T_1 (°F) & $\Delta h'_T$ BTU/#	(2) P_1 PSIA	(3) W #/sec	(4) G_T CFM $\times 10^{-3}$	(5) A_T Sq. In.	(6) h_{bd_T} inches	(7) $D_{T_{tip}}$ inches	(8) G_c CFM $\times 10^{-3}$	(9) A_C Sq. In.	(10) h_{bd_c} inches	(11) $D_{hyd.}$ inches	(12) μ_c #/hr.ft.	(13) Re_c $\times 10^{-4}$	(14) Re_c STP $\times 10^{-4}$	(15) η_c STP	(16) $\Delta \eta_c$ Corr.	(17) η_c Final	(18) HP_T HP $\times 10^{-3}$	(19) η_{TH}
1500°	1000	125.2	39.4	238.5	4.9	21.5	33.2	160	2.69	1.80	.0459	199.4	26.6	.843	.015	.858	124.9	.395
&	700	125.2	56.4	338	5.2	25.7	47.6	228	3.22	2.14	.0459	165.5	32.0	.849	.012	.861	125.0	.399
819	400	125.2	98.6	592	6.9	34.1	83.1	399	4.26	2.83	.0459	125.2	42.1	.860	.008	.868	126.6	.407
1200°	1000	185.5	49.6	298	4.3	26.2	49.2	236	3.28	2.18	.0459	241	32.5	.850	.014	.864	157.3	.319
&	700	185.5	70.9	425	5.1	31.4	70.5	338	3.92	2.61	.0459	202	38.8	.857	.012	.869	158.2	.326
694	400	185.5	124.0	742	6.9	41.5	123	590	5.18	3.45	.0459	153	51.5	.870	.008	.878	160.0	.338
900°	1000	357	78.0	468	4.6	36.5	94.8	455	4.56	3.03	.0459	336	45.0	.864	.014	.878	252.1	.217
&	700	357	111.5	670	5.7	43.5	136	651	5.44	3.60	.0459	279	54.1	.872	.011	.883	253.4	.225
569	400	357	195.0	1170	7.42	57.6	237	1140	7.20	4.78	.0459	211	71.4	.884	.007	.891	256.0	.238

TABLE X—CALCULATIONS FOR GAS TURBINE POWERPLANT

Working Fluid—Helium, T_e = 90°F, Output = 60,000 HP

$P.R._T$ = 2.79, $P.R_c$ = 3.00, D_h/D_t = .75, η_R = .93

NOTE: $\Delta h'_c$ = 336

(1) T_1 (°F) & $\Delta h'_T$ BTU/#	(2) P_1 PSIA	(3) W #/sec	(4) G_T CFM $\times 10^{-3}$	(5) A_T Sq. In.	(6) h_{bd_T} inches	(7) $D_{T_{tip}}$ inches	(8) G_c CFM $\times 10^{-3}$	(9) A_C Sq. In.	(10) h_{bd_c} inches	(11) $D_{hyd.}$ inches	(12) μ_c #/hr.ft	(13) Re_c $\times 10^{-4}$	(14) Re_c STP $\times 10^{-4}$	(15) η_c STP	(16) $\Delta \eta_c$ Corr.	(17) η_c Final	(18) HP_T HP $\times 10^{-3}$	(19) η_{TH}
1500°	1000	41.7	13.1	78.9	2.53	12.4	11.1	53.2	1.55	1.04	.0459	11.52	15.2	.822	+.016	.838	40.6	.370
&	700	41.7	18.8	113.0	3.02	14.9	15.85	76.1	1.86	1.24	.0459	9.62	18.3	.829	+.013	.842	40.7	.375
819	400	41.7	32.8	197.0	4.00	19.7	27.6	133	2.46	1.64	.0459	7.26	24.2	.839	+.009	.848	41.0	.383
	100	41.7	131	789	8.00	39.4	111	533	4.93	3.29	.0459	3.66	490	.867	-.003	.864	41.8	.403
	45	41.7	292	1750	7.20	58.5	246	1180	7.32	4.88	.0459	2.44	72.2	.885	-.009	.876	42.4	.417
1200°	1000	61.8	16.5	99.0	2.49	15.2	16.4	79.2	1.90	1.27	.0459	14.1	19.0	.829	+.015	.844	57.2	.290
&	700	61.8	23.6	142	2.96	18.2	23.5	113	2.27	1.51	.0459	11.7	22.5	.836	+.012	.848	51.5	.296
694	400	61.8	41.4	248	3.92	24.0	41.0	197	3.00	2.00	.0459	8.88	29.5	.846	+.008	.854	51.9	.305
	100	61.8	165	990	7.70	48.0	164	792	6.00	4.00	.0459	4.42	59.0	.876	-.002	.874	53.1	.333
	45	61.8	265	2190	11.8	71.3	365	1750	8.92	5.95	.0459	2.96	88.5	.893	-.008	.885	53.7	.347
900°	1000	119	26.0	156	2.70	21.2	31.6	152	2.63	1.76	.0459	19.5	26.0	.841	+.015	.856	82.0	.180
&	700	119	37.2	223	3.25	25.1	45.1	217	3.70	2.47	.0459	19.1	30.9	.848	+.013	.861	82.5	.189
569	400	119	65.0	390	4.25	33.3	79.0	380	4.16	2.77	.0459	12.3	41.0	.860	+.010	.870	83.4	.204
	100	119	260	1560	8.55	66.5	316	1520	8.32	5.55	.0459	6.24	82.1	.890	-.002	.888	85.1	.233
	45	119	450	2700	9.65	99.3	702	3370	12.4	8.25	.0459	4.12	122	.900	-.008	.892	85.5	.240

TABLE XII — CALCULATIONS FOR GAS TURBINE POWERPLANT

Working Fluid — Helium , T_c = 90°F , Output = 20,000HP

$P.R._T$ = 2.79, $P.R_c$ = 3.00, D_h/D_t = .75, η_R = .93

NOTE: $\Delta h'_c$ = 336

(1) T_1 (°F) & $\Delta h'_T$ BTU/#	(2) P_1 PSIA	(3) W #/sec	(4) G_T CFM $\times 10^{-3}$	(5) A_T Sq. In.	(6) h_{bd_T} inches	(7) $D_{T_{tip}}$ inches	(8) G_c CFM $\times 10^{-3}$	(9) A_C Sq. In.	(10) h_{bd_c} inches	(11) $D_{hyd.}$ inches	(12) μ_c #/hr.ft.	(13) Re_c $\times 10^{-4}$	(14) Re_c STP $\times 10^{-4}$	(15) η_c STP	(16) $\Delta \eta_c$ Corr.	(17) η_c Final	(18) HP_T HP $\times 10^{-3}$	(19) η_{TH}
1500°	1000	13.55	4.26	25.6	1.45	7.08	3.60	17.3	.886	.591	.0459	65.4	8.50	.801	+.018	.819	12.43	.345
&	700	13.55	6.10	36.6	1.72	8.47	5.15	24.7	1.06	.707	.0459	54.8	10.42	.807	+.015	.822	12.41	.349
819	400	13.55	10.70	64.2	2.28	11.20	9.00	43.1	1.40	.938	.0459	41.4	13.9	.818	+.010	.828	12.51	.357
	100	13.55	42.6	256	4.6	22.4	37.0	173	2.80	1.87	.0459	20.6	27.9	.845	-.002	.843	12.72	.377
	45	13.55	95.0	569	6.8	33.4	80.0	383	4.17	2.79	.0459	13.9	41.2	.860	-.010	.850	12.85	.386
1200°	1000	20.7	5.53	33.2	1.43	8.8	5.50	26.4	1.10	.733	.0459	81.2	10.8	.809	+.017	.826	16.78	.262
&	700	20.7	7.90	47.4	1.74	10.48	7.86	37.8	1.31	.875	.0459	67.8	13.1	.815	+.013	.828	16.81	.265
694	400	20.7	13.8	82.9	2.3	13.8	13.7	66.0	1.73	1.16	.0459	51.2	17.2	.826	+.009	.835	16.97	.276
	100	20.7	55.3	332	4.5	27.8	55.0	264	3.46	2.31	.0459	25.6	34.2	.852	-.002	.850	17.28	.299
	45	20.7	123	736	6.7	41.4	122	586	5.17	3.45	.0459	17.2	51.2	.869	-.009	.860	17.48	.313
900°	1000	38.9	8.50	51.0	1.5	12.0	10.32	49.5	1.50	1.00	.0459	110.8	15.1	.820	+.016	.836	26.18	.143
&	700	38.9	12.2	73.0	1.85	14.4	14.8	70.9	1.80	1.20	.0459	92.8	17.8	.827	+.013	.840	26.3	.151
569	400	38.9	21.3	128	2.5	19.0	25.8	124	2.38	1.59	.0459	70.4	23.4	.838	+.009	.847	26.42	.164
	100	38.9	85.0	510	4.9	37.8	103	495	4.74	3.16	.0459	35.0	46.8	.866	-.002	.864	27.0	.194
	45	38.9	199	1200	7.9	56.5	230	1100	7.07	4.71	.0459	23.4	70.1	.883	-.008	.875	27.9	.212

TABLE XII – CALCULATIONS FOR GAS TURBINE POWERPLANT

Working Fluid – Helium , T_c = 90°F , Output = 6,000 HP

$P.R._T$ = 2.79, $P.R_c$ = 3.00, D_h/D_t = .75, η_R = .93

NOTE: $\Delta h'_c$ = 336

(1) T_1 (°F) & $\Delta h'_T$ BTU/#	(2) P_1 PSIA	(3) W #/sec	(4) G_T CFM $\times 10^{-3}$	(5) A_T Sq. In.	(6) h_{bd_T} inches	(7) $D_{T_{tip}}$ inches	(8) G_c CFM $\times 10^{-3}$	(9) A_C Sq. In.	(10) h_{bd_c} inches	(11) D_{hyd} inches	(12) μ_c #/hr.ft	(13) $Re_c \times 10^{-4}$	(14) Re_c STP $\times 10^{-4}$	(15) η_c STP	(16) $\Delta \eta_c$ Corr.	(17) η_c Final	(18) HP_T HP $\times 10^{-3}$	(19) η_{TH}
1500°	1000	5.43	1.71	8.60	.625	5.00	1.44	6.92	*	*	.0459		5.08	.783	—	.783	4.93	.308
"	700	5.43	2.45	14.7	1.05	5.36	2.06	9.90	.671	.947	.0459	34.6	6.50	.790	+.016	.806	5.07	.326
819	400	5.43	4.28	25.7	1.45	7.10	3.61	17.3	.887	.593	.0459	26.2	8.50	.806	+.011	.817	5.14	.342
	100	5.43	17.1	102.5	2.91	14.15	14.4	69.2	1.77	1.18	.0459	13.1	17.4	.827	-.002	.825	5.19	.353
	45	5.43	38.1	228	4.32	21.1	32.0	154	2.64	1.76	.0459	8.76	26.1	.842	-.011	.831	5.23	.361
1200°	1000	8.29	2.22	13.3	.92	5.54	2.20	10.6	.693	.462	.0459	51.2	6.8	.791	+.019	.810	6.59	.236
"	700	8.29	3.16	19.0	1.1	6.60	3.15	15.1	.826	.552	.0459	42.7	8.01	.798	+.017	.815	6.64	.244
694	400	8.29	5.54	33.2	1.96	8.72	5.51	26.4	1.09	.725	.0459	32.0	10.9	.809	+.010	.819	6.66	.251
	100	8.29	22.2	133	2.9	17.5	22.0	106	2.19	1.47	.0459	16.2	21.6	.835	-.004	.831	6.76	.270
	45	8.29	49.0	294	4.27	26.2	48.9	234	3.27	2.19	.0459	10.9	32.3	.849	-.010	.839	6.83	.282
900°	1000	18.2	3.97	23.9	1.06	8.24	4.84	23.2	1.03	.686	.0459	75.8	10.0	.806	+.017	.823	12.04	.118
"	700	18.2	5.69	34.1	1.26	9.84	6.90	33.2	1.23	.819	.0459	63.4	12.2	.813	+.014	.827	12.11	.126
569	400	18.2	9.95	59.6	1.68	12.95	12.1	58.0	1.62	1.08	.0459	47.8	16.2	.823	+.009	.832	12.18	.136
	100	18.2	39.7	239	3.4	25.9	48.3	232	3.24	2.16	.0459	24.0	32.1	.849	-.002	.847	12.41	.164
	45	18.2	93.0	559	5.3	38.7	107	515	4.84	3.22	.0459	16.1	48.1	.867	-.010	.857	12.55	.181

TABLE XIII - CALCULATIONS FOR GAS TURBINE POWERPLANT

Working Fluid — *Helium*, T_6 = 90°F, Output = 2,000 HP

$P.R._T$ = 2.79, $P.R_c$ = 3.00, D_h/D_t = .75, η_R = .93

NOTE: $\Delta h'_c$ = 336

* CENTRIFUGAL COMPRESSOR

(1) T_1 (°F) & $\Delta h'_T$ BTU/#	(2) P_1 PSIA	(3) W #/sec	(4) G_T CFM $\times 10^{-3}$	(5) A_T Sq. In.	(6) h_{bd_T} inches	(7) $D_{T_{tip}}$ inches	(8) G_c CFM $\times 10^{-3}$	(9) A_C Sq. In.	(10) h_{bd_c} inches	(11) $D_{hyd.}$ inches	(12) μ_c #/hr.ft.	(13) Re_c $\times 10^{-4}$	(14) Re_c STP $\times 10^{-4}$	(15) η_c STP	(16) $\Delta \eta_c$ Corr.	(17) η_c Final	(18) HP_T HP $\times 10^{-3}$	(19) η_{TH}
1500°	1000	1.92	.605	8.6	.625	5.00	.510	*	*	*	.0459			.781	—	.781	1.74	.293
&	700	1.86	.837	8.6	.625	5.00	.706	*	*	*	.0459			.787	—	.787	1.70	.297
819	400	1.81	1.43	8.6	.625	5.00	1.20	*	*	*	.0459			.797	—	.797	1.67	.309
	100	1.73	5.45	32.7	1.63	8.00	4.59	22.1	1.00	.667	.0459	7.38	9.8	.806	-.004	.802	1.61	.321
	45	1.64	11.5	69.0	2.58	11.16	9.70	46.6	1.45	.964	.0459	4.82	14.5	.819	-.012	.807	1.53	.328
1200°	1000	3.21	.858	8.6	.625	5.00	.852	*	*	*	.0459			.790	—	.790	2.49	.205
&	700	3.07	.959	8.6	.625	5.00	1.17	*	*	*	.0459			.797	—	.797	2.40	.216
694	400	2.90	1.59	8.6	.625	5.00	1.93	*	*	*	.0459			.806	—	.806	2.29	.226
	100	2.69	7.19	43.1	1.64	10.0	7.14	34.3	1.25	.833	.0459	9.22	12.5	.813	-.003	.810	2.14	.236
	45	2.57	15.2	91.1	2.36	14.6	15.4	72.9	1.82	1.213	.0459	6.06	18.0	.828	-.011	.817	2.06	.248
900°	1000	8.48	1.45	8.6	.625	5.00	2.25	*	*	*	.0459			.806	—	.806	5.5	.088
&	700	7.85	1.91	11.5	.63	6.45	2.98	14.3	.806	.538	.0459	41.6	7.5	.797	+.017	.814	5.14	.100
569	400	7.31	3.12	18.7	.81	8.24	4.86	23.3	1.03	.686	.0459	30.4	10.0	.806	+.010	.816	4.81	.104
	100	5.74	9.80	58.7	1.43	14.6	15.2	73.1	1.82	1.22	.0459	13.5	18.0	.828	-.002	.826	3.82	.124
	45	5.51	20.9	125	2.13	21.3	32.5	156	2.66	1.77	.0459	8.84	26.0	.842	-.012	.830	3.70	.132

TABLE XIV - CALCULATIONS FOR GAS TURBINE POWERPLANT

Working Fluid — Helium, T_c = 90°F, **Output** = 600 HP

$P.R._T$ = 2.79, $P.R_c$ = 3.00, D_h / D_t = .75, η_R = .93

NOTE: $\Delta h'_c$ = 336

*CENTRIFUGAL COMPRESSOR

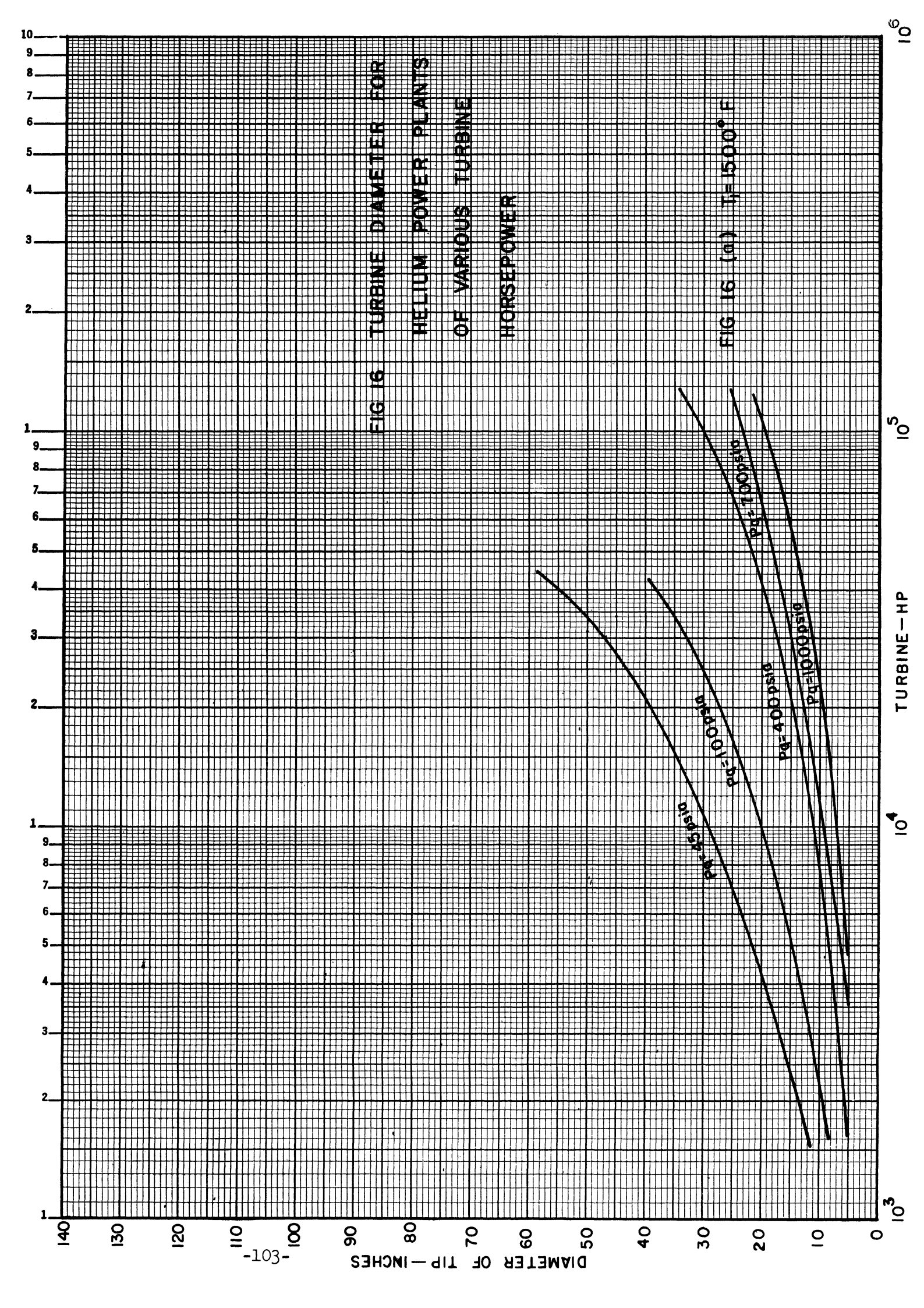
FIG 16 TURBINE DIAMETER FOR HELIUM POWER PLANTS OF VARIOUS TURBINE HORSEPOWER
FIG 16 (a) T1=1500°F
Pd=700 psia
Pd=400 psia
Pd=1000 psia
Pd=100 psia
Pd=50 psia
TURBINE—HP
DIAMETER OF TIP—INCHES

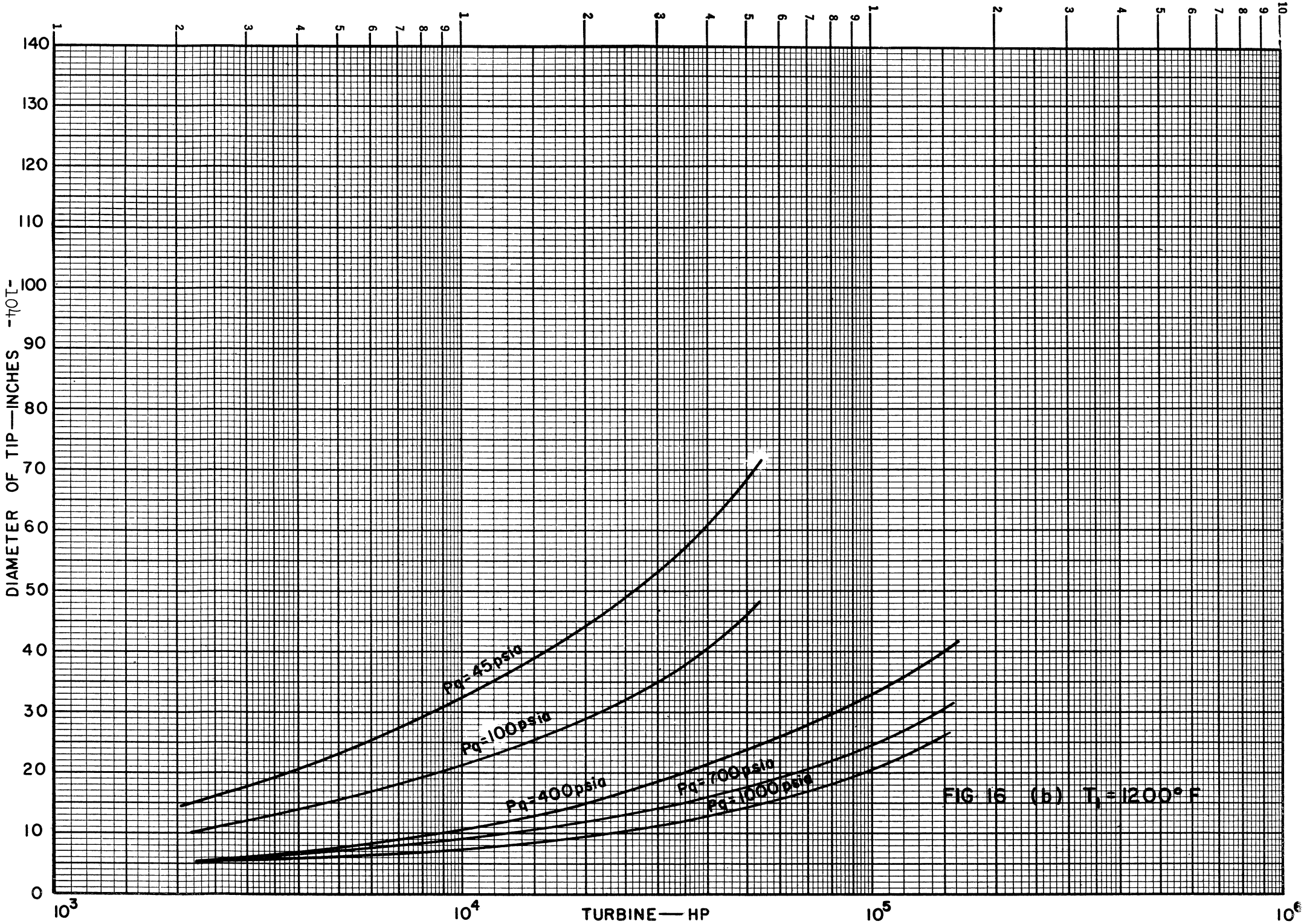

FIG 16 (b) $T_1 = 1200°F$

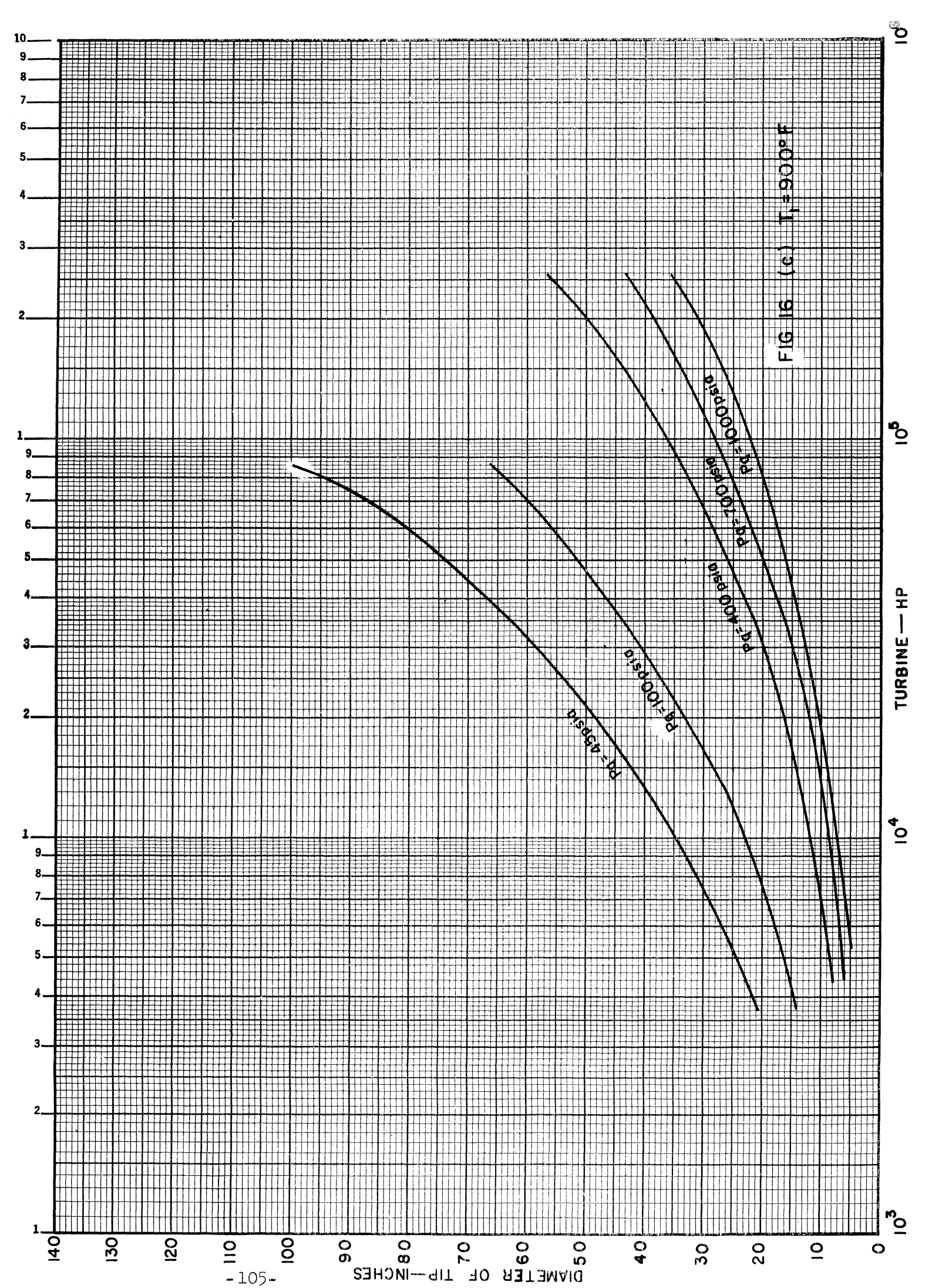
FIG 16 (c) T₁=900°F
P_d=1000psia
P_d=700psia
P_d=400psia
P_d=100psia
P_d=43psia
TURBINE — HP
DIAMETER OF TIP—INCHES
10⁶
10⁵
10⁴
10³

TABLE XV

REQUIRED NUMBER OF COMPRESSOR AND TURBINE STAGES
FOR INCREASED PRESSURE RATIOS

(Pressure Ratio/Stage per Figure 13)

Fluid	Component	Plant Pressure Ratio	No. Stages
Air	Compressor	2	9
		3	14
		4	18
		6	23
		8	26
		10	29
Air	Turbine	2	6
		3	9
		4	12
		6	16
		8	18
		10	20
Helium	Compressor	2	10
		3	16
		4	20
		6	26
		8	30
		10	33
Helium	Turbine	2	13
		3	21
		4	29
		6	37
		8	43
		10	47

previously described, compare its blading Reynold's number with that of the "typical" air machine, and make the proper efficiency adjustment.*

For the closed-cycle air machines, this involves first the calculation of the inlet volumetric flow rate, blading passage dimensions, and Reynold's number. Then comparison is made with the Reynold's number for the same inlet volumetric flow rate (and hence same size machine) which is plotted for the "typical" air machines in Figure 14. For the helium or carbon-dioxide units an additional step is necessary in that the calculated inlet volumetric flow must be corrected for the change in velocity diagram (due to the requirement of constant Mach number) to determine an adjusted flow for comparison with the same size "typical" air design. The results of these calculations are tabulated in Tables V to XIV and sample calculations for typical cases are shown in the Appendix, Section 8.4

It is generally true in fluid flow work that the loss coefficient for any given condition decreases with increasing Reynold's number. A very common case in point is pipe flow. This same trend applies to turbomachinery flow passages; thus blading loss coefficients, which are a function of Reynold's number, are applied to estimate the efficiency of a given machine. Blade loss coefficient data, showing the loss as a function of Reynold's number and turning angle are plotted in Figure 17. This is based on test work conducted by one of the well-known manufacturers of this type of equipment (results not published in the open literature) and is believed to be fairly typical. Certainly the trend illustrated is correct. Somewhat similar results are no doubt available through NACA work in this field, and also through recently reported work at MIT (reference 7).

The compressor designs considered for the study utilize symmetrical blading. Thus the loss coefficient is to be applied both to stator and rotor, and affects each equally. For the purposes of this study, it is simply necessary to note the loss coefficient for the "typical" machine at the given flow rate, and that of the closed cycle machine, and then adjust the "typical" efficiency accordingly. The resulting efficiencies and the major steps in the calculation are shown in Tables V to XIV.

---

* The machine efficiency is assumed to vary in proportion with the blading efficiency because the rotor and stator kinetic heads (to which the loss coefficient is applied) are equal and are always about 1/2 the enthalpy drop per stage for the assumed velocity diagrams. Thus the loss coefficient is effectively applied to 1/2 the stage enthalpy drop for both rotor and stator, or to the whole enthalpy drop for each stage, as is necessary if the assumed type of variation is to exist.

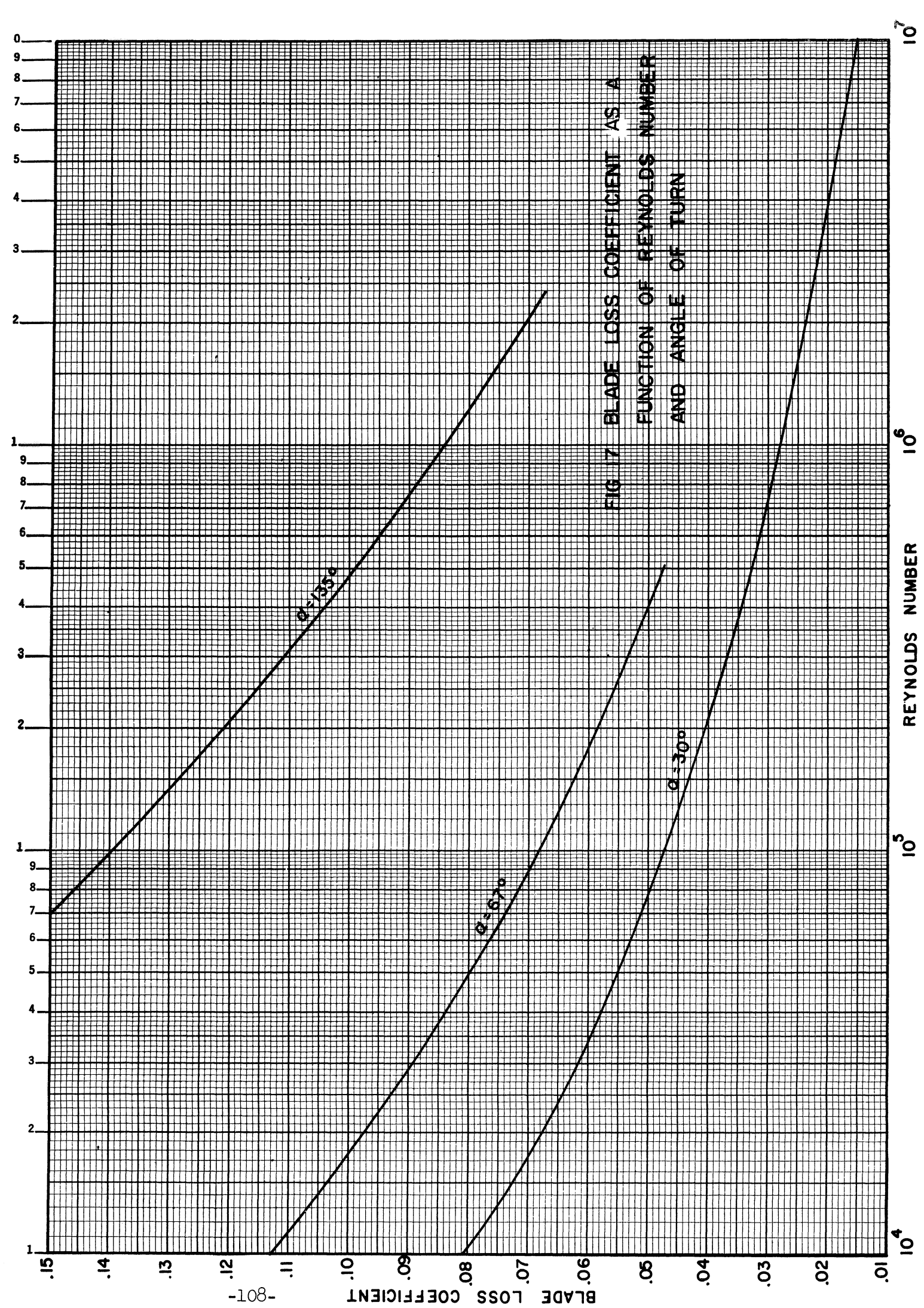
FIG 17 BLADE LOSS COEFFICIENT AS A FUNCTION OF REYNOLDS NUMBER AND ANGLE OF TURN
α=135°
α=67.5°
α=30°
BLADE LOSS COEFFICIENT
REYNOLDS NUMBER
.15
.14
.13
.12
.11
.10
.09
.08
.07
.06
.05
.04
.03
.02
.01
10^7
10^6
10^5
10^4

3.4.2 Centrifugal and Positive Displacement Compressors

As previously explained, and illustrated in Figure 12, it is assumed that positive displacement or centrifugal compressors should replace the axial flow machines below a flow rate of about 2,000 CFM. It seems a reasonable assumption that size of machine alone influences the efficiency in the case of the positive displacement device, particularly if rotary units are considered. Typical efficiencies for Lysholm type rotary positive displacement blowers for standard temperature, pressure air are to be found in reference 6. It is felt that this type of machine, due to its broad operating range, relatively high efficiency, and reasonable size and weight has a good possibility for application in fairly small gas turbine plants. In fact, it has been previously used successfully in such an application by the Elliot Company (reference 8). Hence it is on this type of machine that the efficiencies are based. It is realized that there are other possibilities and that these would give somewhat differing efficiencies. However, the results are more or less typical.

The lower end of the curve of Figure 12 is determined by the positive displacement machine efficiencies and the upper end by the axial flow. While the axial flow efficiencies are affected by Mach number and Reynold's number considerations, the positive displacement efficiencies are not. Between the axial flow and the lower positive displacement ranges, largely overlapping the positive displacement range, is the area of application of the centrifugal compressors. These are affected by Mach number and Reynold's number in the same way as the axial flow machines. Since the range of application is approximately the same as that of the positive displacement machine, and since adequate data relating these effects are not available to the authors, it has been assumed that below about 2,000 CFM there is no Mach or Reynold's number effect. Therefore, to determine the efficiency of a closed cycle compressor, with an inlet CFM below this value the efficiency corresponding to the applicable CFM is simply noted from the curve of "typical" machine efficiencies of Figure 12.

3.4.3 Turbines

As previously stated, it is assumed that axial flow, full admission, impulse turbines are suitable over the entire range of the study. Although centripedal, centrifugal, or positive displacement expanders might be selected for given applications, it is believed that the assumed axial flow machine will give at least comparable efficiency. Thus, it is chosen as the basis for the efficiency estimation.

For the larger flow rates, where both turbine and compressor are of the axial flow type, it is assumed that turbine efficiency and

compressor efficiency are equal. It is realized that in general, for any given set of conditions, it is possible to design a turbine of higher efficiency than the corresponding compressor because of the favorable direction of the boundary layer pressure gradient. However, due to the more difficult mechanical conditions applying to the turbine (i.e. higher temperature), it is usually desirable to increase the work per stage, and thus the Mach numbers in the turbine, over those existing in the compressor. Thus the inherently obtainable efficiency advantage of the turbine tends to be offset to some extent in actual practice. To reduce somewhat the length of the required calculations, it was decided to assume for the purposes of this study, that these opposing factors balanced for the axial flow range and that the turbine and compressor efficiencies are the same.

In the case of air, it is usually assumed that the limitation of the allowable work per stage is one of thermal-centrifugal wheel stresses. From this viewpoint a reasonably conservative value, for the pitch-line velocity, consistent with all but perhaps aircraft practice, is 1000 ft/sec.* However, since the turbine and compressor generally run at the same RPM, a somewhat lower value may be desirable, both to avoid excessive diameters and to allow higher efficiencies. A typical velocity diagram, which is considered applicable throughout the range of the study, is shown in Figure 13. The relative Mach number with air is only .394 even for the case of 900 F inlet. Therefore no possibility of a transonic or supersonic turbine exists and usual data is substantially applicable.

For this reason, in the general case, turbine and compressor rotating speeds will be equal. This assumption is made in the determination of the turbine wheel diameters which are plotted against turbine output for various fluid and operating conditions in Figure 15. To avoid excessive diameters the turbine wheel dimensions are based on the assumption of a peripheral velocity 1.25 times (in the case of air) that for the compressors. In some cases, it may be desirable to reduce the diameter and number of stages by allowing an RPM greater than that of the compressor. Numbers of stages, for different pressure ratios based on the initial assumption, are tabulated in Table XV.

In many installations, there is the likelihood that the compressor may be divided into a two shaft, high and low pressure machine.

---

* The use of a 1000 ft/sec turbine with a 385 ft/sec compressor would of course lead to a considerable mismatching of diameters if direct coupling is assumed. Considering the very large power transmitted between compressor and turbine (several times the output power) any interposed speed reduction mechanism seems a serious handicap.

In this case, the shaft speed for the higher pressure unit will probably exceed that for the low pressure, since volume flow is less, and a higher speed high pressure turbine could be conveniently coupled to the high pressure compressor. For this type of design, the low pressure portion of the turbine would be coupled directly to the low pressure compressor. Thus it is not necessary in all cases that the rotating speed (RPM) of the high pressure turbine match the low pressure portion of the compressor.

For helium, there has been no increase from the compressor design in the assumed turbine peripheral velocities (as there was for air) since the tip speed limitation due to stress is applicable even though the Mach numbers are quite low (Figure 13). The axial turbine velocity was reduced from 500 ft/sec to 400 ft/sec to allow more reasonable blade heights, since in most cases the first stage turbine volume flow is less than the first stage compressor flow. For fluids with a sonic velocity less than air, as carbon-dioxide, it is felt that a reduction in peripheral velocity is necessary to maintain the assumed efficiency (i.e. maintain Mach numbers equal to the air machines) considering the present state of the art. The assumption of equal turbine and compressor efficiencies in the axial flow range is made for helium as well as for air.

An arbitrary ceiling of turbine and compressor efficiency of 0.90 is assumed as the flow rates become increasingly large. This is based on the consideration that it is impractical to build a single machine above a certain physical size and that compromises with optimum velocities, or even the dividing of the flowpath into two parallel machines, becomes advisable. It is for this reason that there is the leveling-off of the efficiency curves shown in Figures 18 and 19 where turbine efficiency is plotted against turbine horsepower output for various pressure and temperature levels. The logarithmic nature of the plot distorts the curve from the intuitive expectation especially at the high flow end. This type of plot is necessitated, however, by the wide range of outputs considered.

As previously mentioned, it is arbitrarily assumed that full admission axial flow turbines are suitable down to a minimum size of 5 inches tip diameter and 5/8 inch blade height. The power levels corresponding to this size, at the different pressure and temperature levels investigated, is used as the lower cut-off point for the assumed velocity diagram (Figure 13). For power outputs below these points, it is assumed that the peripheral speed is reduced, increasing the required number of stages. Efficiencies for each of these designs is estimated on the basis of the blade loss coefficient data previously discussed and plotted in Figures 18 and 19 (these calculations determine the lower portion of these curves). Leakage loss estimation was

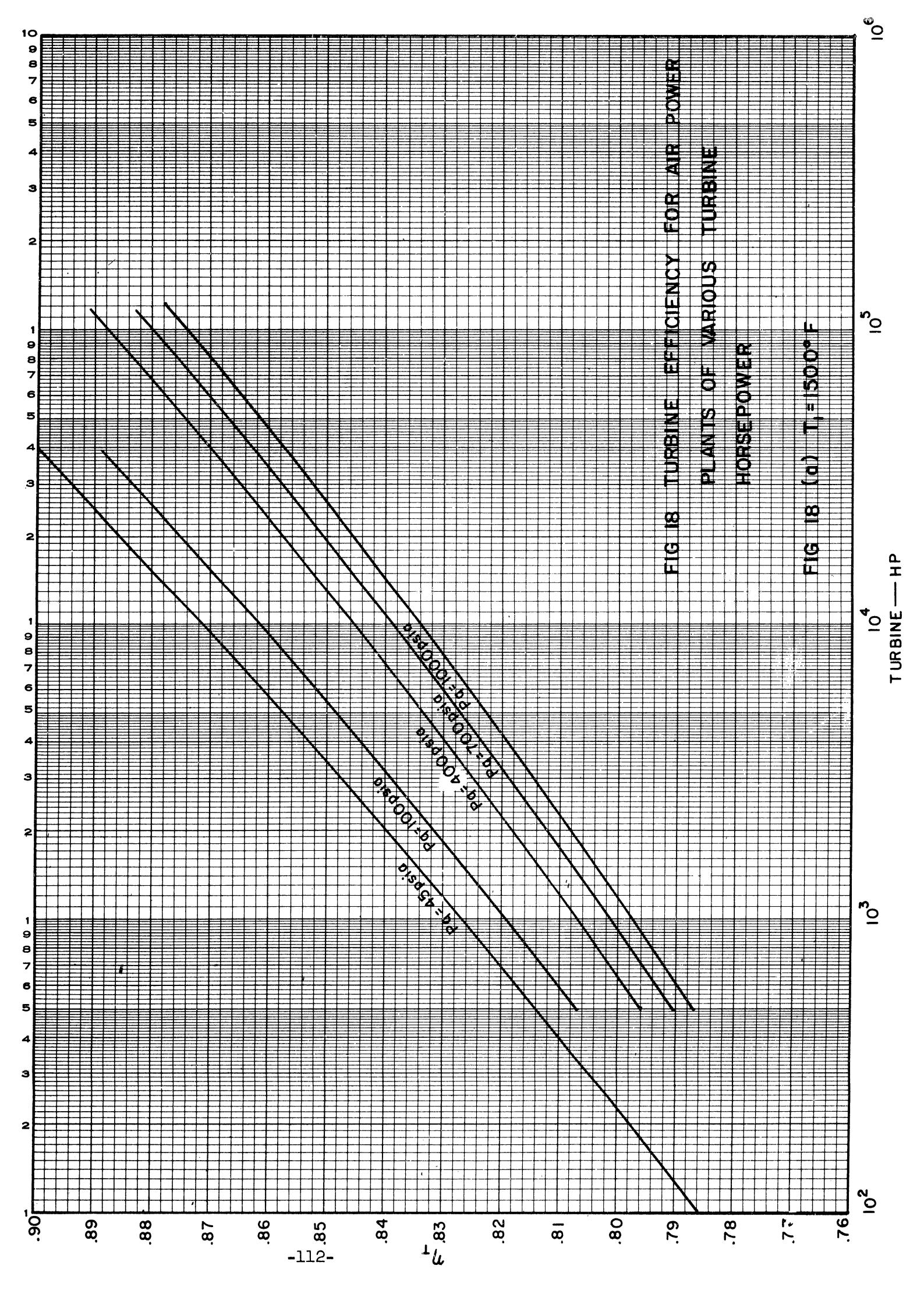
FIG 18 TURBINE EFFICIENCY FOR AIR POWER PLANTS OF VARIOUS TURBINE HORSEPOWER
FIG 18 (a) T_1 = 1500°F
η_t
TURBINE — HP
$P_2 = .45 P_1$
$P_2 = .400 P_1$
$P_2 = .100 P_1$
$P_2 = .0625 P_1$
$P_2 = .001 P_1$

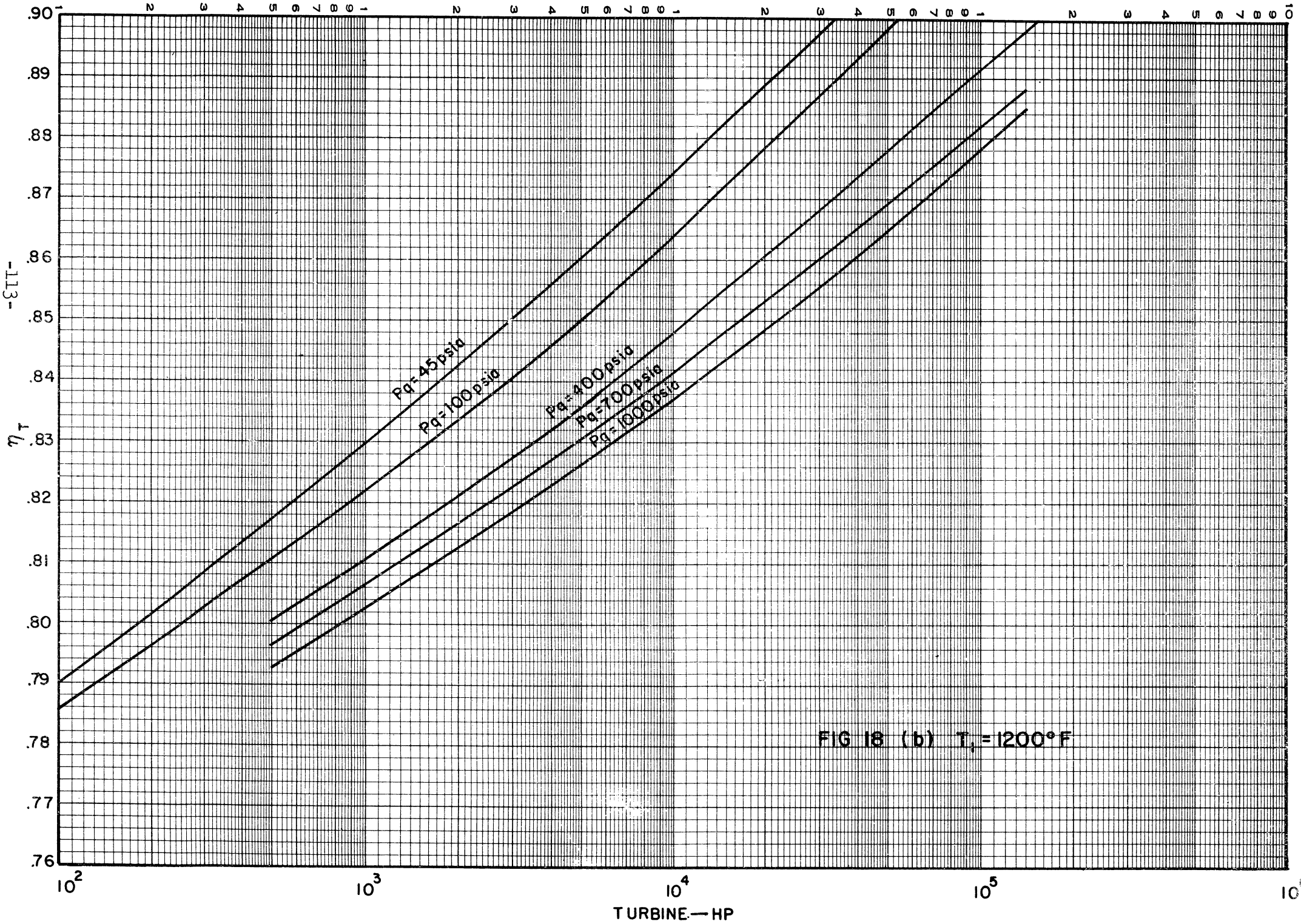

FIG 18 (b) $T_1 = 1200°F$

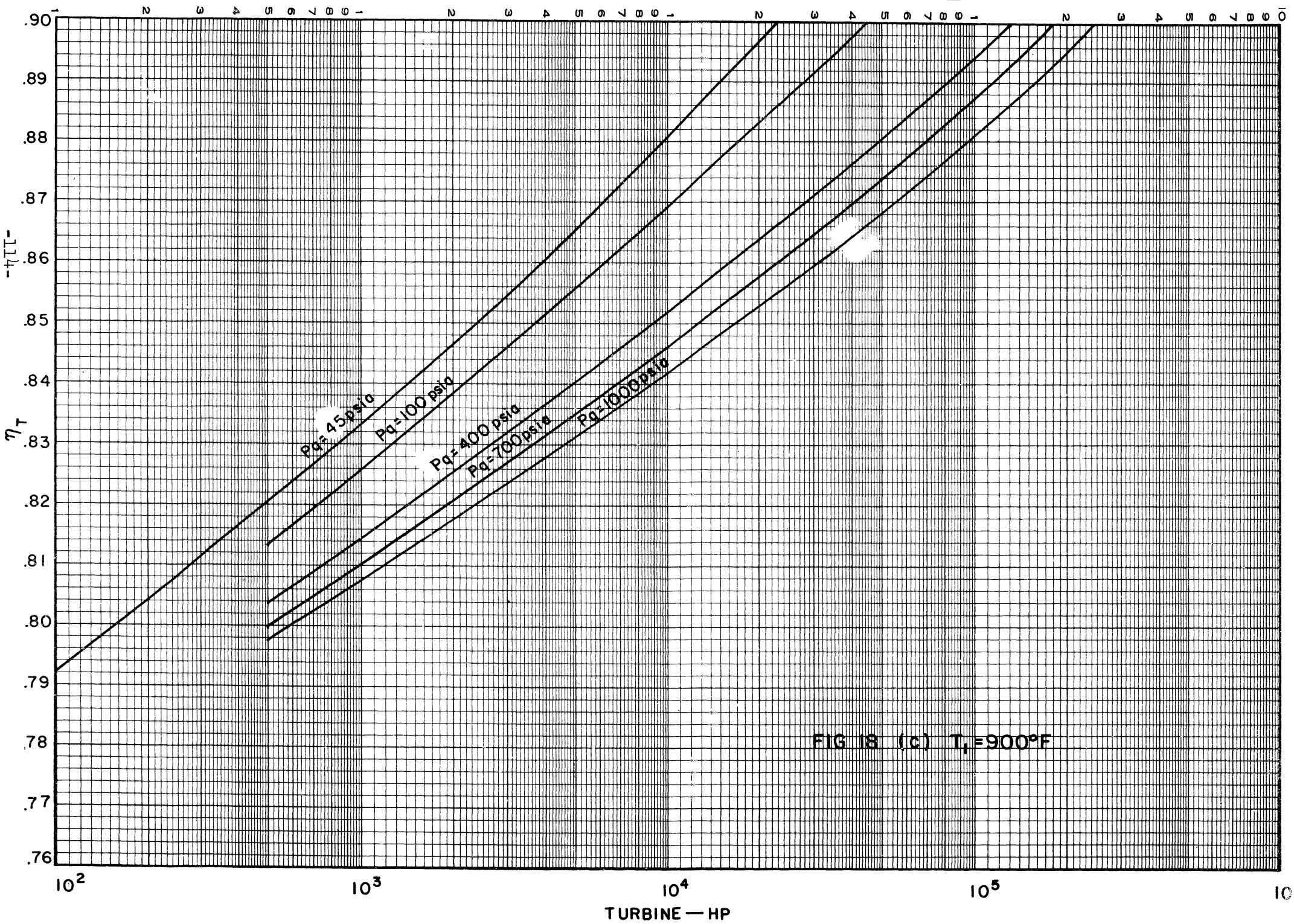

FIG 18 (c) T_1=900°F

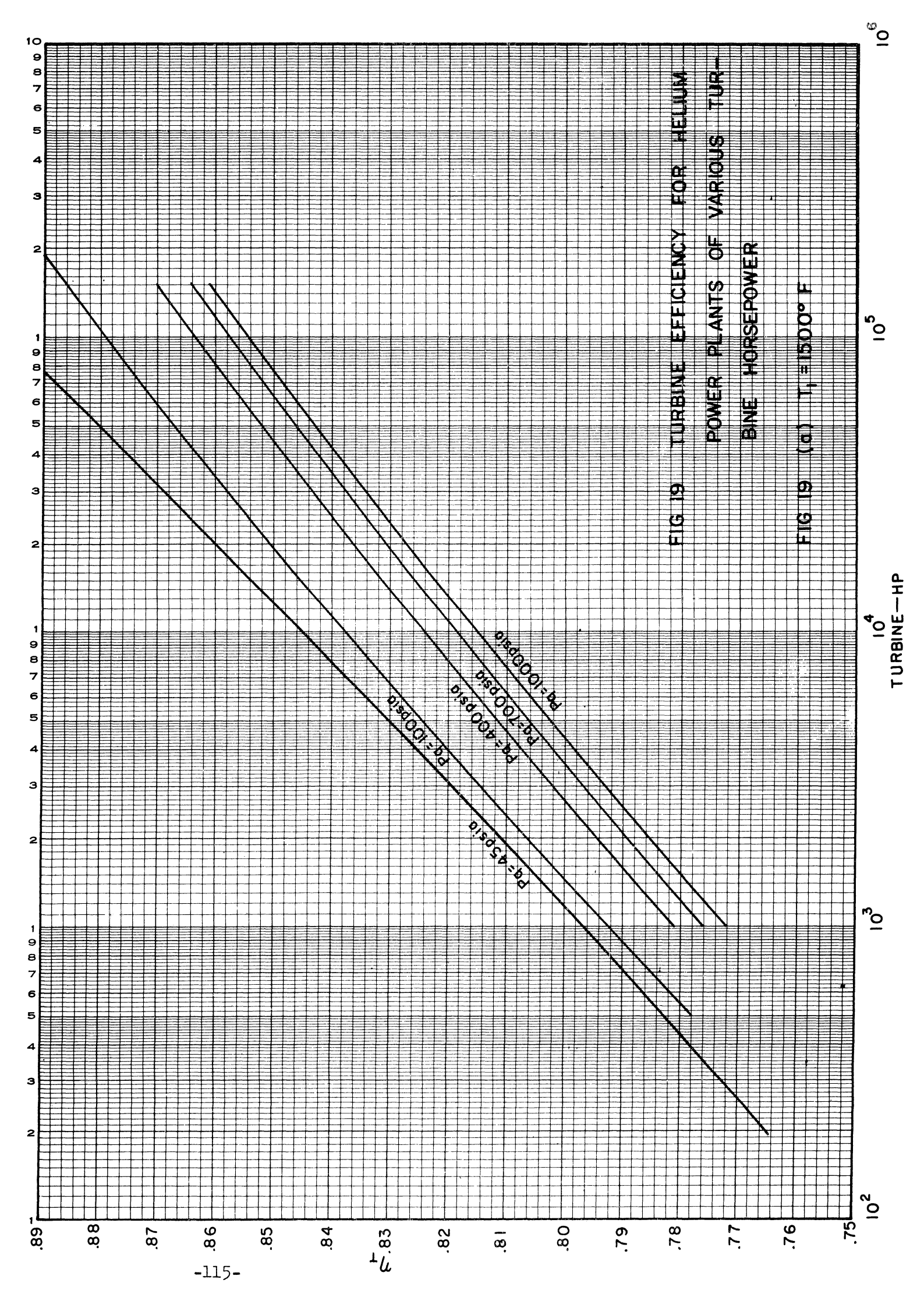
FIG 19 TURBINE EFFICIENCY FOR HELIUM POWER PLANTS OF VARIOUS TURBINE HORSEPOWER
FIG 19 (a) $T_1 = 1500°$ F
$P_d = 1000$ psia
$P_d = 700$ psia
$P_d = 400$ psia
$P_d = 100$ psia
$P_d = 45$ psia
η_t
TURBINE—HP

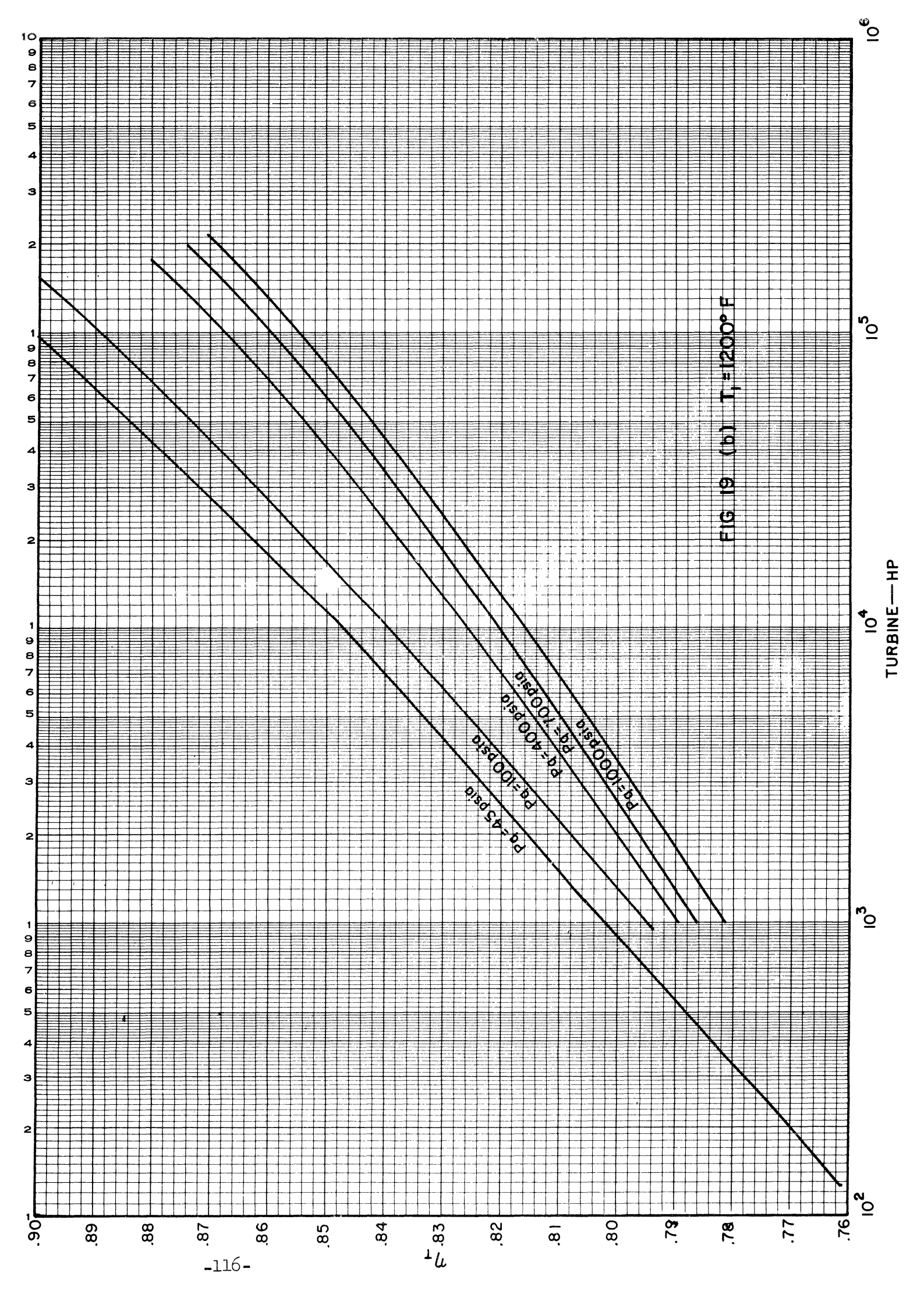
FIG 19 (b) T_1 = 1200° F
p_d = 1000 psia
p_d = 700 psia
p_d = 400 psia
p_d = 100 psia
p_d = 45 psia
η_t
TURBINE — HP

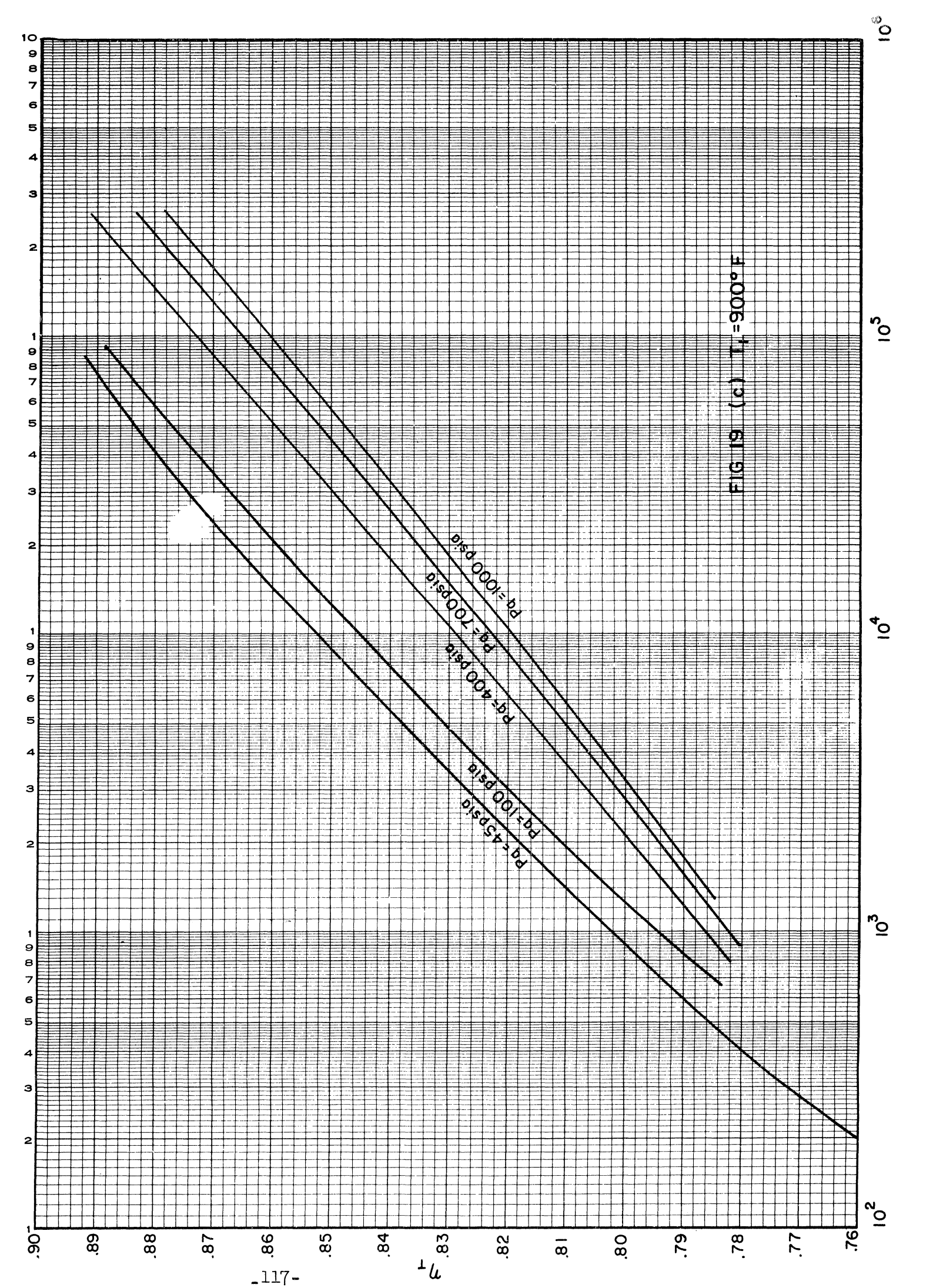
FIG 19 ( ) T_4=900°F
p_d=1000 psia
p_d=700psia
p_d=400 psia
p_d=100 psia
p_d=45psia
η_T
.90 .89 .88 .87 .86 .85 .84 .83 .82 .81 .80 .79 .78 .77 .76
10^6 10^5 10^4 10^3 10^2

based on the assumption of a blade tip clearance of 0.010 inches, which seems reasonable for a 5 inch wheel. Mechanical efficiency of 0.97 was assumed. Sample calculations are shown in the Appendix (Section 8.4).

3.5 Results and Tabulations

The final turbine and compressor efficiencies are tabulated in Tables V through XIV for air and helium plants (carbon-dioxide results will be reported at a later date) ranging in output from 60,000 to 600 horsepower, from 45 to 1000 psia in compressor discharge pressure, and from 1500 to 900 in turbine inlet temperature. In all cases, a compressor pressure ratio of 3.0 is assumed. As previously mentioned, this is fairly near to the optimum for the type of cycle studied, for all the cases. The remainder of the cycle assumptions were given previously in Section 3.1 and include notably a regenerator effectiveness of 0.93 and a ratio of compressor pressure ratio to turbine expansion ratio of 1.07. These latter assumptions appear generally on the optimistic side. However, they appear feasible for an economically optimum closed-cycle plant. In this type plant the heat transfer coefficients are considerably improved over those common to a conventional open cycle installation. For plants varying in the different parameters and arrangement from those assumed for these studies, it is possible to estimate the attainable efficiency on the basis of the curves of Figures 6 through 9. These show the change in efficiency due to a change in any one of the operating parameters with all others constant, as explained in Section 1.

Considering the listed turbine and compressor efficiencies, together with the other cycle assumptions, it is possible to compute the overall cycle efficiency. This has been done for all cases, using the sources for gas data given in Section 3.2. The resulting plant thermal efficiency values are tabulated in Tables V through XIV and plotted in Figures 20 and 21. These efficiencies do not include reduction gear or generator losses, or any shielding or transmission heat losses which may be associated with a given nuclear reactor plant. A 3% radiation loss from the gas turbine ducting was assumed.

3.5.1 Discussion of Results

There are several interesting points which may be mentioned in connection with these tabulated and plotted results. As might be anticipated, the attainable plant efficiency drops considerably with power output, for any given temperature limit and for any pressure level. This, of course, is the result of decreasing turbo-machinery efficiency with decreasing flow rate. Also, except at very high outputs, where the arbitrary physical machine size cut-off is imposed, the efficiency is less for higher operating pressure (not, in general, pressure ratio). This results from two opposing trends. As pressure level is increased, density increases directly in proportion, whereas hydraulic diameter (for a given mass flow under given temperature and

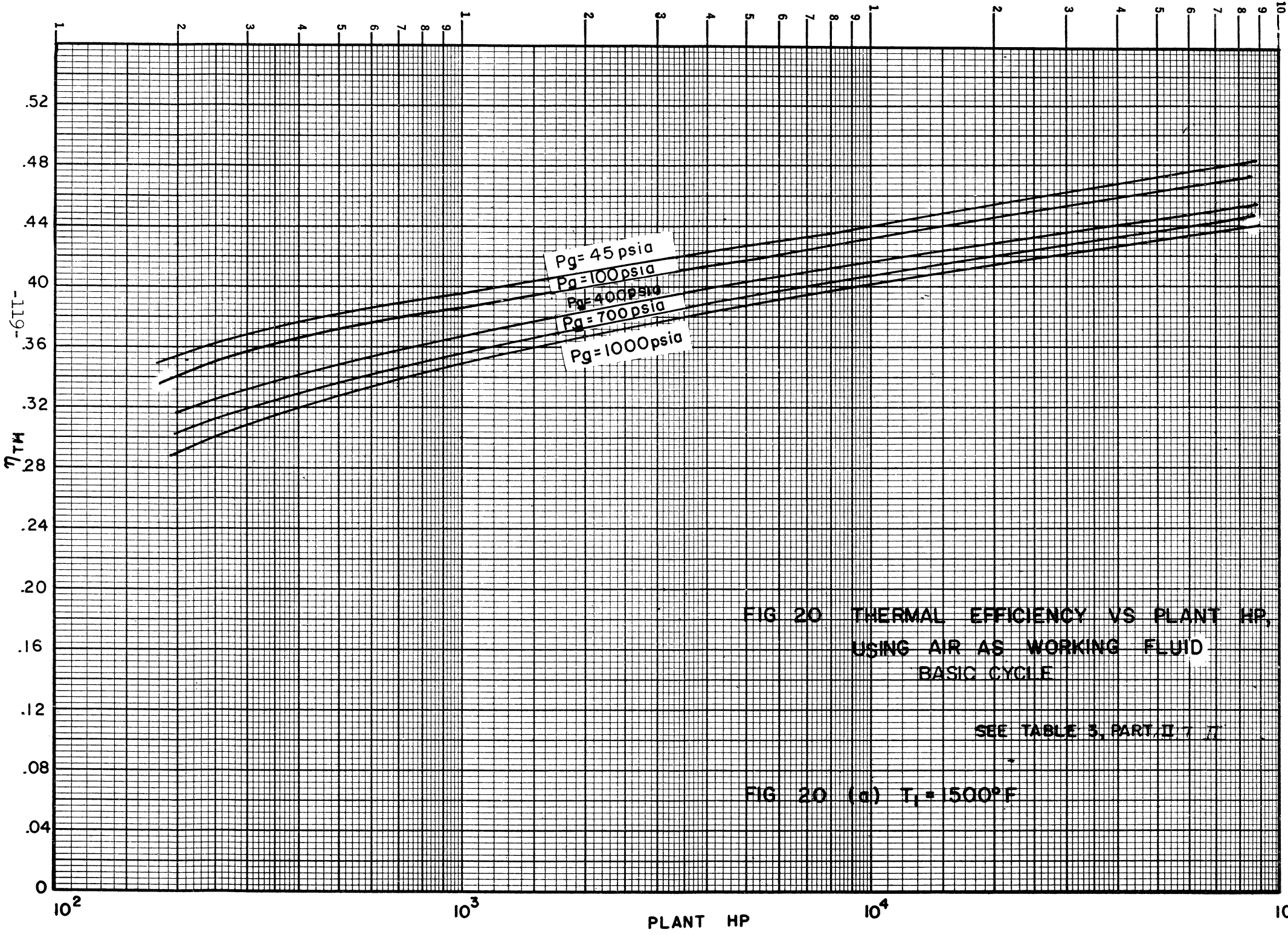

FIG 20 THERMAL EFFICIENCY VS PLANT HP, USING AIR AS WORKING FLUID BASIC CYCLE

SEE TABLE 3, PART II

FIG 20 (a) T_1 = 1500°F

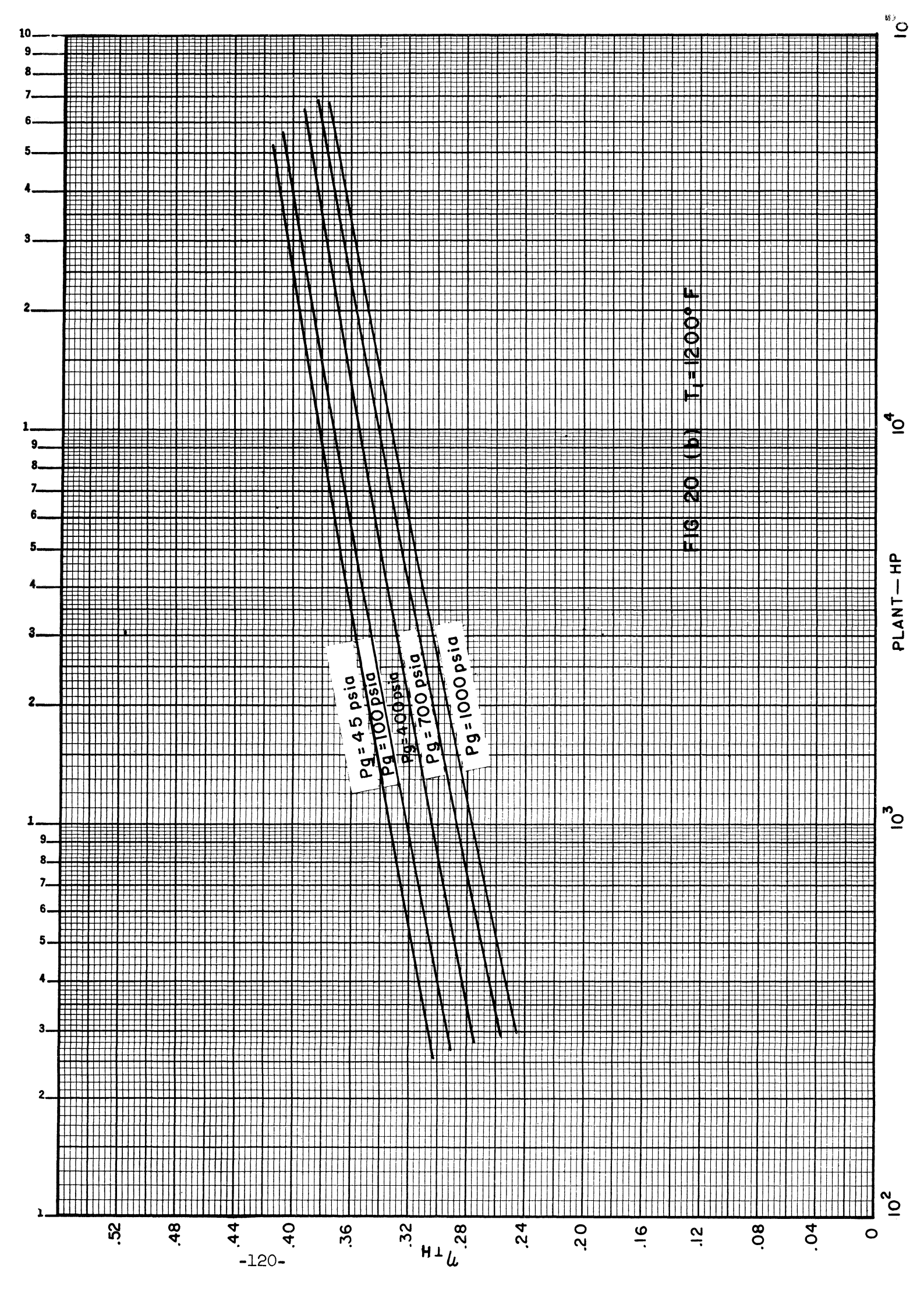
FIG 20 (b) T1 = 1200° F
PLANT — HP
η_{TH}
Pg = 45 psia
Pg = 100 psia
Pg = 400 psia
Pg = 700 psia
Pg = 1000 psia
10
9
8
7
6
5
4
3
2
1
10^4
10^3
10^2
.52
.48
.44
.40
.36
.32
.28
.24
.20
.16
.12
.08
.04
0

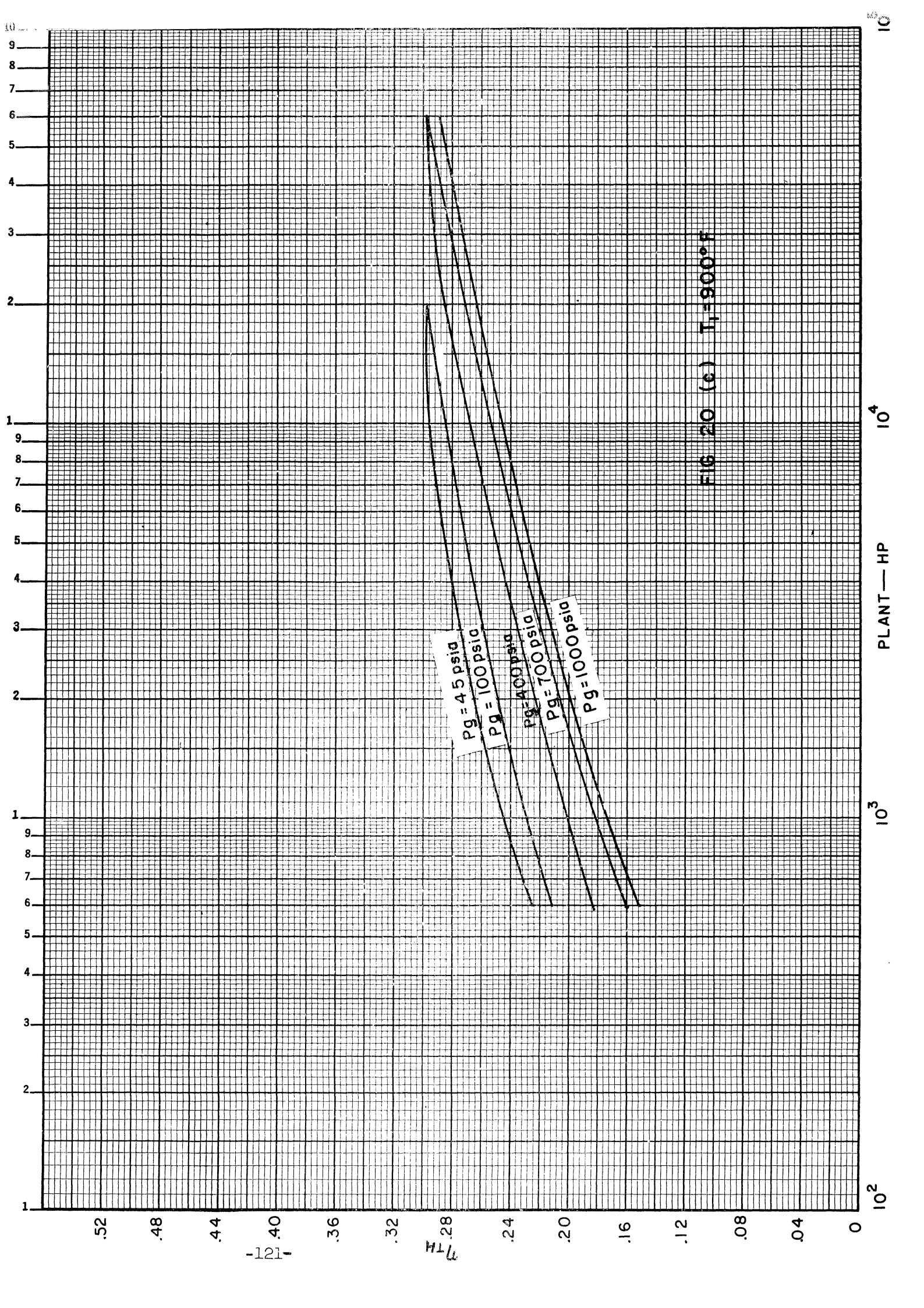
FIG 20 (c) T_1=900°F
PLANT — HP
10^6
10^4
10^3
10^2
η_{TH}
.52
.48
.44
.40
.36
.32
.28
.24
.20
.16
.12
.08
.04
0
Pg = 45 psia
Pg = 100 psia
Pg = 400 psia
Pg = 700 psia
Pg = 1000 psia

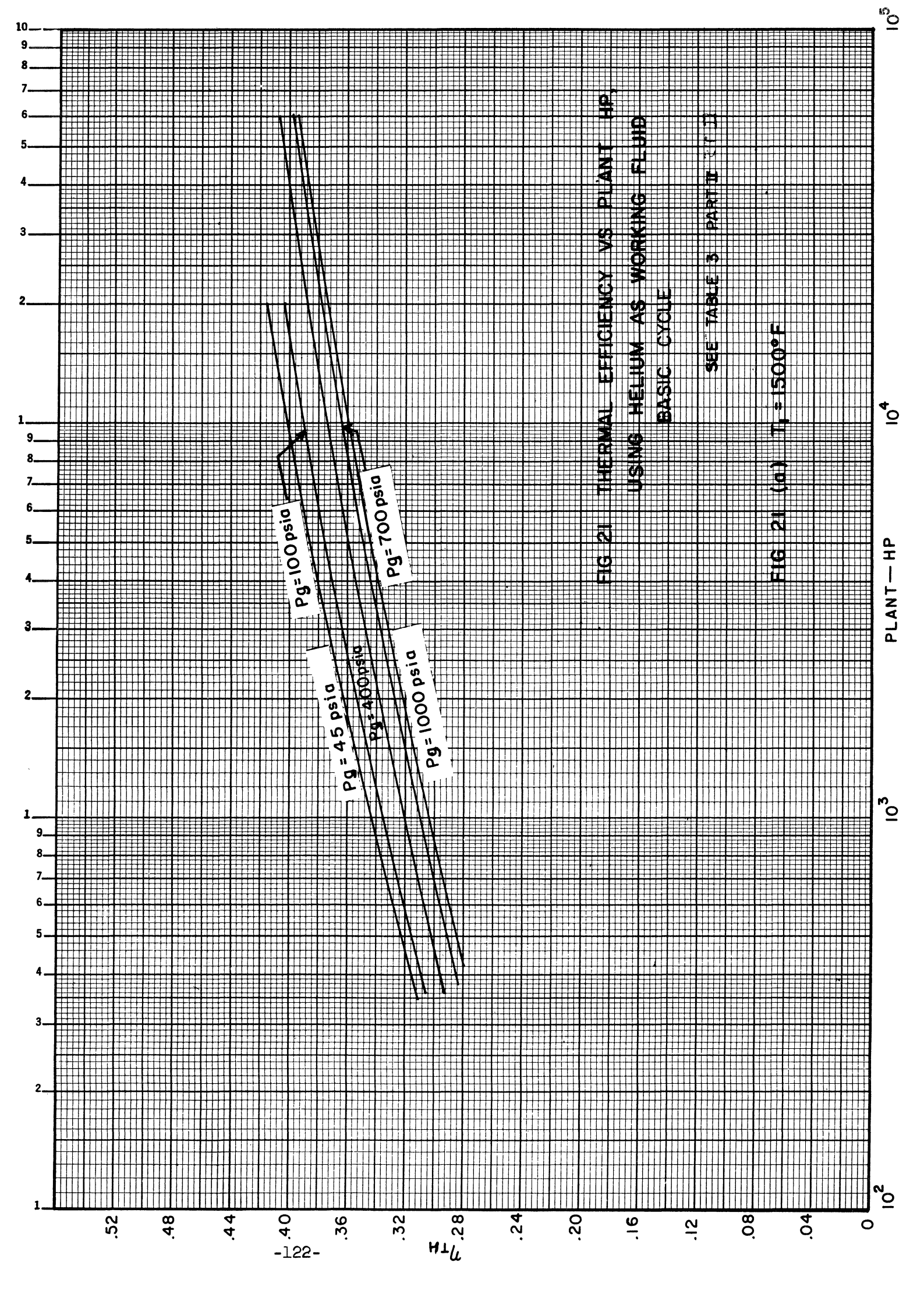
FIG 21 THERMAL EFFICIENCY VS PLANT HP
USING HELIUM AS WORKING FLUID
BASIC CYCLE
SEE TABLE 3 PART II
FIG 21 (a) T_1 = 1500°F
Pg=100 psia
Pg=700 psia
Pg = 45 psia
Pg=400 psia
Pg=1000 psia
η_{TH}
PLANT—HP
10
9
8
7
6
5
4
3
2
1
10^5
10^4
10^3
10^2
.52
.48
.44
.40
.36
.32
.28
.24
.20
.16
.12
.08
.04
0

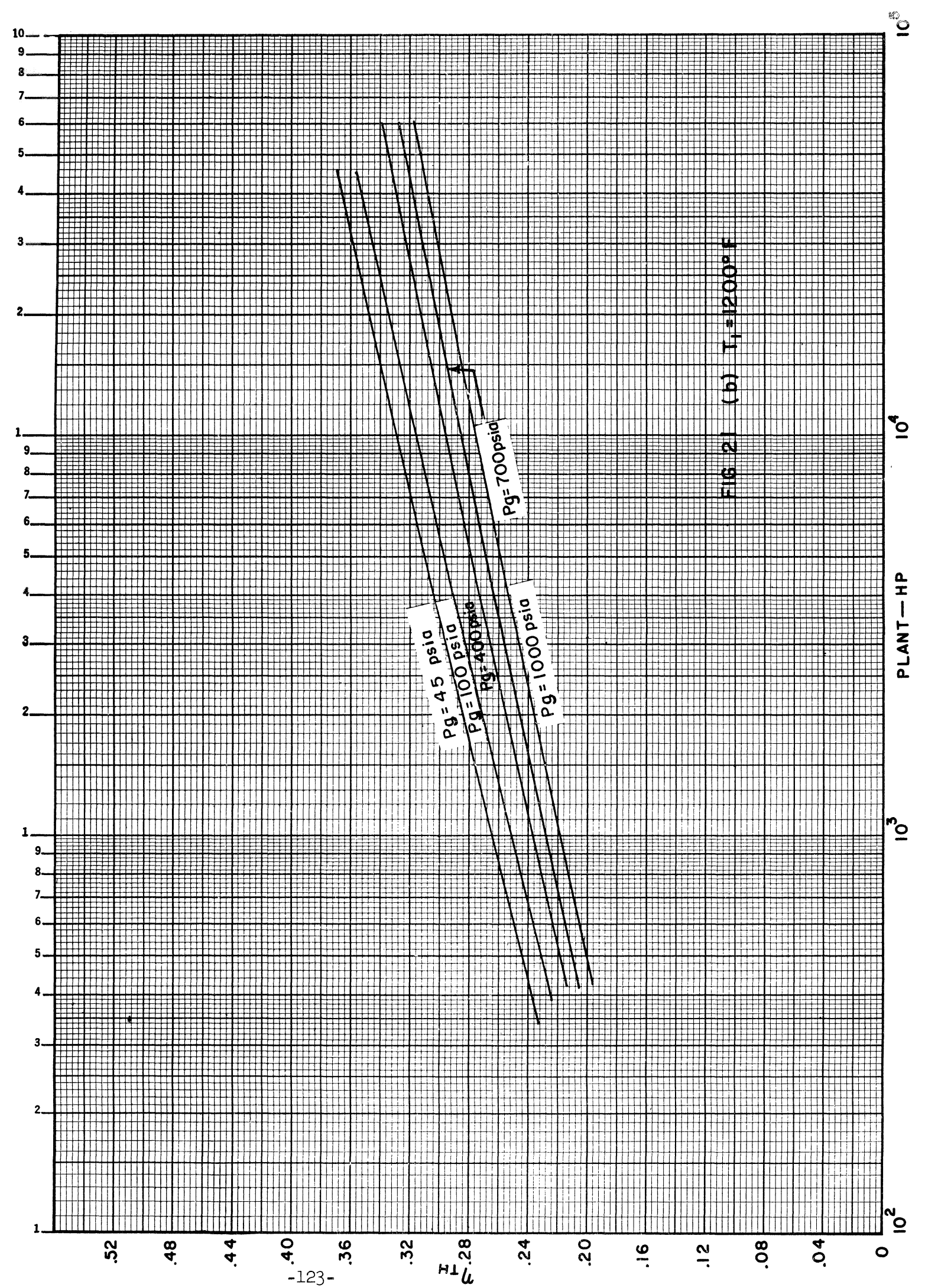

FIG 21 (b) T_1 = 1200° F

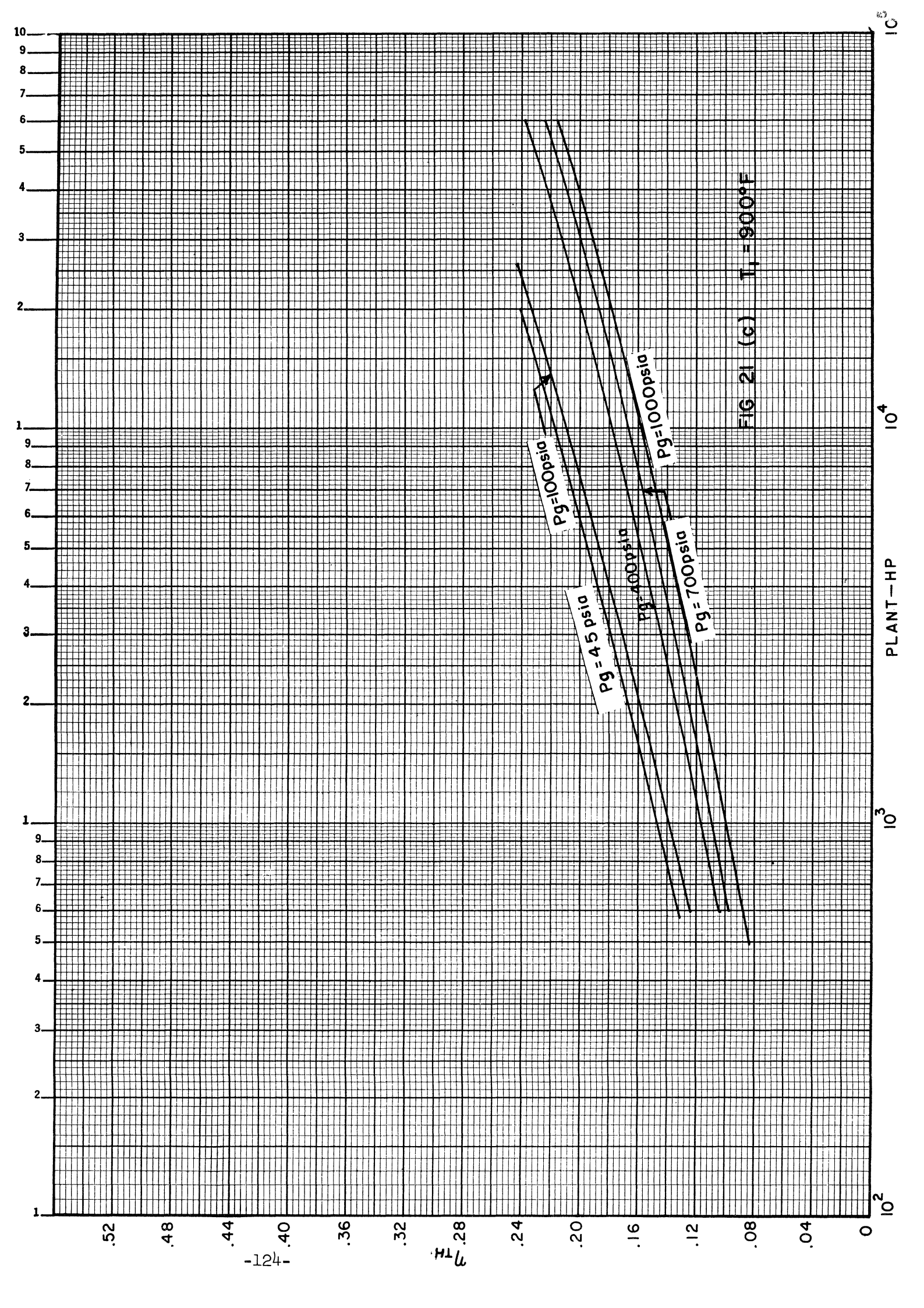
Pg=100psia
Pg=45 psia
Pg=400psia
Pg=1000psia
Pg=700psia
PLANT—HP
η_{TH}
FIG 21 (c) T_1 = 900°F

velocity conditions) decreases only as the square root of the pressure. Since viscosity does not change substantially with pressure, (not at all for a perfect gas), the Reynold's number increases with pressure. However, the physical size of the machine decreases. The effect of this change on the component efficiency as abstracted from the data of reference 6 and plotted in Figure 12 is more pronounced than the effect of the increasing Reynold's number (see Tables V through XIV). Therefore, the component efficiency decreases. In practice of course, the use of high pressure will result, up to a point, in the reduction of equipment cost and weight. This factor will, in many cases, overcome in an economic analysis the corresponding efficiency loss. Stated another way, for a given capital outlay, it may be possible to achieve higher efficiency at higher pressure because a more highly effective regenerator, more adequate ducting, and a more nearly optimum (in number of stages) turbomachine design can be obtained. The balance of these various factors is of extreme importance and will be the subject of additional analytical effort.

There is, of course, a large decrease of efficiency with source temperature level. This is of extreme importance in many cases. A further disadvantage of low source temperature is that the flow rate and hence machinery size (see Tables V to XIV and Figures 15 and 16) becomes excessive. This factor may be as important in an economic balance for a given application as the reduced efficiency, since it results in a greatly increased machinery capital cost. Additional investigation of these factors will be conducted.

It will be noted (Figure 21) that the cycle efficiencies shown for helium under given power, temperature, and pressure conditions are considerably less than for air under the same conditions. Partially, this is the result of an inherently lower monatomic gas efficiency (Figure 6a for example) with the same component efficiencies. It is also the result of the fact that the pressure ratio assumed for this study gives theoretical efficiencies further reduced from the optimum for helium than for air (monatomic gas efficiency is considerably more sensitive to pressure ratio than diatomic which is a real disadvantage of the monatomic gases). An additional factor is the use of higher velocities (almost equal Mach numbers) for helium than for air. This results in smaller machinery than would otherwise be the case and hence reduced efficiency (Figure 12). However, it appears likely that the additional efficiency obtainable from a reduced velocity design could not balance economically the increased machinery cost. These factors will be further evaluated in the continuation of these studies.

A very high regenerator effectiveness has been assumed for these studies. Even though this may be feasible, it may not be desirable where there is a requirement for low temperature heat, as

perhaps for area heating, low pressure steam, etc. In these cases, a low regenerator effectiveness is advantageous from the viewpoint of capital cost reduction, without prejudice to overall thermal efficiency, since, as with steam extractions in a steam plant, extraction of low level heat at this point is thermodynamically more advantageous than the supplying of the heat requirement directly from the high level heat source.

4.0 FUTURE WORK

The work to this point has furnished a basis for the estimation of the attainable cycle efficiencies and the general size of the turbomachinery for gas turbine cycles operating with either air or helium over a wide range of power outputs, pressures, and temperatures. However, this basic work suggests the desirability of various avenues of extended effort which would help to complete the overall picture of the gas turbine plant as applied to nuclear reactor power-plants. Among those additional desirable points of investigation which will be pursued are the following:

1) An extension of the basic study to include economic optimization of typical nuclear plants. This would then include the effects of heat exchanger effectiveness, operating pressure level, working fluid, temperature, etc. vs. capital and fuel costs.

2) Extension of the work to include carbon-dioxide to give a broader range of molecular weights and the corresponding basic fluid quantities. Other gases of particular interest from the viewpoint of nuclear or other special desirability may be included.

3) Study of the effects of radiation on the various gases and the degree of machinery contamination involved in their use as direct reactor coolants. This phase of the study can be broadened to include an estimation of the mechanical and developmental difficulties which may be expected with the various fluids, for cases where they are, and also where they are not, used as direct reactor coolants.

4) Problems of control of an integrated reactor-gas turbine set. This will involve feedback to the reactor through such parameters as the reactor temperature coefficient.

5) Preliminary study of the possibility and desirability of the design and erection of a small-scale gas turbine plant, capable of operation with a minimum of alteration with various fluids under various operating conditions. Eventually, such a plant could be a portion of a reactor mock-up, and would serve to pinpoint the problems likely to be encountered in a full scale design.

5.0 CONCLUSIONS

A broad investigation of the gas turbine cycle as it applies to nuclear powerplants has been conducted. On the assumption that efficiency is likely to be of more importance than size and weight for this type of device, the study has emphasized the regenerative cycle with highly effective heat exchanger components and relatively low pressure ratios. A "basic cycle" was assumed and optimized with respect to pressure ratio for both diatomic and monatomic perfect gases. Variations of each of the significant parameters including cycle arrangement and operation were assumed singly, and the effects on the plant efficiency computed. Thus a basis is provided for the estimation of any gas turbine cycle efficiency if the component efficiencies and arrangement are known. An interesting result of the study is the fact that the perfect gas efficiencies do not depend on molecular weight, but only on pressure ratio and ratio of specific heats. As it turns out, the attainable cycle efficiency with given component efficiencies is somewhat greater for diatomic than for monatomic gases. However, if a cost balance is included, the balance may in some cases favor the monatomic gas on the basis of higher component efficiencies for a given capital outlay.

A further detailed study for air and helium plants, utilizing the "basic cycle" over a wide range of power output, pressure, and temperature is included. This has resulted in the tabulation of overall cycle efficiency, turbomachine component efficiencies, turbomachine sizes and types. The study assumed constant heat exchanger effectiveness at a rather high level, with the variations due solely to the change in attainable turbomachinery efficiency with power level, pressure, and temperature. As expected, this has shown the very serious disadvantage of low inlet temperature, both with respect to efficiency and machinery size and cost. Under the assumptions of the study, it has been shown that increasing pressure level results in reduced component size, but, in general, also in somewhat reduced turbomachine efficiency due to the lower volumetric flow rate. Also, the overall efficiency for a helium plant, with optimized turbomachinery, but fixed heat exchanger effectivenesses, is considerably less than that of an air plant with the same heat exchanger values and optimized turbomachinery. However, it is a question of optimization between efficiency and capital cost for the heat exchangers as well as the turbomachinery. Such an optimization has been beyond the scope of the investigation to date. A listing of desirable future endeavors along the lines of this work is included.

6.0 NOMENCLATURE

T	-	temperature (noted as F or R)
p	-	pressure (psia)
PR	-	pressure ratio
TR	-	temperature ratio
A	-	area (sq. in.)
h_{bd}	-	blade height (in.)
D	-	diameter (in.)
W	-	mass flow or work (lb/sec or ft-lb)
G	-	volume flow (cu. ft/min)
R_e	-	Reynold's number
R	-	gas constant (53.3 for air)
Q	-	heat input from prime heat source (BTU)
Q_R	-	heat input from reheater (BTU)
J	-	778 ft-lb/BTU
C_p	-	specific heat at constant pressure
C_v	-	specific heat at constant volume
k	-	ratio of specific heats (C_p/C_v)
μ	-	viscosity (lb/hr. ft)
h	-	enthalpy (BTU/lb)
η	-	efficiency
HP	-	horsepower
w	-	relative velocity (ft/sec)
Cu	-	absolute velocity (ft/sec)
u	-	wheel velocity (ft/sec)
v	-	axial velocity (ft/sec)

a - sonic velocity (ft/sec)

ℓ - blade spacing normal to relative velocity (inches)

Subscripts

T - turbine

C - compressor

th - thermal

hyd - hydraulic

h - hub

t - tip

R - regenerator

p - friction pressure

u - peripheral

Numerical subscripts refer to Figures 1 through 5 of Part II.

Superscripts

Prime refers to the ideal state.

7.0 BIBLIOGRAPHY

1. Keenan and Kaye, Gas Tables, 1948, John Wiley and Sons, New York.

2. McAdams, William H., Heat Transmissions, 3rd Edition, 1954, McGraw-Hill, New York.

3. Kestin, J. and Pilarczyk, K., Measurement of the Viscosity of Five Gases at Elevated Pressure by the Oscillating Disk Method, ASME Paper No. 53-A-67.

4. Worthington Research Bulletin P-7637, July, 1949, Compressibility Charts and Their Application to....Real Gases, Worthington Corporation, Harrison, New Jersey.

5. Akin, S. W., The Thermodynamic Properties of Helium, ASME Paper No. 49-A-96.

6. Kent's Mechanical Engineers Handbook, 12th Edition, Power Volume, Section 10, John Wiley and Sons, New York.

7. Nguyen, Van Le, Report on Loss Coefficients in Turbine Blade Passages, Gas Turbine Laboratory, Massachusetts Institute of Technology, Cambridge, Massachusetts.

8. Dolan, W. A. Jr., Hafer, A. A., Gas Turbine Progress Report-Naval Vessels, Trans. ASME, Vol. 75, No. 2, February, 1953.

8.0 APPENDIX

8.1 Derivation of Thermal Efficiency Equations

The derivation of the equation of thermal efficiency for the basic cycle (Figure 1) is based on the following:

$$W_T = \frac{k}{k-1}\,\eta_T\,R\,T_1\left[\frac{PR_T^{\,k-1/k} - 1}{PR_T^{\,k-1/k}}\right]$$

$$W_C = \frac{2}{\eta_C}\,R\,T_6\,\frac{k}{k-1}\left[PR_C^{\,k-1/2k} - 1\right]$$

$$\eta_R = \frac{T_{10} - T_9}{T_4 - T_9}$$

$$\eta_P = \frac{PR_T}{PR_C}$$

$$PR_C = PR$$

$$\gamma = \frac{k-1}{k} = \frac{R}{C_p J}$$

$$TR = \frac{T_1}{T_6}$$

$$Q = (T_1 - T_{10})\,C_p J$$

$$T_9 - T_6 = \frac{W_C}{2C_p J}$$

$$T_1 - T_4 = \frac{W_T}{C_p J}$$

$$\eta_{th} = \frac{\text{output}}{\text{input}} = \frac{W_T - W_C}{Q}$$

from which

$$\eta_{th} = \frac{TR\,\eta_T\,[\,1 - (\eta_p PR)^{-\gamma}\,] - \frac{2}{\eta_C}\,[\,PR^{\gamma/2} - 1]}{TR\left\{1 - \eta_R + \eta_R\eta_T\,[\,1 - (\eta_p PR)^{-\gamma}\,]\right\} + \frac{\eta_R - 1}{\eta_C}\,[PR^{\gamma/2} + \eta_C - 1]}$$

The derivations for the other cycles are similar. The elimination of the recuperator (Figure 2) can be considered simply by letting $\eta_R = 0$ in the previous equation.

For the case of the basic cycle without intercooler (Figure 3) the work of the compressor becomes

$$W_C = \frac{1}{\eta_C} \frac{k}{k-1} R T_6 [PR_C^{k-1/k} - 1],$$

hence,

$$\eta_{th} = \frac{TR\eta_T [1 - (\eta_p PR)^{-\gamma}] - \frac{1}{\eta_C} [PR^{\gamma} - 1]}{TR \{ 1 - \eta_R + \eta_R\eta_T [1 - (\eta_p PR)^{-\gamma}]\} + \frac{\eta_R - 1}{\eta_C} [PR^{\gamma} + \eta_C - 1]}$$

Considering a simple cycle of compressor, turbine, heat source and sink, i.e. without intercooler and recuperator (Figure 4), the thermal efficiency reduces to:

$$\eta_{th} = \frac{TR\eta_T [1 - (\eta_p PR)^{-\gamma}] - \frac{1}{\eta_C} [PR^{\gamma} - 1]}{TR - \frac{1}{\eta_C} [PR^{\gamma} + \eta_C - 1]}$$

With the basic cycle supplemented by reheat between turbine stages the thermal efficiency is affected by both the increased work of the turbine and the additional heat input to the system.

Thus,

$$W_T = 2\eta_T \frac{k}{k-1} R T_1 \left[\frac{PR_T^{k-1/2k} - 1}{PR_T^{k-1/2k}} \right]$$

and the heat added by the reheater, Q_R, equals $(T_3 - T_2) C_p J$. The resulting thermal efficiency is

$$\eta_{th} = \frac{2\eta_T TR [1 - (\eta_p PR)^{-\gamma/2}] - \frac{2}{\eta_C} [PR^{\gamma/2} - 1]}{TR\{ 1-\eta_R + \eta_R\eta_T[1-(\eta_p PR)^{-\gamma/2}]\} + \frac{\eta_R-1}{\eta_C} [PR^{\gamma/2} + \eta_C-1]+TR[1 - \left(\frac{1}{\eta_p PR}\right)^{\gamma/2}]}$$

8.2 Velocity Vector Diagram Calculations

Velocity vector diagrams of approximate designs for both the turbine and compressor were made considering axial flow symmetrical stage machines. A pressure ratio per stage within the range of current industrial practice was used. The diagrams which are shown in Figure 13 for the first stage only of the turbine and compressor of the air and helium powerplants, i.e. the temperature assumed was for the inlet to the turbine and compressor.

The overall pressure ratio of the compressor is 3.00 and of the turbine 2.79 due to 7% frictional duct and heat exchanger pressure losses. The pressure ratio per stage of the compressor is maintained at approximately 1.08. In the case of the helium compressor the peripheral velocity of the wheel was reduced to keep within a tolerable wheel stress level. Similar velocity diagrams were considered for both helium and air machines, so that the helium pressure ratio per stage is reduced to 1.07.

The compressor calculations were based on the following perfect gas relations.

$$W_C = - J C_p T_6 \left[1 - PR^{k-1/k} \right] \tag{1}$$

$$W_C = \frac{u\Delta Cu}{g} \tag{2}$$

$$M_u = \frac{u}{a} \tag{3}$$

$$a = \sqrt{gkRT_6} \tag{4}$$

$$R/J = C_p - C_v = C_p \left(\frac{k-1}{k}\right) \tag{5}$$

$$W_T = JC_pT_1 \left[1 - \left(\frac{p_1}{p_2}\right)^{-(k-1/k)} \right] \tag{6}$$

$$W_T = \frac{u\Delta Cu}{g} \tag{7}$$

For the compressor,

$$-JC_pT_6 \left[1 - \left(\frac{p_1}{p_2}\right)^{k-1/k} \right] = \frac{u\Delta Cu}{g} = \frac{\Delta Cu\ u^2}{ug}$$

$$T_6 = \frac{a^2}{gkR} \; ; \; \frac{R}{JC_p} = \frac{k-1}{k}$$

Then,

$$- \left[1 - \left(\frac{p_1}{p_2}\right)^{k-1/k} \right] = \frac{\Delta Cu}{u} M_u^2 (k-1)$$

or

$$(PR)_{stage} = \left(\frac{p_1}{p_2}\right)_{stage} = \left[1 + \frac{\Delta Cu}{u} (k-1) M_u^2 \right]^{k/k-1} \tag{8}$$

and,

$$(PR)_{tot} = \left(\frac{p_1}{p_2}\right)_{Tot} = \left[1 + \frac{\Delta Cu}{u} (k-1) M_u^2 \right]^{Zk/k-1} \tag{9}$$

where Z is the number of stages, and where the subscripts 1 and 2 refer to the higher and lower pressures respectively.

The derivation for the turbine follows a similar pattern, and gives

$$(PR)_{stage} = 1 / \left[1 - \frac{\Delta Cu}{u} (k-1) M_u^2 \right]^{k/k-1} \tag{10}$$

As a sample calculation consider the case of the compressor for air.

Overall P.R. = 3.00

v = 200 fps

k = 1.4

Assume initially:

P.R./stage = 1.08

$\Delta Cu/u = .368$

Overall P.R. = [P.R./stage]^Z

where Z is the number of stages

$3.00 = (1.08)^Z$

Z = 14.35

Since the number of stages must be an integral number it is taken as 14 and the P.R./stage is then 1.082.

Then using equation 8:

$$M_u = \sqrt{\frac{-\left[1 - (\text{P.R./stage})^{k-1/k}\right]}{\left(\frac{\Delta Cu}{u}\right)\quad (k-1)}}$$

$$M_u = \sqrt{\frac{1\left[1 - (1.082)^{0.286}\right]}{(.368)\ (.4)}} = .394$$

$$u = M_u a = (.394)\ (1150) = 453 \text{ fps}$$

$$Cu = \frac{\Delta Cu}{u} \times u = (.368)\ 453 = 167 \text{ fps}$$

The calculations of the triangles (assuming symmetrical blading) through triganometric identities gives $C_1 = W_2 = 246$ fps, $C_2 = W_1 = 369$ fps, $\Theta_2 = \beta_1 = 32.8°$, and $\Theta_1 = \beta_2 = 54.5°$. The blade turning angle (angle between the two relative velocities, W_1 and W_2) is then equal to 21.7°.

Since it is desired to have a blade turning angle of approximately 30°, the calculations were repeated with a $\Delta Cu/u = .510$. Mach no. then = .335, u = 385 fps, ΔCu = 196.5 fps, and the blade turning angle = 30.3°. The compressor velocity diagram in Figure 13a presents the complete results of this calculation.

The helium compressor velocity vector diagram was determined through the same procedure. Table XVI summarizes the results.

8.3 Effects of Gas Turbine Plant Size. Sample Calculations

As typical examples, consider sample calculations for a 1500 F, 100 psia, 20,000 HP helium plant with axial flow compressor and also an air plant of the same size. In addition a 1200 F, 100 psia, 600 HP helium and also an air plant are shown. The cycle schematic for all cases is shown in Figure 1.

8.3.1 Helium Plant, 20,000 HP, 1500 F, 1000 psia

8.3.1.1 Compressor

The compressor inlet conditions are:

$$p = 1000/3 = 333 \text{ psia}$$

TABLE XVI. AXIAL COMPRESSOR AND TURBINE VECTOR DIAGRAM TABULATION

	Compressor		Turbine	
	Air	Helium	Air	Helium
Pressure Ratio	3.00	3.00	2.79	2.79
Pressure Ratio Stage	1.082	1.0712	1.121	1.0502
No. of Stages	14	16	9	21
Axial Velocity (v)	200 fps	500 fps	400 fps	400 fps
Wheel Velocity (u)	385 fps	962.5 fps	481 fps	962.5 fps
Mu	.335	.286	.240*	.164*
Blade Turning Angle	30.3°	30.3°	76.3°	76.2°

* Based on the 1200 F case which represents the mean of the inlet temperatures used.

$$t = 90\ F = 550\ R$$

$$P = \frac{333 \times 144}{1545/4 \times 550} = 0.226\ lb/ft^3.$$

It was estimated from approximate efficiencies that required flow rate is

$$w = 41.7\ lb/sec.$$

Then the volumetric flow rate at compressor inlet is

$$G = w/P = 41.7/.226 = 184.5\ ft^3/sec = 11{,}100\ ft^3/min.$$

Referring to Figure 13 it is noted that the axial inlet velocity is 500 ft/sec compared to 200 ft/sec for a typical air machine. Therefore, the physical size of the helium machine is similar to that of an air unit handling 200/500 x CFM = 200/500 x 11,100 = 4440 CFM.

The efficiency of such an air unit is taken from Figure 12 and is noted to be .822. The blading Reynold's number for the air unit is taken from Figure 14 (derivation of these figures is shown in Section 8.3.2) and is 152,000.

The blading Reynold's number for the helium unit is computed as below. All calculations are for the first stage of both compressor and turbine. It is assumed that the efficiency of subsequent stages will be similarly affected.

The absolute viscosity for helium at 90 F is taken from reference 2 and is .0459 lb/hr. ft. (viscosity is substantially independent of pressure).

The blade height is computed from continuity utilizing the assumption that $D_h/D_t = .75$. (1)

$$\text{Then } A = .785\ (D_t^2 - D_h^2) \tag{2}$$

$$h_{bd} = \frac{D_t - D_h}{2} \tag{3}$$

Substituting (1) in (3) we get

$$h_{bd} = \frac{D_t}{8} \tag{4}$$

Substituting (3) and (1) into (2) we get

$$A = .785\ (D_t^2 - .75^2\ D_t^2) = .344\ D_t^2 \qquad (5)$$

or

$$D_t = \sqrt{A}\ /\ .586 \qquad (6)$$

$$h_{bd} = \frac{\sqrt{A}}{8 \times .586} = \frac{\sqrt{A}}{4.68} \qquad (7)$$

$$A_c = \frac{G \times 144}{500} = \frac{184.5 \times 144}{500} = 53.2 \text{ sq. in.}$$

$$h_{bd} = \frac{\sqrt{53.2}}{4.68} = 1.55 \text{ in.} \qquad D_t = 8 \times 1.55 = 12.4 \text{ in.}$$

The blading Reynold's number is

$$R_{e_c} = \frac{V\ D_{hyd}\ P}{\eta}$$, and it is necessary to evaluate D_{hyd}.

By definition $D_{hyd} = \dfrac{4A}{\text{Wetted Perimeter}}$

If it is assumed that the blade height is 2 blade spacing (ℓ) normal to the relative velocity, then

$$A = h_{bd} \times \ell = \frac{h_{bd}^2}{22}$$

$$\text{Wetted Perimeter} = 2(h_{bd} + \ell) = 3\ h_{bd}$$

$$\therefore D_{hyd} = \frac{4\ h_{bd}^2/2}{3\ h_{bd}} = .667\ h_{bd} = .667 \times 1.55 = 1.04 \text{ in.}$$

From the velocity diagram of Figure 13 the mean relative velocity is about 300 ft/sec. Then,

$$R_{e_c} = \frac{750 \times 1.04 \times .226 \times 3600}{12 \times .0459} = 1152 \times 10^3.$$

The efficiency for the helium compressor is assumed to be equal to that of the "typical" air machine of the same physical size, operating with STP suction, corrected for the difference in R_e. The air machine efficiency (Figure 12) is .822, and the corresponding R_e (Figure 14) is 152,000.

Since the machines are compared on the basis of the same physical size (i.e. same leakage, etc.) and same Mach number, the only efficiency difference is that due to Reynold's number.

Blading loss coefficients from typical test data from one of the manufacturers in this field are plotted in Figure 17 as a function of Reynold's number and turning angle. These coefficients are expressed in terms of energy loss. Since symmetrical staging is assumed they apply equally to stator and rotor and thus directly to the efficiency of the machine.

The blade loss coefficients applying to the air machine (R_e = 152,000) is 0.043; that applying to the helium machine (R_e = 1,152,000) is 0.027. The correction to the helium machine is +.016. Since the loss for the helium machine is less than for the air unit, the efficiency must be corrected upward. Thus compressor efficiency for this case is 0.838.

8.3.1.2 Turbine

It is assumed that turbine efficiency is the same as compressor efficiency. This reflects a counterbalancing, as explained in the text, of the more favorable flow conditions in a turbine against the mechanical desirability of a reduced number of stages.

Thus turbine efficiency is also 0.838.

8.3.1.2.1 Turbine Dimensions

It is generally necessary that turbine and compressor RPM be the same, since interposed gearing would necessarily handle 3 to 4 times the output power. Thus it is not usually possible to design an optimum turbine flow path as considered on its own merits.

In a conventional air plant, the turbine diameter would be somewhat greater than the compressor diameter, since a greater pressure ratio per stage and peripheral velocity is permissible. However, for the helium compressor, allowing reasonable Mach numbers, the tip speed is limited by stress considerations. Therefore, since stress is even more important for the high temperature turbine, it has been assumed that the turbine wheel tip diameter is equal to that of the compressor.

Then the blade heights are computed on the basis

of continuity. Since the volumetric flow for the turbine over most of the temperature range studied is less than for the compressor, the axial velocity has been reduced to 400 ft/sec (at least for the first stage) to allow more reasonable blade height (see the velocity triangle of Figure 13).

$$w = 41.7 \text{ lb/sec.}$$

$$\rho = p/RT = \frac{1000 \times 144}{1545/4 \times 1960} = .1905 \text{ lb/ft}^3$$

$$G = w/\rho = \frac{41.7}{.1905} = 219 \text{ ft}^3/\text{sec.}$$

$$A = \frac{G \times 144}{400} = \frac{219 \times 144}{400} = 78.9 \text{ in.}^2$$

$$D_t^2 - D_h^2 = \frac{A}{.785} \tag{1}$$

$$(D_t - D_h) = 2 h_{bd} \tag{2}$$

$$(D_t - D_h)(D_t + D_h) = \frac{A}{.785} \tag{3}$$

Substituting (2) into (3)

$$2h_{bd}(D_t + D_t - 2h_{bd}) = \frac{A}{.785} \tag{4}$$

$$4h_{bd}(D_t - h_{bd}) = \frac{A}{.785} \tag{5}$$

$$h_{bd}^2 - h_{bd}D_t + \frac{A}{4 \times .785} = 0 \tag{6}$$

$$h_{bd}^2 - h_{bd}D_t + \frac{A}{\pi} = 0 \tag{7}$$

$$h_{bd} = \frac{D_t - \sqrt{D_t^2 - 4A/\pi}}{2} \tag{8}$$

In this case:

$$h_{bd} = \frac{12.4 - \sqrt{12.4^2 - 4 \times 78.9/\pi}}{2} = 2.53 \text{ in.}$$

$$D_t = 12.4$$

8.3.1.3 Thermodynamic Cycle Calculations

The following assumptions have been made:

a) Compressor ratio/turbine ratio = 1.07

b) Regenerator effectiveness = .93

c) Heat sink at 90 F

d) Perfect gas data applicable.

8.3.1.4 Compressor Work

$$W_c = \frac{2}{\eta_T} C_p T_1 \left[PR_c^{k-1/2k} - 1 \right]$$

$R = \frac{1545}{4} = 386$ $\qquad \eta_c = .838$

$k = 1.66$ $\qquad C_p = 1.25$

$PR_c = 3.0$

$T_6 = 550$ R

Then

$$W_c = \frac{2}{.838} \times 1.25 \times 550 \left[3.0^{.66/3.32} - 1 \right] = 401.0 \text{ Btu/lb.}$$

8.3.1.5 Turbine Work

$$W_T = \eta_T C_p T_1 \left[1 - \frac{1}{PR^{k-1/k}} \right]$$

$\eta_T = .838$

$T_1 = 1960$ R

$PR_T = 3.0/1.07 = 2.79$

$$W_T = .838 \times 1.25 \times 1960 \left[1 - \frac{1}{2.79^{.66/1.66}} \right] = 686.3 \text{ Btu/lb.}$$

8.3.1.6 Regenerator

Compressor discharge temperature:

$$T_9 = T_6 + \frac{W_c}{2C_p} = 550 + \frac{401}{1.25 \times 2} = 710 \text{ R} = 250 \text{ F}$$

Turbine discharge temperature:

$$T_4 = T_1 - \frac{W_T}{C_p} = 1960 - \frac{686.3}{1.25} = 1412 \text{ R} = 952 \text{ F}$$

Regenerator Outlet Temperature = (Effectiveness) $(T_4 - T_9) + T_9$

$$T_{10} = .93\ (952 - 250) + 250 = 903\ F$$

8.3.1.7 Heat Input to Cycle

$$Q_{in} = C_p\ (T_1 - T_{10}) = (1500 - 903)\ \frac{1.25}{.97} = 771$$

(a 3% radiation loss is assumed.)

T_{10} = regenerator outlet temperature

T_1 = maximum cycle temperature

Combining of previous relations gives,

$$Q_{in} = .092\ (T_1 - 550) - .0361\ W_C + .959\ W_T$$

for the assumptions previously listed.

8.3.1.8 Work from Cycle

$$W_{net} = W_T - W_C = 686.3 - 401.0 = 285.3\ \text{Btu/lb.}$$

8.3.1.9 Cycle Efficiency

$$\eta_{th} = \frac{W_{net}}{Q_{in}} = \frac{285.3}{771} = .370$$

8.3.1.10 Mass Flow Rate

$$w = \frac{20{,}000 \times 2545}{W_{net} \times 3600} = \frac{20{,}000 \times 2545}{285.3 \times 3600} = 49.5\ \text{lb/sec.}$$

This compares with the originally assumed value of 41.7 lb/sec based on approximate efficiency assumptions. A recalculation based on the corrected value would have little effect on the efficiency. It would affect only the Reynold's number, and the corresponding efficiency effect is small. The diameters and blade heights should theoretically be corrected. However, the assumption of velocities is not rigid and may easily be changed by this amount.

8.3.1.11 Air Machine Efficiencies

The data from Table IX given in Section 10 of reference 6 for typical air machines was plotted in Figure 12. It was extrapolated as required. It was arbitrarily assumed (as explained in

the text) that an efficiency of over .90 was not feasible for a standard air machine since the size would become prohibitive and compromises at the expense of efficiency would be necessary. Thus the efficiency curve is assumed asymptotic to .90.

It was assumed that the compressor and turbine designs were similar to those shown in the velocity diagrams of Figure 13. The Reynold's numbers were computed on the assumption that $D_h = h_{bd} \times .667$ as shown in Section 8.3.1 and that the relative velocity was 300 ft/sec (Figure 13).

The absolute viscosity for air at 90 F, 14.7 psia is .0436 lb/hr.ft. and $\rho = \frac{p}{RT} = \frac{14.7 \times 144}{53.3 \times 550} = .0723$ lb/ft^3.

Assume for example a 10,000 CFM unit

$$A = \frac{G \times 144}{u} = \frac{10{,}000 \times 144}{200 \times 60} = 120 \text{ in.}^2$$

as shown in Section 8.3.1

$$h_{bd} = \frac{\sqrt{A}}{4.68} = \frac{\sqrt{120}}{4.68} = 2.34 \text{ in.}$$

and,

$$D_h = .667\ h_{bd} = .667 \times 2.34 = 1.56$$

Then

$$R_e = \frac{w\rho D_{hyd}}{\eta} = \frac{300 \times .0723 \times 1.56 \times 3600}{12 \times .0436} = 233.0 \times 10^3$$

8.3.2 Air Plant, 20,000 HP, 1500 F, 1000 psia

The air plant differs in several particulars from the helium.

8.3.2.1 Compressor

The compressor calculations follow the same procedure as for the helium plant with the following exception. No velocity correction is necessary between the "typical" air machine and the closed cycle machine under consideration. Thus the volumetric flow for the closed cycle machine can be applied directly to the "typical" efficiency curve of Figure 12. The remainder of the procedure is identical.

The resulting diameter and blade height values are

h_{bd_c} = 2.23 inches

D_{t_c} = 17.8 inches

It is noted that these are larger than the helium machine by a factor of about 1.45 (the helium blade height and diameter are 1.55 and 12.4 respectively).

The estimated compressor efficiency is .416 compared to the helium plant efficiency of .370.

8.3.2.2 Turbine

Again it was assumed that the turbine efficiency was equal to that of the compressor.

Although an optimum turbine design might utilize peripheral velocities about double that of the compressor, (for the case of air, this would be allowable with respect to both Mach number and stress), the factor of constant RPM would then lead to inconveniently short blading and large wheel diameters. Thus it has been assumed that the turbine diameter will be 1.25 x compressor diameter. The air turbine velocity diagram (Figure 13) is identical to that for helium. The blade heights are computed in the same manner as shown in Section 8.3.1.2.1 for the helium turbine. The resulting height and diameter are

h_{bd_c} = 1.05 inches

D_{t_c} = 21.4 inches

It will be noted that this diameter is about 1.7 times that for the comparable helium case, but the blade height is less than 1/2 that of the helium turbine.

8.3.2.3 Thermodynamic Calculations

The remainder of the calculations and assumptions are the same as for the helium case. Thermodynamic data from reference 1 was used instead of perfect gas data.

The resulting cycle efficiency and mass flow rate are

η_{th} = .416

W = 275 lb/sec

G_c = 11,900 CFM

compared to

$$\eta_{th} = .370$$

$$W = 49.5 \text{ lb/sec}$$

$$G_c = 13{,}200 \text{ CFM}$$

for the helium cycle.

8.3.3 Helium Plant, 600 HP, 1200 F, 100 psia

8.3.3.1 Compressor

The compressor inlet conditions are computed as before and an approximate flow rate estimated. The volumetric flow rate is computed to be 7140 CFM.

Referring to Figure 12, it is noted that a machine of this volumetric capacity falls within the centrifugal or positive displacement range. Therefore, it is assumed as explained in the text that the efficiency is not strongly affected by Reynold's number or Mach number, but is primarily influenced only by volumetric flow rate. Consequently the compressor efficiency is simply read from Figure 12 and is .810.

8.3.3.2 Turbine

The volumetric flow rate for the turbine is computed as shown in Section 8.3.1.2.1 and is 7190 CFM. If the 400 ft/sec axial velocity previously considered were used, along with a reasonable D_t/D_h ratio, the turbine would become extremely small. It was arbitrarily assumed that the minimum turbine of practical interest would be one with a tip diameter of 5.0 inches and a blade height of .625 inches. It was assumed that this turbine would be operated at whatever speed (and hence velocity) was required in view of the available flow (i.e. the possibility of partial admission was excluded on the basis of efficiency).

Typical turbines were computed for 1500, 1200, and 900 F at 1000 and 45 psia, for air and helium. These were plotted to show the trend for intermediate machines (Figures 18 and 19;i.e. pressures).

The efficiency of a typical air machine was estimated, operating under the following conditions:

$$T_{in} = 1200 \text{ F} \qquad PR = 2.79$$

P_{in} = 45 psia h' = 102.8 Btu/lb

v_{axial} = 438 fps C' = 2269 fps

ρ = .0731 lb/ft^3

The impulse velocity diagram sketched below was assumed, since the simple highly-loaded impulse turbine seems desirable for such small units.

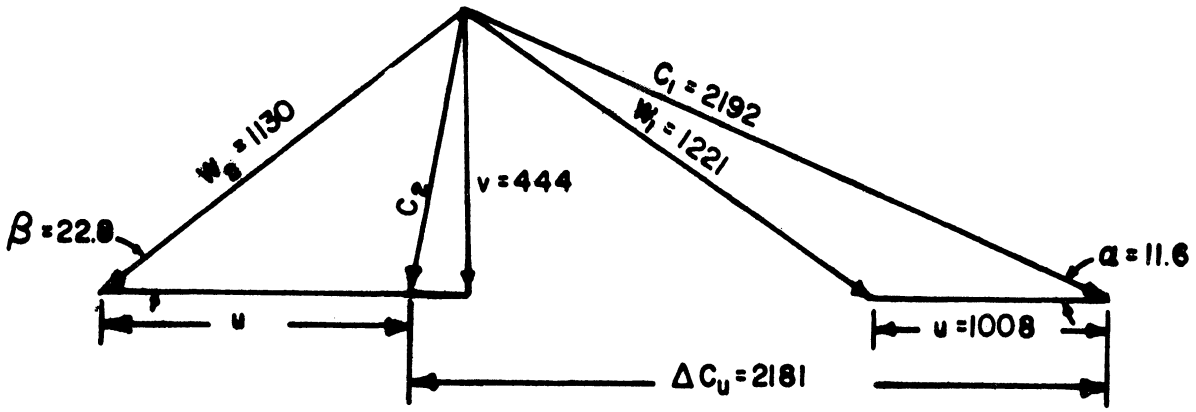

Figure 22. Small Turbine Velocity Diagram

There is no problem of matching between compressor and turbine in these cases, since centrifugal compressor design is quite unrestricted compared to axial compressor design in this respect, and, if a positive displacement unit is employed, gearing will be necessary in any case.

The loss coefficient vs. Reynold's number data of Figure 17 was utilized to estimate the efficiency.

For the stator:

The nozzle angle of turn is about 67°. The nozzle Reynold's numbers were computed assuming blade spacing (normal to flow) = .48 blade height (as for the compressor).

On this basis the R_e is 154 x 10^3 and the loss coefficient for 67° angle from Figure 17 is .067. Thus nozzle efficiency for this case is .933 and the velocity coefficient for the nozzle is $\sqrt{.933}$ = .966.

For the rotor:

$$h_{bd} = .625 \text{ inches}, \quad D_{hyd} = .405.$$

A blade spacing normal to flow of .3 inches for the .625 inch blade was assumed.

$$Re_{bd} = \frac{w_1 \rho D_{hyd}}{\eta} = \frac{1221 \times .0731 \times .404 \times 3600}{.0944 \times 12} = 114.9 \times 10^3$$

ξ_{bd} = .136 based on 135° turning angle (See Figure 17 and vector diagram)

ξ_{AR} = .0085 (estimated = aspect ratio loss)

$\eta_{bd} = 1 - \xi_{bd} - \xi_{AR} = .856$

$C_{v_{bd}} = .9255$

$w_1 = 1221$

$w_2 = 1130$

$$\text{Work} = \frac{u\Delta Cu}{g} = \frac{1008 \times 2181}{32.2 \times 778} = 87.8 \text{ Btu/lb}$$

$$\text{Input} = \frac{C_1'^2}{2g} = \frac{2269^2}{64.4 \times 778} = 103.0 \text{ Btu/lb}$$

$$\eta_T' = \frac{\text{Work}}{\text{Input}} = \frac{87.8}{103} = .852$$

Assume mechanical efficiency = .97

Leakage loss = .060 (This assumes .040 for tips and .020 for seals: based on a tip clearance of .010 giving leakage loss =

$$\frac{D_t t}{h D_t \sin \beta} = \frac{.010}{.625 \times \sin 22.8} = .040).$$

Then stage efficiency = .852 x .97 x .94 = .778 for a standard air machine of these dimensions.

The ratio of turbine efficiency to stage efficiency for these conditions is estimated to be 1.02. Then the turbine efficiency is .793.

The turbine horsepowers are computed on the basis of continuity, utilizing the axial velocity, density, $\Delta h'$, and the computed efficiency.

For the case of 1200 F, 45 psia air inlet, the horsepower is computed as shown below.

Axial area through the first stage of blading is

$$A = \frac{.625\ (5.0 - .625)\pi}{144} = .597\ ft^2$$

$$BHP = G\Delta h'_T \eta_T; \quad G = Av\rho$$

$$\rho_{bd} = \rho_1 \left(\frac{p_2}{p_1}\right)^{1/kZ}$$

$$\rho_1 = .0731$$

$$\frac{p_2}{p_1} = \frac{1}{2.79} \qquad Z = 1$$

$$BHP = .597 \times \frac{778}{550} \times 438 \times .0731 \times \left(\frac{1}{2.79}\right)^{1/1.4} \times 102.8 \times .793 = 106\ h\rho$$

For other cases of pressure and temperature, the volumetric flows were computed and the blading Reynold's number for a machine of these dimensions. The efficiency was then corrected according to the differences in loss coefficient from Figure 17. The turbine horsepower output for each of these units was computed and plotted in the curves of Figures 18 and 19 where the variation of turbine efficiency with power, pressure and temperature is shown. The computed values are shown below for both air and helium. Slight variations were made in the plotted values to allow smooth curves.

Ratio of Stage to Turbine Efficiency:

For turbine stage work -

$$W_{st} = \eta_{st} C_p T_{1_1} \left[1 - \frac{1}{(p_1/p_2)^{k-1/k}} \right]$$

then for the second stage -

$$T_{1_2} = T_{1_1} - \eta_{st} \left[T_{1_1} - \frac{T_{1_1}}{(p_1/p_2)^{k-1/Zk}} \right] = T_{1_1} \left[1 - \eta_{st} \left(1 - \frac{1}{(p_1/p_2)^{k-1/Zk}} \right) \right]$$

$$T_{l_3} = T_{l_2}\left[1 - \eta_{st}\left(1 - \frac{1}{(p_1/p_2)^{k-1/Zk}}\right)\right] = T_{l}\left[1 - \eta_{st}\left(1 - \frac{1}{(p_1/p_2)^{k-1/Zk}}\right)\right]^2$$

etc. If we define

$$r = \left[1 - \eta_{st}\left(1 - \frac{1}{(p_1/p_2)^{k-1/Zk}}\right)\right]$$

then

$$W_{turbine} = \eta_{st} C_p T_{l_1}\left[1 - \frac{1}{(p_1/p_2)^{k-1/k}}\right](1 + r + r^2 + \ldots r^{Z-1})$$

then

$$\frac{W_T}{W_{st}} = \frac{\left[1 - \frac{1}{(p_1/p_2)^{k-1/Zk}}\right]}{1 - \frac{1}{(p_1/p_2)^{k-1/k}}}\left(\frac{r^Z - 1}{r - 1}\right)$$

If an evaluation is made for the air and helium cases it is found that

$$\left(\frac{W_T}{W_{st}}\right)_{air} \sim 1.02 \text{ for 2 stages and total pressure ratio of } 2.79.$$

and

$$\left(\frac{W_T}{W_{st}}\right)_{helium} \sim 1.03 \text{ for 8 stages and total pressure ratio of } 2.79.$$

The upper portion of the curves of Figures 18 and 19 apply to the large axial flow compressor units, where it was assumed that turbine and compressor efficiencies were equal. Some slight alteration of the points to achieve smooth curves was necessary.

The turbine efficiency for all cases where centrifugal or positive displacement compressors were used was read from Figures 18 and 19.

Thus for the 600 HP, 1200 F, 100 psi helium unit, turbine efficiency is .810.

TABLE XVII. SMALL TURBINE DESIGN TABULATION

Fluid	p psia	t °F	No. Stages	u	η	BHP
Air	45	1500	2	771	.792	117
		1200	1	1008	.793	106
		900	1	931	.799	95.5
	1000	1500	2	806	.837	2820
		1200	1	1048	.839	2530
		900	1	949	.848	2280
Helium	45	1500	10	881	.748	159
		1200	9	858	.757	156
		900	7	885	.767	159
	1000	1500	10	946	.822	4000
		1200	9	920	.826	3890
		900	7	946	.832	3930

8.3.3.3 Thermodynamic Calculations

These are identical to the helium calculations previously discussed as is the remainder of the calculating procedure.

The resulting plant efficiency is .236.

8.3.4 Air Plant, 600 HP, 1200 F, 100 psia

The calculating procedures and methods are identical to those explained in Section 8.3.3 for the 600 HP helium unit.

The air plant resulting efficiency is .310 as compared to .236 for the helium.

This large difference is the result of the fact that helium is inherently less efficient at the same component efficiency, that it is further from optimum pressure ratio at 3.0, and that the turbine efficiency under the assumptions of this study is lower.

8.4 Number of Compressor Stages for Air and Helium if Velocities are Equal

$$W_c = C_p T_1 \left[(p_2/p_1)^{k-1/k} - 1 \right] ; \quad \text{Assume } (p_2/p_1)_{air} = 1.08 \text{ per stage}$$

$$= \frac{u \Delta C_u}{gJ} = \text{constant under the basic assumption.}$$

Then

$$W_{c_{air}} = .24\ T_1 \times .0223 = .00535\ T_1$$

$$W_{c_{helium}} = 1.25\ T_1\ [\ (p_2/p_1)^{.398} - 1] = .00535\ T_1$$

$$(p_2/p_1)^{.398}_{hel} = 1 + .00428 = 1.00428$$

$$(p_2/p_1)_{hel} = 1.0108$$

For $p_2/p_1 = 1.08$, seven helium stages are required.